UNIVERSITY OF OKLAHOMA

GRADUATE COLLEGE

ELECTRIC CIRCUIT FOUNDATION FOR STRUCTURAL ANALYSIS AND APPLICATIONS IN LARGE-SCALE POWER NETWORKS

A DISSERTATION

SUBMITTED TO THE GRADUATE FACULTY

in partial fulfillment of the requirements for the

Degree of

DOCTOR OF PHILOSOPHY

BY

DHRUV SHARMA
Norman, Oklahoma
2019

ELECTRIC CIRCUIT FOUNDATION FOR STRUCTURAL ANALYSIS AND APPLICATIONS IN LARGE-SCALE POWER NETWORKS

A THESIS APPROVED FOR THE
SCHOOL OF ELECTRICAL AND COMPUTER ENGINEERING

BY

Dr. John N. Jiang, Chair

Dr. Theodore Trafalis, Outside Member

Dr. Paul S. Moses, Member

Dr. Ronald Barnes, Member

Dr. Krishnaiya Thulasiraman, Member

Acknowledgments

Throughout the writing of this dissertation I have received a great deal of support and assistance. Firstly, I would like to thank my advisor, Dr. John N. Jiang who gave me the opportunity to come to the University of Oklahoma to pursue my PhD studies. He guided me all these years through my work and helped me develop my research and writing skills while also imparting in me the strong work ethic required to write a doctoral dissertation. His support and leadership have been the primary contributing factors in my becoming the researcher that I am today.

I would also like to thank my co-advisors and committee members Dr. Paul Moses, Dr. Krishnaiyan Thulasiraman, Dr. Ronald Barnes and Dr. Theodore Trafalis whose advice and guidance has always been instrumental. I want to give special thanks to Dr. Paul Moses and Dr. Krishnaiyan Thulasiraman for their extended guidance and support during our collaborations which has been influential in developing this dissertation.

I would like to thank my wife, Shreyasi, who stood by me and showed all the love, support and patience during these years. I want to thank my parents, my sister for supporting me through my education since my childhood years.

I am grateful to my colleagues at the ECE Dept. at University of Oklahoma, for being friendly and having contributed to a good working environment. I would like to thank Rodney Keele, Abe Hartley and Jack Bailey for their continued administrative support in every way possible. I would like to express gratitude to Lisa Wilkins for her extended support during my early PhD years.

Finally, as a contributor to the field of education, I would like to dedicate this dissertation to everyone who is directly or indirectly working towards improving the quality of education across the globe.

Dhruv Sharma

Table of Contents

List of Figures

List of Tables

Abstract

The modern power grid is increasing in size and with that becoming more complex. The recent evolution of grids has made an impact on power system planning studies and analyses. On the other hand, the developments in the field of complex networks and the range of application areas have allowed their extension to the field of power systems. The application of complex network-based analysis on power system networks has been helpful in solving many long-standing challenges.

This research focuses on presenting the underlying foundation of structural analysis of power system network. The structural analysis of power systems is an important approach and has the ability to address various issues, particularly, dynamic and transient real-time issues and identification of critical components. Steady-state, dynamic and transient power system models may differ with change in applications when analyzed from an electric circuit theory perspective, however they demonstrate an embedded consistency from a structure perspective. To this end, Chapter 2 gives a primer on the concept of distance in power system networks from different perspectives.

The research highlights the key features of structural analysis in order to allow the use of only structure information for various analyses in power systems. This is highlighted in Chapter 3 through port-Hamiltonian formalism. Further the basis of the newly developed structural analysis is introduced and described in Chapter 4. Next, using the electric circuit foundation of structural analysis for power systems from network perspectives, in Chapter 5, the underlying similarity in various networks is identified. This chapter also highlights the key structural features such as decoupling of state variables from structure parameters, connection information and link strength.

The research also highlights the use of network methodology in analyzing power system networks. The importance of link strength, determined by the weights of the links connecting the nodes is highlighted by with associating electrical power network parameters

with the structure information. This allows us to derive the network topology of the system and then do the analysis on structural information.

Based on the insights obtained from the preceding chapters, Chapter 6 and Chapter 7 show the evidence of the use of structural analysis for addressing long-standing problems. Power system restoration is one such area, where a solution is presented solely based by applying complex network techniques to obtain the solution. Further, the network-based electrical distance parameter is used to address the issue of complexity of analysis involved in making economic and dispatch decisions. These applications demonstrates how structural analysis from a networks perspective helps in bridging the gap between power system and complex network science.

CHAPTER 1

Introduction

The last few decades have witnessed expansion of modern power systems in terms of scale and with that added complexity. With climate change in mind, the developments in the area of renewable energy have increased. Also due to various economic and political reasons, the modern power system has become more complex with distributed generation and load centers. These recent changes have also made an impact on planning studies and power system market analyses. With such enormity of scale, conventional studies based on full model representations are proving to be computationally challenging.

At the other end of the spectrum, a new movement of interest and research has evolved in the study of complex networks, i.e. networks whose structure is irregular, complex and dynamically evolving in time such as power grids, communication networks, biological networks, social networks, etc. Investigating dynamics in such complex networks requires an understanding of the interaction between network topology and specific domain constraints. For example, the study of power grids requires basic circuit laws, relating voltages and currents, to be incorporated along with the network topology. One such illustration of topological representation of a complex power system network is shown in Fig. 1.1.

Structural analysis of a power system networks as an approach has been given emphasis in analyzing and addressing various issues related to the operation of power grids. The analytical foundation of structural analysis is based on power system representation from various perspectives, such as steady-state, electromagnetic transient and electromechanical dynamic perspectives. These types of models, which from an electric circuit theory perspective may differ with change in applications, demonstrate an embedded consistency from a structure perspective and suggest possible solutions. Given the re-

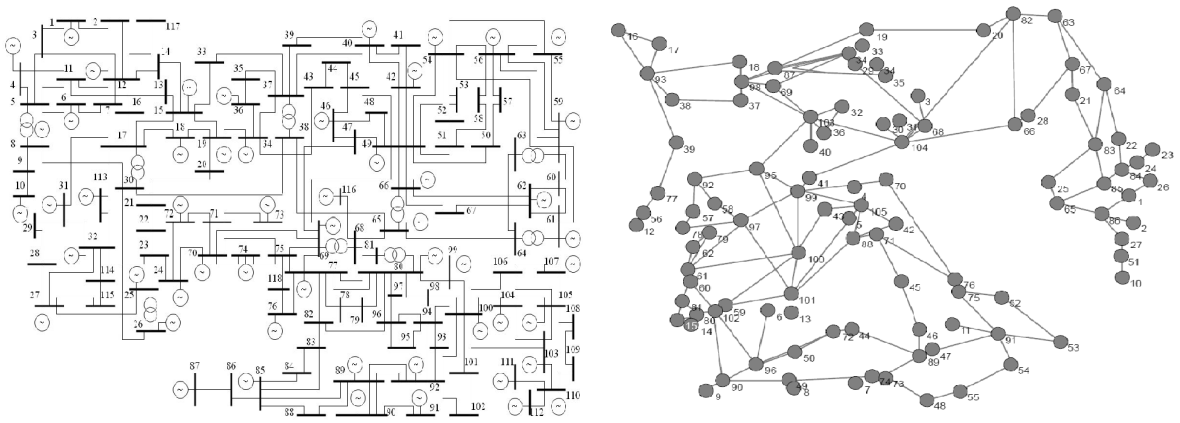

Fig. 1.1: One-line diagram and topological representation of a power system [1]

quirements from optimal objectives of planning or operation, the overarching goals of this thesis has been to reduce the complexity of analysis in modern power systems including economic, political and environmental factors. The simplified electrical network analysis is the pressing need for utilities and network operators to make informed dispatch decisions across power network interconnections. Such incorporation of domain specific information can result in simplified analysis, the significance of which has been shown in this thesis. As a result, the long standing gap between power system and complex network analysis can be seen to be closed down and bridged. The evidence of this is illustrated in this thesis with various applications dealing with the current issues related to the structural analysis of power systems.

1.1 Motivation

The network structure aspect of power grids has received a fair amount of attention in the network science and complex system literature. For example, the characteristic path length has been measured in [10] which resulted in determining clusters in power grids, and exhibits similarities to "small-world" network models. A number of studies measure the degree distribution of various power grids with some reporting exponential [11, 12] and others reporting power-law/scale-free degree distributions [13, 14]. It is

evident that different countries or regions require different topological structures for the study of their respective power grids. But even different analyses of identical grids, for instance, the Western Interconnection transmission system in the U.S., have yielded different structural results [13, 14]. Such varying results and analyses along with the practical issues stated in the following paragraphs have provided the motivation for the work presented in this thesis.

Though historically negligible and infrequent, power system outages across the U.S. for the last 15 years are on the rise at an alarming rate [15]. The outages are mainly caused from disruptions on the transmission system, both in terms of the duration and frequency of outages. This becomes one of the most critical scenarios in modern power system. In such a situation, the pressing need is to be able to quickly restore the system to an optimal operating configuration such that it can be re-synchronized to the grid. The complexity of the power system requires such restoration process to be subject to steady state and dynamic constraints of the network including those related to the generation, transmission and distribution, and load.

While not very frequent, any damage to the transmission system can result in major power outages that can affect large numbers of customers and can cause major economic disruptions [16]. Power system operators have to deal with the most important task of system restoration following a disruption. The formalism of a restoration process can be highly complex involving a large number of generation, transmission and distribution, and load constraints. Such complexities warrant the operators to employ off-line solution plans to re-synchronize the newly formed islands post disruption. Therefore in practice, power system restoration should be achieved optimally according to different objectives such as maximizing generation capacity and quickly re-energizing major transmission corridors in order to minimize the impact of blackout and recover the load.

In addition to the issues related to the restoration of power systems, the complexity of interconnection has always been a constraint for network operators for power mar-

ket analyses and economic dispatch decision making. Due to economic, political and environmental reasons, the degree of interconnections in modern power systems has increased which makes the electrical market analysis involving power exchange complex [17]. The analysis can be computationally challenging especially when a full AC implementation approach is used [18]. As compared to the full AC analysis, a simplified analysis of the network can be done by using full network DC power flow model [19]. But due to the enormity of the power systems, full network DC analysis still remains to be computationally taxing. As an alternative, various network equivalence models have been used to analyze the electricity market [18, 20].

The work presented here is motivated by the need of analyzing the power system networks from structural perspective in a more efficient manner. The results will provide a better understanding of the significance of structure parameters along with the behavior under different operating conditions. The outcomes will also allow us to solve long-standing problems of power system networks that have not been efficiently solved using conventional methodologies. Further in a broad spectrum, the work allows us to bridge the gap between traditional power system analyses and complex network theory.

1.2 Objective and highlights of the work

The thesis mainly deals with the electric circuit foundation of structural analysis for power systems from a networks perspective. The focus is on the identification and interpretation of electrical distance measures that incorporate system topology with power systems considerations. The main objective is thus the identification of key features of structural analysis in order to allow the use of only structure information for various analyses in power systems. This highlights the dominating influence of the structure. The thesis also highlights the use of network methodology in analyzing power system networks. The other objective is to use the methodology in existing problems of power system restoration followed by introduction of an electrical distance measure

which is used in equivalencing of power system networks.

Using the structure information combined with network methodology are shown to provide solutions to long-standing problems that have not been efficiently solved using conventional methodologies. This is one of the motivation for this work. The investigation of various electrical distance measures done in the thesis highlights the differences in scope of each measure. The study is directed towards uncovering the underlying similarities which is provided by port-Hamiltonian formalism and is reflected in the structural analysis covered in the thesis.

Next, structural analysis from networks perspective is utilized to address the power system restoration issue. The power system structure information is utilized and network topology is generated. At this point, for further analysis, the thesis is aimed at utilizing only network methodologies to obtain the solution to system restoration. The link strength between two nodes is used as a parameter for identification of critical components along with approximate dynamic programming to reduce the solution space. Compared to the conventional methodologies, the network-based method aims to highlight how the simplified methodology addresses the system restoration problem in large-scale power systems. This is illustrated by development of system restoration plans on large-scale power systems.

Another application is in the area of network equivalencing to reduce the complexity of the interconnected network and thus simplify analyses. This is illustrated with the introduction of electrical distance measure which is based on the network connection information.

Further the results of these applications are presented. These applications demonstrate the use of structural analysis from a network perspective helps in bridging the gap between power system and complex network analyses.

1.3 Publications

Some results of this thesis have already been published and the details are given below. Chapters 3 and 5 describes the contents of [5]. The results in [1] and [4] are discussed in Chapter 7 and the fundamental study is published in [3]. The main content and results in Chapter 6 are described in [2] and [6].

[1] D. Sharma, K. Thulasiraman, D. Wu, and J. N. Jiang. A network science-based k-means++ clustering method for power network equivalence. Computational Social Networks, SpringerOpen, 2019.

[2] D. Sharma, C. Lin, X. Luo, D. Wu, K. Thulasiraman, and J. N. Jiang. Advanced techniques of system restoration and practical applications. Electric Power System Research. *(under review)*

[3] M. N. Rafiq, D. Sharma, D. Wu, J. N. Jiang, and C. Kang. Average electrical distance based bus clustering method for network equivalence. In 19th International Conference on Intelligent System Application to Power Systems, San Antonio, USA, Sept 2017.

[4] D. Sharma, K. Thulasiraman, D. Wu, and J. N. Jiang. Power network equivalents: A network science based k-means clustering method integrated with silhouette analysis. In Complex Networks & Their Applications VI, vol. 689, pages 78-89, Cham, 2018.

[5] D. Sharma, G. Ji, W. Fei, D. Wu, P. Moses, and J. N. Jiang. Electric Circuit Foundation of Structural Analysis for Power Systems from a Network Perspective. In 11th Int. Conf. on Power Generation, Transmission, Distribution and Energy Conversion, Dubrovnik, Croatia, Nov. 2018.

[6] D. Sharma, C. Lin, X. Luo, D. Wu, K. Thulasiraman, and J. N. Jiang. Advanced techniques of system restoration and practical applications. In 11th Int. Conf. on

Power Generation, Transmission, Distribution and Energy Conversion, Dubrovnik, Croatia, Nov 2018. (Ranked #5)

CHAPTER 2

Primer for distance from different perspectives

The power grid has been evolving ever since its inception and is mainly driven by economical and societal demands. Historically, the electric power grid has evolved to meet increasing electricity demand. For example, in the United States, the energy consumption has risen from 10% of the energy consumption in 1940 to 40% by 2002. This evolution has also affected the electrical power grid size as well with demands ranging from big load centers such as cities, towns etc. to isolated areas with loads spread few and far between. This evolution of the electrical power grid has made it an interconnected complex network. The electrical power grid faces different requirements and challenges, such as its organization, its technical ability to meet increasing electricity needs, and its capacity to increase efficiency without diminishing reliability and security. In order to analyze such network with electrical properties, this chapter discusses the concept of distance in an interconnected system from different analytical perspectives.

2.1 Distance from networks perspective

The concept of graph distance, also known as geodesic distance, in simple connected graphs (introduced in [21]), is defined in [22] and further used in [23, 24, 25]. It has two variants:

1 The simple one considering only the number of edges;

2 The weighted one having a "length" for each edge.

Distance $d_G(u, v)$ between two vertices u, v of a graph G is defined as the length of the shortest path between u and v in G. A path in a graph is a sequence of distinct

vertices, such that adjacent vertices in the sequence are adjacent in the graph. For an unweighted graph, the length of a path is the number of edges on the path. For an (edge) weighted graph, the length of a path is the sum of the weights of the edges on the path. The distance function is a metric on the vertex set of a (weighted) graph G. In particular, it satisfies the triangle inequality:

$$d_G(u, v) \leq d_G(u, w) + d_G(w, v)$$

for all vertices u, v, w of G. This follows from the fact that, if we want to get from u to v, then one possibility is to go via vertex w.

The average distance of a graph $G = (V, E)$ of order n, denoted by $\mu(G)$, is the expected distance between a randomly chosen pair of distinct vertices given by

$$\mu(G) = \frac{1}{\binom{n}{2}} \sum_{u,v \subset V} d(u, v). \tag{2.1}$$

Further, considering a finite directed graph G with a directed edge e having an associated length $w(e)$, the authors in [26] consider the measure of distance between two vertices v_i and v_j defined by (2.2).

$$d_{ij} = \min_{P(v_i, v_j)} w(P(v_i, v_j)), \tag{2.2}$$

where $P(v_i, v_j)$ ranges over all directed paths from v_i to v_j and $w(P(v_i, v_j))$ represents the sum of all edge-lengths in $P(v_i, v_j)$. This assumes that the graph G is strongly connected or $d_{i,j}$ always exists where $d_{i,j}$ is the $(i, j)th$ entry of the distance matrix $D(G)$ of G.

Considering a strongly connected graph G which is divided into various blocks G_i. In [27], a relation given in (2.3) between the ratio of determinant and co-factors of graph G and sum of corresponding determinants and sum of co-factors of the blocks of graph G. This is given as

$$\frac{det\{D(G)\}}{cof\{D(G)\}} = \sum_i \frac{det\{D(G_i)\}}{cof\{D(G_i)\}}, \tag{2.3}$$

where $det\{D(G)\}$ and $det\{D(G_i)\}$ are the determinants of graph G and block G_i respectively while $cof\{D(G)\}$ and $cof\{D(G_i)\}$ represent the respective co-factors of graph G and block G_i of the graph. Note that the determinants and co-factors of the Laplacian matrix to be defined later.

2.1.1 Networks perspective

The resistance distance of a graph, because of its structural meaning, has become a useful tool to analyze structural properties of graphs, or more generally of networks. In this context, a network is a connected graph in which each edge has been assigned a positive value, named the conductance of the edge. In contrast with the standard geodesic distance, defined as the length of the shortest path between vertices, the resistance distance takes into account all paths between vertices. The high sensibility of this metric with respect to small perturbations, makes it suitable to compare different network structures.

The identification of effective resistance as distances is done in [28]. The resistance distance $R(G)$, of a connected undirected graph $G = (V, E)$ with vertex set $V = 1, 2, \cdots, N$ and edge set E, was defined by Klein *et.al.* [28] as

$$R(G) = \sum_{i<j} R_{ij}, \tag{2.4}$$

where R_{ij} is the effective resistance between vertices i and j as computed with Ohm's law when all the edges of G are considered to be unit resistors. The quantity R_{ij} is shown in [28] to be a distance function on the set of vertices, and it is introduced together with the index $R(G)$ as an alternative to the usual graph theoretical distance. The indexing is so done that the resistance distance can be compared with that of conventional graphical distance. Resistance distance $R(G)$ is also called Kirchhoff index of G.

The properties of resistance distance are discussed in [29] and further [30, 31, 32] present the applications of resistance distance in a network along with various indices such as

Kirchhoff index and Wiener index.

2.1.2 Topological perspective

2.1.2.1 Centrality measure-based index

The authors in [33] builds resistor networks by representing each link by a 1Ω resistor. For each network, the resistance matrix is calculated, which is essentially equivalent to the admittance matrix for an equivalent electrical network. The resistance matrix R, defines a relationship between voltages and currents, as shown below.

$$\Delta V = R\Delta I. \tag{2.5}$$

From this, the ratio of different elements in R matrix can be calculated and assessed. The ratio can be defined as

$$S_{kl} = \frac{R_{kl}}{R_{kk}}. \tag{2.6}$$

The elements of S, describe the extent to which a state change at location k will affect a similar change at location l. Essentially this matrix tells the extent to which information flowing through the system will propagate through each network, or conversely, the extent to which information can be contained within a small area.

The weighted degree distributions along the topology of a network is discussed in [34] where the weights are based on the physical capacity constraints of the paths for a system. The degree distribution as a centrality measure is used in various domains ranging from non-linear science, mechanics, medicine, social networks, engineering etc. [35, 36].

2.1.2.2 Connectivity distance-based index

While electrical distance does not perfectly represent all of the ways in which components in a network connect, it is a useful starting point for structural analysis. There are numerous variant measures of electrical distance, but one of the simplest is the absolute value of the inverse of the system admittance matrix as described in [37] and shown below

$$E = |Y^{-1}|. \tag{2.7}$$

This electrical distance matrix, E with elements e_{ab}, gives the relation between voltage and current changes for every node pair ab. The impact of voltage and current changes for a node with respect to the other nodes in the network can be seen as the connectivity distance. Specifically, e_a is used to define the measure of connectivity distance for node a as shown below

$$e_a = \sum_{b=1;b\neq a}^{n} \frac{e_{ab}}{n-1}. \tag{2.8}$$

Given the electrical distance matrix E, it is possible to rank nodes by the amount of load/demand that is within a given electrical distance threshold. Such a measure of distance to load enables additional insight to the electrical network structure. A similar measure has been discussed in [33] while the concept of electrical distance has been used in [38].

2.1.3 Remarks

The representation of distance from a networks perspective provides a unique insight on the sensitivity of different structure-based variables. The distance as seen from a networks perspective has been broadly divided into categories defining the proximity of a bus on the basis of topology of the network and on the basis of actual resistance distance.

The resistance distance is based on electrical network theory, wherein a fixed resistor is imagined on each edge connecting the nodes. The resistance function is defined as a distance function. On the other hand, from a topological perspective, the aim is to simplify the network to demonstrate the structure of the network. The ratio matrix adds an information regarding the validity of state change across the network. The connectivity distance is possibly the simplest measure of electrical distance based on the admittance matrix of the network.

The distances from networks and topological perspective are studied and various indices defining the measurements are mentioned. From the networks perspective, [28] identifies the distance as effective resistance as shown in (2.4) which is calculated using Ohm's law where resistance can be defined as a sensitivity parameter. Further, from a topological perspective, authors in [33], defines the resistance matrix in (2.5) and the ratio in (2.6). Finally in [37], the elements e_{ab} gives the sensitivity between current and voltage changes in (2.8). Hence it can be seen that the distance described by various methods is actually the sensitivity depending on different parameter changes in the network.

The distances as seen from networks and topological perspectives are classified in Table 2.1 highlighting significant properties and applications.

Table 2.1: Classification of distance estimation from networks perspective

		Topological Perspective	
	Network Resistance Perspective	Centrality measure-based Index	Connectivity Distance-based Index
Measure/Index	Effective resistance or Kirchhoff Index	Resistance matrix	System Admittance matrix
Equation	$R(G) = \sum_{i<j} R_{ij}$	$S_{kl} = \frac{R_{kl}}{R_{kk}}$	$e_a = \sum_{b=1;b\neq a}^{n} \frac{e_{ab}}{n-1}$
Similarities	1. Gives the sensitivity index of a network 2. All are based on the equivalent network impedance		
Differences	Takes into account all the paths between vertices.	Defines the effective proximity of a state change across the network	Retains the links representing strong electrical connections irrespective of direct physical connection
Applications	Simplifies the network by "multiple-route distance diminishment" feature	Gives a new dimension to scale-free networks and defines the effective boundaries of any state change	Used in creating synthetic electrical network topologies

2.2 Distance from power grid perspective

It is a well-known empirical evidence that electric power grids are inherently prone to frequent disturbances of different severities. In [13], authors follow a different approach based on the development of the science of complex networks i.e. the details of the electromagnetic processes were neglected while focusing only on the topological properties of the grid. The aim was to demonstrate that the structure of an electric power grid highlights important information on the vulnerability of the system. However in order to get a more accurate measure with the changing system dynamics, the concept of distance is discussed from a power systems perspective.

2.2.1 Electro-mechanical perspective

With expansion and heavy interconnections, large-scale power systems can no longer be studied in isolation. The concept of electro-mechanical distance (EMD) into area division of dynamic equivalence for transient stability in power systems was introduced in [2] and later pursued in [39]. In order to reduce the complex analysis and computation, the precise mathematical models are adopted within the studying system, but for the external systems, each coherent sub-system is subjected to dynamic equivalence which simplifies it into small quantities of aggregate generators. EMD is a concept of evaluating the electro-mechanical disturbance propagation between generators.

2.2.1.1 Reflection distance-based index

The definitions of subsystems within the interconnected network based on electrical equivalencing and electro-mechanical equivalencing was introduced in 1971 by J.M. Undrill *et.al.* [40]. However as discussed earlier, the concept of EMD was introduced in 1973 by S.T.Y. Lee *et.al.* [2] and later discussed by Podmore [39] which suggested a method to identify coherent groups without conducting a transient stability study. The study used the concept of a *distance measure* which could be a means of assessing the impacts of generators. It is defined in two ways: 1) electrical perspective, and 2) electro-mechanical perspective. Electrical perspective gives the simplest distance measure which is the transfer admittance between generators and describes how closely coupled two generators are electrically close to each other. While the admittance-based distance is a purely electrical distance, the reflection distance is designed to measure the dynamical effect of a generator on the stability of inner circle generators. The inner circle is drawn around the group of generators the stability of which in response to local disturbances is to be studied. This is illustrated in Fig. 2.1.

The reflection distance of a generator k which is in the set Ω measured with respect to

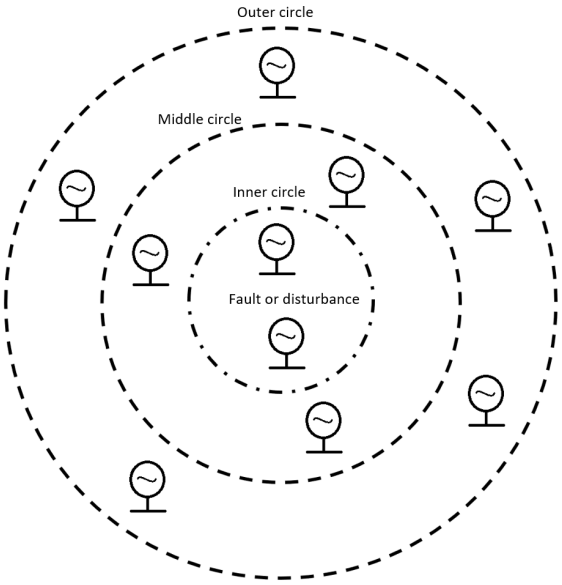

Fig. 2.1: Interpretation of closeness of generators [2]

the inner circle ϕ is defined as follows.

$$R_d(k) = \max_{f \in \phi} \Big\{ \max_{i \in \phi} \frac{\Delta P_{ki}}{M_i} \Big\}, \qquad k \in \Omega, \tag{2.9}$$

where

$$\Delta P_{ki} = \frac{\partial P_{ik}}{\partial \delta_k} \Delta \delta_k. \tag{2.10}$$

ΔP_{ki} in (2.10) is the change in electrical power of a generator i owing to a small change in the angle of generator k. Also $R_d(k)$ in (2.9) can be defined as the inverse distance in the sense that the bigger it is, the closer is that generator to the inner circle. ϕ is the set of inner circle generators, and Ω is the set of all generators outside the inner circle. In (2.10), $\Delta\delta_k$ is the change in power angle of the generator k and is caused by a fault at one of the inner circle generators for a duration t_c seconds and is given by

$$\Delta \delta_k \approx \frac{1}{2} a_k t_c^2, \tag{2.11}$$

where a_k is the acceleration of generator k at the instant of fault, however it does not change much during the short duration of fault.

The reflection distance measure can be interpreted as the synchronizing force between a

generator close to a fault and the generator whose distance is to be measured. Applying this to generators existing in the network, a relative distance can be measured with respect to the location of fault. Generators showing the same response are coherent generators and hence can be grouped together.

2.2.1.2 Coherency-based index

The coherency-based technique is introduced in [41] which is based on the property of equal acceleration for coherent machines. The concept of coherency is discussed in various studies such as [39, 42, 43] which focuses on the dynamic equivalence of a network. In an operating condition, two generators are said to be coherent if their angular difference is constant within a certain tolerance limit, ϵ, over a certain time interval. For the two machines i and j

$$|\delta_{ij} - \delta_{ij}^{s}| \leq \epsilon.$$

Then the coherency factor can be defined as

$$CF = \frac{max|\delta_{ij}|}{|\delta_{ij}^{s}|}. \tag{2.12}$$

For a machine i, the dynamic equation is

$$M_i \Delta\ddot{\delta}_i = \Delta P_{m,i} - \Delta P_{G,i}. \tag{2.13}$$

After simplifying, the relation is of the form

$$[M][\Delta\ddot{\delta}] = [M]^{-1}[Y][\Delta\delta]. \tag{2.14}$$

Here $[M]^{-1}[Y]$ is the Jacobian matrix J. This method compares only the elements of the Jacobian matrix to identify the coherent group. A normalized quantity β is defined such that

$$\beta = \frac{|j_{ij} - j_{ji}|}{max(j_{ij}, j_{ji})}, \tag{2.15}$$

where the term $|j_{ij} - j_{ji}|$ can be taken as a measure to estimate the relative variation between $\Delta\delta_i$ and $\Delta\delta_j$. When the moments of inertias M_i and M_j are equal, then $\beta = 0$, which means that the machines are perfectly coherent.

2.2.1.3 Electro-mechanical distance-based index

The EMD between two machines is defined in [44] as a measure of the maximum angular movement between the machines during the transient period. A logical measure of the electro-mechanical interaction between a pair of machines during the transient period could be the synchronizing power flow or the maximum angular deviation. The EMD between the generator i and the reference generator n is defined as

$$d_{in} = \Big[\sum_{l=1}^{m} (p_{il}^2 + q_{il}^2) + \sum_{l=2m+1}^{2n-1} s_{il}^2 \Big]^{1/2}. \tag{2.16}$$

The elements p_{il}, q_{il} and s_{il} represent the amplitudes of the complex modes and the real modes, respectively corresponding to $\Delta\delta_{in}$. A measure (the Euclidean norm) of such amplitudes for all the modes is taken and defined as the EMD. Thus the EMD d_{in} reflects the maximum angular excursion between the generator i and the reference generator n. Similarly, the EMD between generators i and j is derived from the expression $(\Delta\delta_{in} - \Delta\delta_{jn})$ and is given by

$$d_{ij} = \Big[\sum_{l=1}^{m} [(p_{il} - p_{il})^2 + (q_{il} - q_{jl})^2] + \sum_{l=2m+1}^{2n-1} (s_{il} - s_{jl})^2 \Big]^{1/2}. \tag{2.17}$$

Based on d_{ij}, the coherent generators can be included in a single area depending on the threshold for that network such that the power system is decomposed into several regions. The distance measure under transient conditions is discussed in [2, 41, 45] under different scenarios and assumptions.

2.2.1.4 Composite EMD-based index

EMD is a concept of evaluating the electro-mechanical disturbance propagation between generators. Since EMD is a relative index to evaluate the propagation of dynamic phenomena associated with a given disturbance, its definition varies with different conditions. According to the basic definition of EMD, the concept of composite EMD was presented in [46, 47]. The application scope of EMD was also extended. It could not only deal with some emergent situations under some given operation conditions, but also the stability problems of a special emergent situation under different operation conditions and the degree of influencing the different parts of a power system. Highlighted in [48], the following definitions of EMD are given with a combination of these to form composite EMD.

1 The absolute value of initial power angle acceleration (ED_{1i}).

2 The absolute value of initial acceleration power (ED_{2i}).

3 Transfer admittance before disturbance (ED_{3i}).

4 Inertia constant (ED_{4i}).

Combining the above mentioned definitions of EMD, we get EMD between buses j and i is

$$ED_{ij} = w\sqrt{2H_j/B_{ij}}, \tag{2.18}$$

and similarly the EMD between buses i and j is

$$ED_{ji} = w\sqrt{2H_i/B_{ji}}, \tag{2.19}$$

where H_i is the inertia constant of the generator at bus i and B is the susceptance matrix which is symmetrical giving $B_{ij} = B_{ji}$. For a real power system, it is difficult to confirm the direction of electro-mechanical disturbance propagation, so the algebraic

average value of EMD between the generator buses i and j can be obtained as

$$ED_{ij}^{av} = ED_{ji}^{av} = \frac{w}{2}(ED_{ij} + ED_{ji}). \tag{2.20}$$

2.2.2 Voltage interaction perspective

A given power system can be separated into some non-overlapping voltage-control areas comprising coherent bus groups. A set of buses can be classified as a voltage-control area if they are sufficiently uncoupled electrically, from its neighboring areas. The controllable reactive power in the area should be enough to master the voltage changes at the buses in the area.

As mentioned in [38] and later used in [49, 50, 51], electrical distance measures the voltage interactions between different buses of the system. With the usual hypothesis of the active-reactive decoupled system, the reactive model is written as

$$[\Delta Q] = \left[\frac{\delta Q}{\delta V}\right][\Delta V], \tag{2.21}$$

or

$$[\Delta V] = \left[\frac{\delta V}{\delta Q}\right][\Delta Q], \tag{2.22}$$

where $\left[\frac{\delta Q}{\delta V}\right]$ is part of power flow Jacobian matrix and $\left[\frac{\delta V}{\delta Q}\right]$ is its inverse.

Electrical distance between bus i and bus j is defined as

$$D_{ij} = D_{ji} = -log(\alpha_{ij} \cdot \alpha_{ji}), \tag{2.23}$$

where $\alpha_{ij} = \frac{(\delta V_i/\delta Q_j)}{(\delta V_j/\delta Q_j)}$ represents normalized voltage attenuation on bus i with respect to the perturbation at bus j. In practice, the matrix $\left[\frac{\delta V}{\delta Q}\right]$ can be approximated by the inverse of the system susceptance matrix $[B']$, which is with the rows and columns corresponding to PV buses.

2.2.3 Steady state perspective

2.2.3.1 Reactive Power support capability-based Index (RPSC)

In [52], an index is proposed to estimate the reactive power support capabilities that load buses can obtain from generation units in a power system by using the reactive power capacities of generation units and the electrical distances between load buses and generation units. The electrical distances between loads and generation units can be derived based on reactive power equations. In a power system with N_g generation units and N_d loads, the reactive power at bus i can be represented as

$$Q_i = V_i \sum_{j=1}^{N_g+N_d} V_j \Big[G_{ij} sin(\delta_i - \delta_j) - B_{ij} cos(\delta_i - \delta_j) \Big],$$

$$i = 1, \ldots, N_g + N_d,$$

where V_i and δ_i are the voltage magnitude and angle of the i^{th} bus respectively; G_{ij} is the real part of the negative of the branch admittance between buses i and j; G_{ii} is the sum of real parts of all branch admittances connected to the i^{th} bus; B_{ij} is the imaginary part of the negative of the branch admittance between buses i and j; and B_{ii} is the sum of imaginary parts of all branch admittances connected to the i^{th} bus. Reactive power change at the generator and load buses can be represented as

$$\begin{bmatrix} \Delta Q_G \\ \Delta Q_D \end{bmatrix} = - \begin{bmatrix} B_{GG} & B_{GD} \\ B_{DG} & B_{DD} \end{bmatrix} \begin{bmatrix} \Delta V_G \\ \Delta V_D \end{bmatrix}, \tag{2.24}$$

where B_{GG}, B_{GD}, B_{DG} and B_{DD} are the sub-matrices in the susceptance matrix, which is the imaginary part of the bus admittance matrix.

Therefore the electrical distances between loads and generation units can be presented as

$$\Delta Q_G = D \cdot \Delta Q_D, \tag{2.25}$$

where

$$D = B_{GD} B_{DD}^{-1}, \tag{2.26}$$

and the elements (i, j) of D (i.e. $|d_{ij}|$) represents the electrical distance between the j^{th} load and i^{th} generation unit. The larger $|d_{ij}|$ means j^{th} load and i^{th} generation unit are electrically closer. Furthermore, $|d_{ij}|$ is also the reactive power distribution factor, which indicates the reactive power that i^{th} generation unit distributes to the j^{th} load when a unit of reactive power change occurs at the j^{th} load. A larger $|d_{ij}|$ means that the i^{th} generation unit distributes more reactive power to the j^{th} load than the other generation units when a unit of reactive power change occurs at the j^{th} load. Different techniques related to reactive power monitoring and calculations with respect to voltage stability criterion had been investigated in [53, 54, 55, 56].

2.2.3.2 Relative electrical distance-based index

The method presented by authors in [57] is used for allocating transmission transaction charges among users in transmission services for various combinations of power contracts. The method allocates the transaction charges over the participants/contracts based on the relative electrical distance i.e., the relative locations of load points with respect to the generator points in open access. The method is based on the fundamentals of the impact of transactions in a transmission system which are discussed in [58, 59, 60, 61].

The relative electrical distances (RED) is a representation of the relative locations of load nodes with respect to the generator nodes and is given by $[R_{LG}]$.

$$[R_{LG}] = 1 - abs\{[F_{LG}]\}, \tag{2.27}$$

where

$$[F_{LG}] = -[Y_{LL}]^{-1}[Y_{LG}],$$

and Y_{LL} and Y_{LG} are partitioned portions of network Y-bus matrix obtained from the equation given below.

$$\begin{bmatrix} I_G \\ I_L \end{bmatrix} = \begin{bmatrix} Y_{GG} & Y_{GL} \\ Y_{LG} & Y_{LL} \end{bmatrix} \begin{bmatrix} V_G \\ V_L \end{bmatrix}, \tag{2.28}$$

where I_G, I_L and V_G, V_L represent complex current and voltage vectors at the generator nodes and load nodes.

The elements of $[F_{LG}]$ matrix are complex and its columns correspond to the generator bus numbers and rows correspond to the load bus numbers. This matrix gives the relation between load bus voltages and source bus voltages. It also gives information about the location of load nodes with respect to generator nodes that is termed as relative electrical distance between load nodes and generator nodes.

2.2.3.3 Generation shift factor-based index

When performing power market studies, the most accurate approach would be to model the transmission system using a full AC implementation, including the impacts of all germane contingencies. However, for a large network this can be computationally prohibitive for long-term market simulations. The use of DC power flow model reduces the computation drastically. In [62, 63, 64, 65], the authors use the concept of GSF in order to define the proximity of a bus to a tie-line.

GSF is defined by the change in power flows on a line due to the change in the injection at a generator bus, and a corresponding withdrawal at slack generator. GSF is based on change in phase angles with respect to bus injections and change in line flows with respect to phase angles. Hence, GSFs can be considered as the impact of bus injections on tie-line flows. The DC load flow model in matrix form is given by

$$P = [B]\delta,$$

where, P is the power vector of net injection where each element represents the individ-

ual power injection, $[B]$ is the susceptance matrix and δ is the vector of phase angles of the respective buses.

GSF of tie-line ab with respect to bus i can be calculated using elements of inverse of susceptance matrix as shown in equation below

$$g_{ab,i} = \frac{\bar{X}_{a,i} - \bar{X}_{b,i}}{x_{ab}}, \tag{2.29}$$

where $g_{ab,i}$ is the GSF of tie-line ab with respect to bus i, $\bar{X}_{a,i}$ and $\bar{X}_{b,i}$ are the elements of inverse of susceptance matrix and x_{ab} is the reactance of tie-line ab.

2.2.4 Average Electrical Distance-based Index

In [66], authors present a novel technique to define the distance of a bus from a tie-line which is used in clustering the buses to reduce the computational effort required for market analysis. As compared to the full AC analysis, a simplified analysis of the network can be done by using full network DC power flow model. But due to the scale of power systems, full network DC analysis still remains to be computationally taxing. As an alternative, various network equivalence models have been used to analyze the electricity market where the buses are aggregated on the basis of electrical distances. Average Electrical Distance (AED) is defined as the average of electrical distances from a particular bus to the two buses of the tie-line of interest.

$$d_{ab,i} = \frac{|Z_{th,ai} - Z_{th,bi}|}{2}, \tag{2.30}$$

where $d_{ab,i}$ is the AED of a bus i from a tie-line ab and $Z_{th,ai}$ is given by

$$Z_{th,ai} = Z_{aa} - 2Z_{ai} + Z_{ii}. \tag{2.31}$$

Electrical distance between two buses is represented by the equivalent impedance between the same buses. In the equation above, Z_{aa}, Z_{ai} and Z_{ii} are the elements of impedance matrix of the network.

2.2.5 Electromagnetic transient perspective

Electromagnetic transients (EMTs) are fast transients caused by switching operation and as a result produces transient overvoltage. The property of EMTs is such that the steady-state phasor respresentation is not possible and hence instantaneous voltage and current variables are considered. Additionally, the initial status for voltages and currents are steady state variables result from the power flow simulation. On the other hand, in the case of extreme and accurate EMT models which need more than traditional parameters, reduced and equivalent representation illustrates the main electromagnetic behavior of a branch switching.

In the assessment of the time responses of electromagnetic transients in single or multi-phase networks, Dommel in [67] formulated a method of solving networks by nodal admittance matrix which was pursued later in [68, 69, 70, 71]. The formulation is based on the method of characteristics for distributed parameters and the trapezoidal rule of integration for lumped parameters. The method of characteristics and the trapezoidal rule can easily be combined into a generalized algorithm capable of solving transients in any network with distributed as well as lumped parameters. Numerically this leads to the solution of a system of linear (nodal) equations in each time step.

Starting from initial condition at $t = 0$, the state of the system is found at $t = \Delta t, 2\Delta t, 3\Delta t, \ldots$ until the maximum time t_{max} for the particular case has been reached. While solving for the state at t, the previous states at $t - \Delta t, t - 2\Delta t, \ldots$ are known. With a record of this past history, the equations of both methods can be represented by simple equivalent impedance networks. A nodal formulation of the problem is shown below from these networks.

A solution for transients is necessarily a step-by-step procedure that proceeds along the time axis with a variable or fixed step width Δt. Based on this, equivalent impedance networks are used to describe different elements in the system.

- ***Lossless Line:*** Considering a lossless line with inductance L' and capacitance C' per unit length. Then at a point x along the line voltage and current are related by

$$-\frac{\partial e}{\partial x} = L'\Big(\frac{\partial i}{\partial t}\Big),$$
$$-\frac{\partial i}{\partial x} = C'\Big(\frac{\partial e}{\partial t}\Big).$$

Considering the voltage at node m at time $t - \Delta t$ remains same as that at node

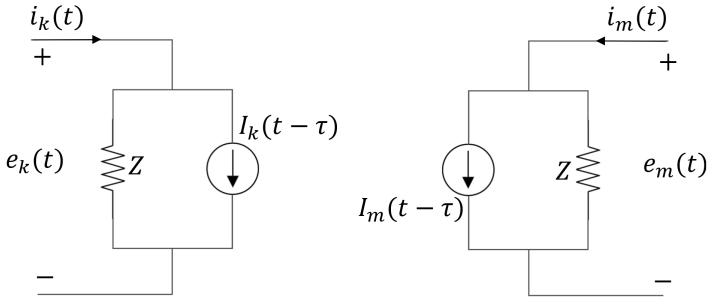

Fig. 2.2: Lossless line equivalent impedance network

k at time t, the line can be seen as a two-port network. With equivalent current sources I_k and I_m which are known at state t from the past history at time $t-\Delta t$,

$$I_k(t-\Delta t) = -\Big(\frac{1}{Z}\Big)e_m(t-\Delta t) - i_{m,k}(t-\Delta t), \tag{2.32}$$

$$I_m(t-\Delta t) = -\Big(\frac{1}{Z}\Big)e_k(t-\Delta t) - i_{k,m}(t-\Delta t). \tag{2.33}$$

Equations (2.32) and (2.33) describe the corresponding equivalent impedance network. Topologically, the terminals are not connected; the conditions at the other end are only seen indirectly and with a time delay Δt through the equivalent current sources $I_k(t-\Delta t)$ and $I_m(t-\Delta t)$.

- ***Inductance:*** For the inductance L of a branch km and consider the equivalent current source $I_{k,m}$ is known for past history, which yields $I_{k,m}(t-\Delta t)$ between the nodes k and m given in (2.34).

$$I_{k,m}(t-\Delta t) = i_{k,m}(t-\Delta t) + \Big(\frac{\Delta t}{2L}\Big)(e_k(t-\Delta t) - e_m(t-\Delta t)). \tag{2.34}$$

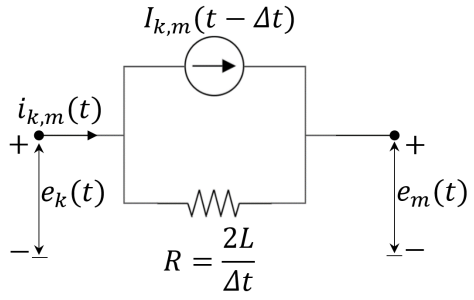

Fig. 2.3: Inductance equivalent impedance network

- ***Capacitance:*** Similar relation is derived for capacitance C of branch km

$$I_{k,m}(t-\Delta t) = -i_{k,m}(t-\Delta t) - \left(\frac{2C}{\Delta t}\right)(e_k(t-\Delta t) - e_m(t-\Delta t)). \tag{2.35}$$

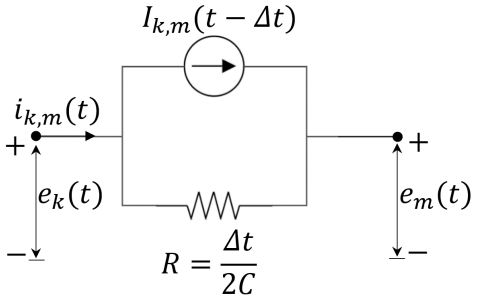

Fig. 2.4: Capacitance equivalent impedance network

- ***Resistance:*** For completeness the branch equation for the resistance is also added

$$i_{k,m}(t) = \left(\frac{1}{R}\right)(e_k(t) - e_m(t)). \tag{2.36}$$

- ***Nodal equations:*** With all network elements replaced by equivalent impedance networks, it becomes very simple to establish the nodal equations for any arbitrary system. The result is a system of linear algebraic equations in (2.37) that describes the state of the system at time t.

$$[Y][e(t)] = [i(t)] - [I], \tag{2.37}$$

where $[Y]$ is nodal conductance matrix, $[e(t)]$ is column vector of node voltages at time t, $[i(t)]$ is column vector of injected node currents at time t, $[I]$ column vector of known equivalent current sources.

The real symmetric conductance matrix $[Y]$ remains unchanged as long as Δt remains unchanged. It is, therefore, preferable, to fix the time step width at Δt. The formation of $[Y]$ follows the rules for forming the nodal admittance matrix in steady-state analysis.

2.2.6 Modeling of load

Stable operation of a power system depends on the ability to continuously match the electrical output of generating units to the electrical load on the system. The modeling of loads is complicated because of composition of each load comprising large number of devices. It is a common practice to represent the composite load characteristics as seen from the bulk power delivery points [72]. The load models are traditionally classified into two major categories: static models and dynamic models.

2.2.6.1 Static load models

A static load model represents the load characteristics as algebraic function of bus voltage magnitude and frequency at an instant [72]. The active and reactive power components of the load can be determined on the basis of initial operating conditions by the exponential model as shown in (2.38).

$$\begin{aligned} P &= P_0(\bar{V})^a, \\ Q &= Q_0(\bar{V})^b, \\ \bar{V} &= \frac{V}{V_0}, \end{aligned} \tag{2.38}$$

where P_0, Q_0 and V_0 represents the initial operating values for each variable respectively. The parameters a and b represents whether the load model has constant power,

constant current or constant impedance characteristics ranging 0, 1 or 2 respectively. For composite system loads, the voltage dependency is shown through a polynomial model mentioned in (2.39).

$$\begin{aligned} P &= P_0[p_1\bar{V}^2 + p_2\bar{V} + p_3], \\ Q &= Q_0[q_1\bar{V}^2 + q_2\bar{V} + q_3]. \end{aligned} \tag{2.39}$$

This models is referred to as ZIP model since it is composed of constant impedance, constant current and constant power components.

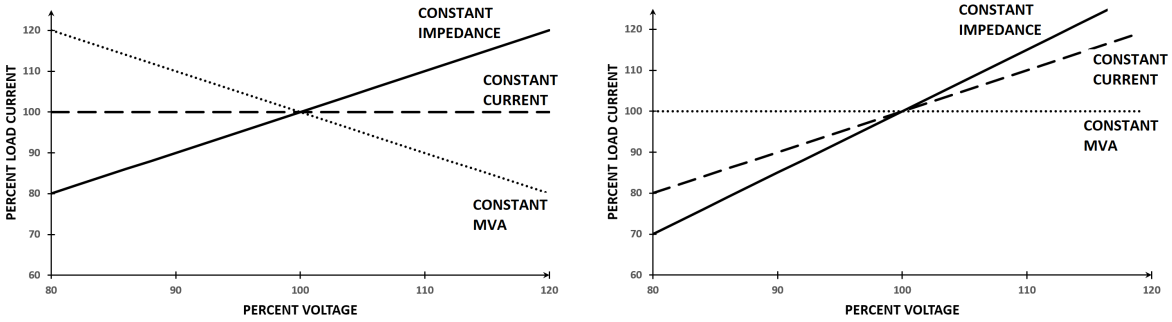

(a) Relationship between load current and bus voltage

(b) Relationship between load MVA and bus voltage

Fig. 2.5: ZIP load models [3]

The model for frequency dependency of load characteristics is obtained by including the frequency component in the voltage dependent ZIP model and is shown in (2.40).

$$\begin{aligned} P &= P_0[p_1\bar{V}^2 + p_2\bar{V} + p_3](1 + K_{pf}\Delta f), \\ Q &= Q_0[q_1\bar{V}^2 + q_2\bar{V} + q_3](1 + K_{qf}\Delta f), \end{aligned} \tag{2.40}$$

where Δf is the frequency deviation $(f - f_0)$. The bus frequency f is usually not a state variable in the system model used for analysis, therefore it is evaluated by computing the time derivative of the bus voltage angle.

2.2.6.2 Dynamic load models

The response of most composite loads to voltage and frequency changes is fast and the steady state of the response is reached very quickly. Hence the use of static models is

justified for such cases. There are, however, many cases which accounts for the dynamics of load components especially the dynamics of motors which is a significant aspect of system loads. Induction motors form the majority of motor loads across the power system network. Since there is no field winding in the induction motor, the cage rotor is modeled by two coils in quadrature while the armature is modeled by d- and q-axis armature coil. Since it does not rotate at synchronous speed, the two rotor equations include a rotational emf term proportional to the rotor slip speed $s\omega_s$. These equations are in the form given by (2.41).

$$\begin{aligned} v_d = 0 &= Ri_d + \dot{\Psi}_d - s\omega_s\Psi_q, \\ v_q = 0 &= Ri_q + \dot{\Psi}_q + s\omega_s\Psi_d, \end{aligned} \tag{2.41}$$

where slip $s = \frac{(\omega_s - \omega)}{\omega_s}$, Ψ_d and Ψ_q are the flux linkages.

2.2.6.3 Impact on electrical distance

The response of nearly all loads to voltage changes can be represented by some combination of constant impedance, constant current, and constant power devices. It is also important to recognize that the total active power of the motor load depends not only on the system frequency, but also on the rate of the frequency change which is evaluated by computing the time derivative of the bus voltage angle. Large induction motor loads can cause relatively severe instability conditions. Contrary to the active power, a major portion of which is consumed by load as systems are so designed and operated, the reactive power flow depend not only on component characteristics, but also on the network parameters between major buses and end-use devices.

2.2.7 Modeling of FACTS devices

The typical problems encountered in large interconnected transmission systems are with respect to voltage control, reactive power control, steady state and dynamic stability

as well as inter-area oscillations in an interconnected power system [73]. Apart from the steady-state considerations, a sudden change in real power demand in the power system can be observed due to rapid changes in reactive power and the corresponding voltage variations, caused by line switching, faults, load rejection, and various other disturbances. This rapid change in real power demand can cause some power generators to accelerate, and others to decelerate, from their steady-state synchronous speed resulting in transients in frequency and power angle which if gets worse can result in total loss of synchronism between the generators [74].

2.2.7.1 Static VAR systems

Static var systems are applied by utilities in transmission applications for several purposes. The primary purpose is usually rapid control of voltage at weak points in a network. CIGRE defines a static var system (SVS) as a coordinated combination of a static var compensator (SVC) and switching capacitors and reactors [75, 76]. Components of SVS may include thyristor-controlled reactors (TCRs), thyristor-switched reactors (TSRs), thyristor-switched capacitors (TSCs), mechanically-switched capacitors (MSCs) or reactors (MSRs).

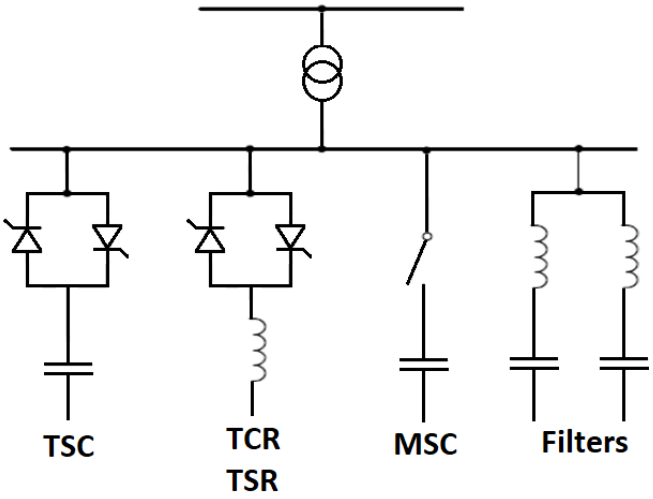

Fig. 2.6: Static VAR system structure

A typical SVS for transmission application is shown in Fig. 2.6. In the figure, the system is assumed to contain one TCR and two TSCs, along with a MSC. The TCR reactive power rating is typically slightly larger than the discrete TSC and MSC blocks which allows continuous (smooth) control over the entire SVS rating. In the active control range, reactive power is varied to regulate voltage according to the required voltage regulation and the requirement of compensating reactive power in the system. At the capacitive limit, the SVC becomes a shunt capacitor while at the inductive limit, it behaves as a shunt reactor [77].

2.2.7.2 Variable VAR generation

The dynamic reactive compensation in a system can be achieved by addition of supplementary reactive devices attached to the system. The major dynamic reactive requirements are in the areas of, (1) transient stability improvement, (2) power oscillation damping, (3) voltage support.

2.2.7.2.1 Thyristor controlled reactor: An elementary single-phase thyristor-controlled reactor (TCR) consists of a fixed reactor of inductance L, and a bi-directional thyristor switch. A typical TCR along with its associated waveform output is shown in Fig. 2.7.

The current in the reactor can be controlled and varied from maximum to zero by the function of switching thyristors using the method of firing delay angle control. This method of current control is illustrated in Fig. 2.7, where the reactor current $i_L(\alpha)$ and its fundamental component $i_{FL}(\alpha)$ are shown at various firing delay angles, α.

2.2.7.2.2 Thyristor switched capacitor: A single-phase thyristor-switched capacitor (TSC) is shown in Fig. 2.8. It consists of a capacitor, a bidirectional thyristor valve, and a relatively small surge current limiting reactor. This reactor is needed

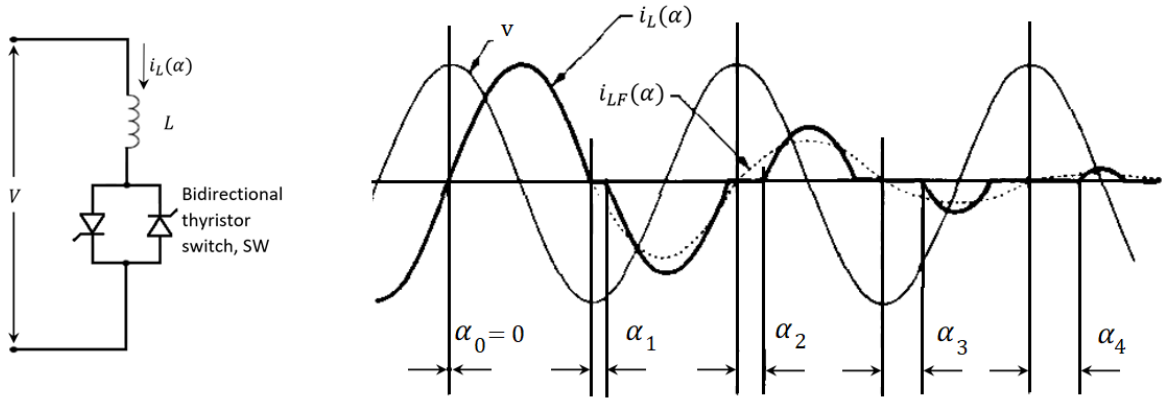

Fig. 2.7: Basic thyristor controlled reactor and associated waveforms

primarily to limit the surge current in the thyristor valve under abnormal operating conditions and may also be used to avoid resonances with the AC system impedance at particular frequencies.

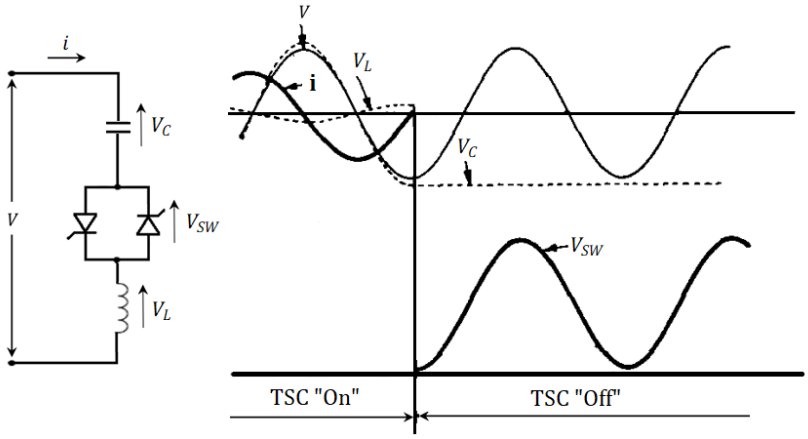

Fig. 2.8: Basic thyristor switched capacitor and associated waveforms

Under steady-state conditions, when the thyristor valve is closed and the TSC branch is connected to a sinusoidal AC voltage source, $v = V\sin\omega t$, the current in the branch is given by

$$i = V\frac{n^2}{n^2-1}\omega C\cos\omega t, \tag{2.42}$$

where,

$$n = \frac{1}{\sqrt{\omega^2 LC}} = \sqrt{\frac{X_C}{X_L}} \tag{2.43}$$

The TSC branch can be disconnected at any current zero by prior removal of the signal to the thyristor valve. At the current zero crossing, the capacitor voltage is at its peak value, $V = V_n^2/(n^2 - 1)$. The disconnected capacitor stays charged to this voltage and, consequently, the voltage across the non-conducting thyristor valve varies between zero and the peak-to-peak value of the applied AC voltage. This is illustrated in Fig. 2.8. Further, removal and re-connection of the capacitor may induce some transients which can be minimized if the thyristor valve is turned on at those instants at which the voltage across the thyristor is zero.

2.2.7.3 Static synchronous compensator

Static synchronous compensator (STATCOM) can be seen as a controllable reactive power, which can change voltage and current waveform of the inverter through power electronic means, and which also can improve the power quality [78]. STATCOM can be divided into two types of circuits namely: voltage-bridge circuit and current-bridge circuits. As shown in Fig. 2.9, the main circuit of STATCOM is composed of voltage-bridge circuit and the structure is composed of the following parts: the DC side capacitor, which plays a role in providing voltage support; voltage source converter (VSC), which constitutes self-commutating solid-state electronic switching devices such as GTOs/IGBTs. It uses a pulse width modulation (PWM) technology to control the power electronic switching. The primary objective of STATCOM is to obtain a harmonic free and controllable three-phase AC output voltage waveforms at the point of common interaction (PCI) to regulate reactive current flow by generation and absorption of controllable reactive power by the solid-state switching algorithm .

2.2.7.4 Unified power flow controller

Unified power flow controller (UPFC) can be described as a combination of a static synchronous compensator (STATCOM) and a static synchronous series compensator

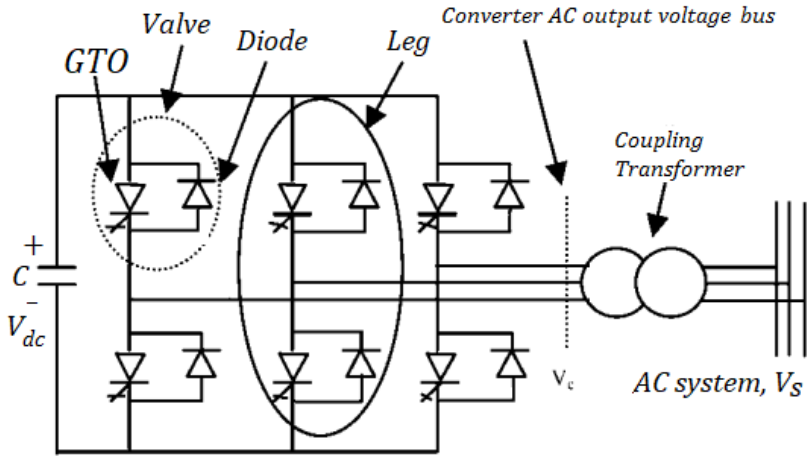

Fig. 2.9: Static synchronous compensator (STATCOM)

(SSSC). It can provide the benefits of both, shunt connected FACTS device as well as that of series connected FACTS device and most of all it can also provide active power flow control. The steady state power flow control using a UPFC is attained by injecting a voltage with controllable magnitude and phase angle in series with the line via series inverter. The UPFC injection model is derived enabling three parameters to be simultaneously controlled namely, shunt reactive power, the magnitude, and the angle, of injected series voltage [79, 80]. Sub-synchronous resonance mitigation in UPFC is carried out by modulating the real power flowing through the DC link capacitor. Figure (2.10) shows the structure of UPFC.

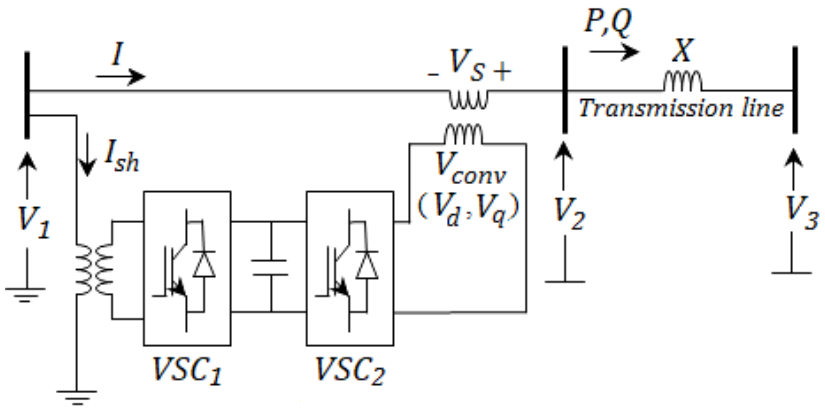

Fig. 2.10: Unified power flow controller (UPFC)

UPFC along with the many benefits has limitations. For example, the real power series voltage injection will be limited when the UPFC is operating in a STATCOM mode. As the series transformer is in the line, the leakage reactance of the series transformer adds to the series line impedance, which the UPFC is compensating. High and low operating voltage limitations on the bus will limit the effective range of the UPFC.

2.2.7.5 HVDC

HVDC power transmission systems and technologies associated with the FACTS continue to advance as they make their way to commercial applications [81]. HVDC, like FACTS, were also based initially on thyristor technology and more recently on fully controlled semiconductors and voltage-source converter (VSC) topologies. The ever increasing penetration of the power electronics technologies into the power systems is mainly due to the continuous progress of the high-voltage high power fully controlled semiconductors [82]. The current HVDC installations employ two major technologies, (1) line commutated current source converters (CSCs) that use thyristors, and (2) Forced commutated voltage source converters (VSCs) that use IGBTs.

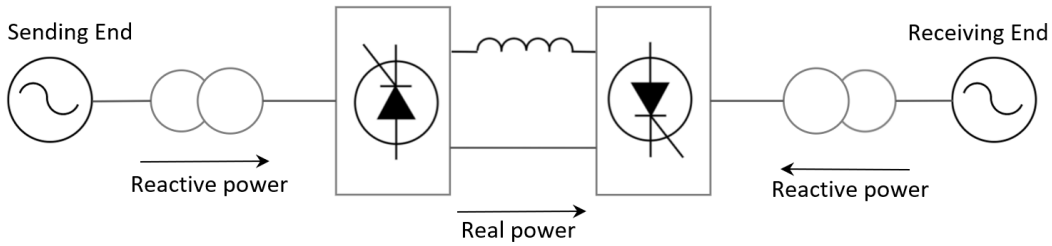

Fig. 2.11: HVDC system based on CSC technology with thyristors.

In a general setting of two AC voltage sources shown in Fig. 2.13 connected via a reactor where one voltage is generated by the VSC and the other one is the voltage of the AC system the active and reactive powers are defined by the relationships given by (2.44) and (2.45). The relationships are based on the fundamental frequency and assuming

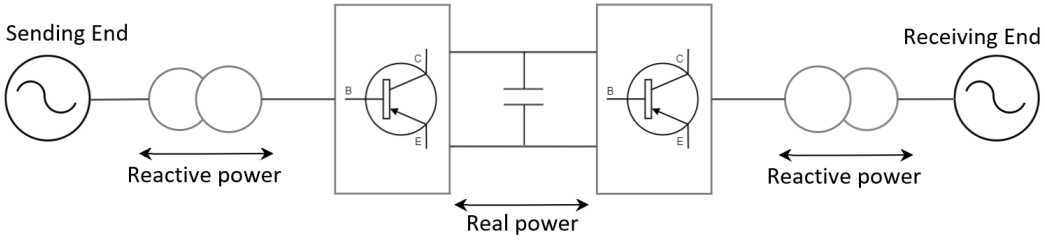

Fig. 2.12: HVDC system based on VSC technology built with IGBTs.

that the reactor between the converter and the AC system is ideal (i.e. lossless).

$$P = \frac{V_s \sin \delta}{X_L} V_r, \tag{2.44}$$

$$Q = \frac{V_s \cos \delta - V_r}{X_L} V_r, \tag{2.45}$$

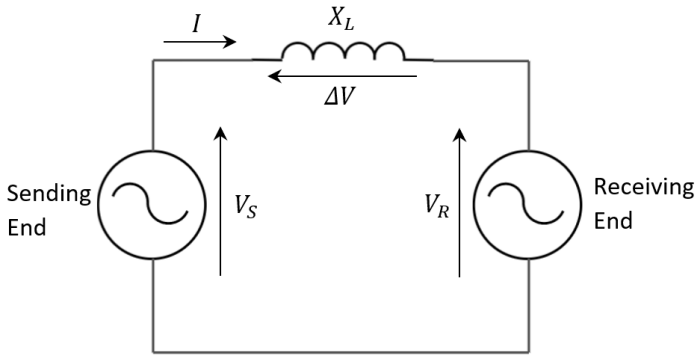

Fig. 2.13: General setting of interaction of two sources.

2.2.8 Reduction of dynamic model of power system

As discussed in previous chapters and previous methods of network equivalencing using the concept of electrical distance, a power system can be divided into internal subsystems and external subsystems. The internal subsystem is modeled in detail while remainder of the system is approximated in order to simplify the computational requirements. The model reduction methods can be further divided into three groups: 1) *Physical reduction*,

which requires the electrical distance parameter in order to determine the proximity from the area of disturbance; 2) *Topological reduction*, eliminates certain nodes thus reducing the size of the equivalent network; 3) *Modal reduction*, uses linearized models of the external subsystem that neglects the unexcited modes.

The equivalent model is obtained using modal reduction in the form of a reduced set of linear differential equations [83]. This type of technique is rarely used in practice as it is difficult to achieve standardization of the technique in order to apply it to different operating scenarios.

Topological reduction, along with physical reduction, gives an equivalent model that retains the equivalent system elements. The topological reduction gives a good representation of the system static performance as well as the dynamic performance during the short time following a disturbance. The reduced model can therefore be used for load flow analysis and transient stability analysis when disturbances occur in the internal system.

2.2.8.1 Network transformation

Topological reduction is achieved by transforming a large network into an equivalent smaller network by either elimination or by aggregation of nodes.

2.2.8.1.1 Elimination of nodes: It is evident from the basis of analysis of structure of power network that the elimination of nodes from the network model must be done in such a way that currents and nodal voltages at the retained nodes are unchanged. The network is defined by nodal equation shown in (2.46).

$$\begin{bmatrix} I_R \\ I_E \end{bmatrix} = \begin{bmatrix} Y_{RR} & Y_{RE} \\ Y_{ER} & Y_{EE} \end{bmatrix} \begin{bmatrix} V_R \\ V_E \end{bmatrix}. \tag{2.46}$$

The equation shown above considers all the nodes with classification such as set of eliminated nodes given by {E} and set of retained nodes given by {R}. The eliminated

voltages and currents in (2.46) can be swapped to modify it to (2.47).

$$\begin{bmatrix} I_R \\ V_E \end{bmatrix} = \begin{bmatrix} Y_R & K_I \\ K_V & Y_{EE}^{-1} \end{bmatrix} \begin{bmatrix} V_R \\ I_E \end{bmatrix}. \tag{2.47}$$

where $Y_R = Y_{RR} - Y_{RE}Y_{EE}^{-1}Y_{ER}$, $K_I = Y_{RE}Y_{EE}^{-1}$, $K_V = -Y_{EE}^{-1}Y_{ER}$.

The nodal currents in the set {R} are given by

$$I_R = Y_R V_R + \Delta I_R, \tag{2.48}$$

where $\Delta I_R = K_I I_E$.

Eq. (2.48) refers to the relationship between the currents and voltages of the retained nodes in the reduced network. The matrix Y_R corresponds to a reduced equivalent network that consists of the retained nodes and equivalent branches linking them. This network is often referred to as the transfer network and the matrix describing it as the transfer impedance matrix. K_I gives a relation between the nodal currents from the eliminated nodes to the retained nodes and is known as distribution matrix. The method is illustrated in Fig. 2.14.

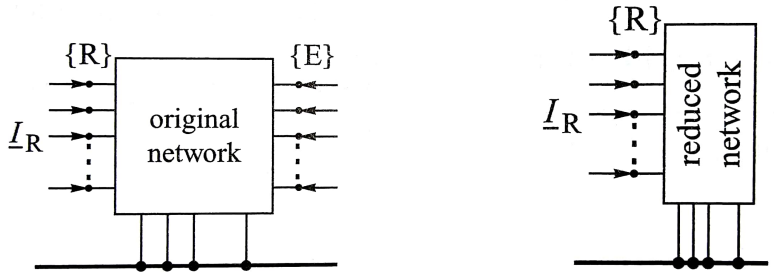

(a) Network before elimination **(b)** Network after elimination

Fig. 2.14: Elimination of nodes

2.2.8.1.2 Sparse matrix techniques: Sparse matrix techniques are used in order to reduce the complexity of elimination algorithm shown in (2.48) [84, 85]. This form is equivalent to Gauss elimination of a corresponding row and column from the admittance matrix.

For each eliminating node, k, of set {E}, the matrix Y_R is updated. This is given in (2.49) for each element Y_{ij}^{new} of matrix Y_R.

$$Y_{ij}^{new} = Y_{ij}^{old} - \frac{Y_{ik}Y_{kj}}{Y_{kk}}, \qquad \text{for } i \neq k, j \neq k, \tag{2.49}$$

where Y_{ij}^{old} is an element of matrix Y_{RR}.

It is worth noting that if nodes i and j are not adjacent to node k, then elimination of k does not modify the admittance matrix Y_{ij}. Also, self admittances of all the nodes adjacent to k are modified with the elimination of k. Therefore, while using sparse matrix techniques the order in which the rows/columns of a matrix are processed is important. Simple heuristic methods [86, 85] are used to carry out the node elimination techniques based on the following rules: 1) Nodes with least number of adjacent nodes are eliminated; 2) Nodes which introduce the least number of new connections are eliminated. Following these rules ensure that the elimination have a minimum impact on the structure of the power system and hence the equivalent network can be a closer representation to the full complex network.

2.2.8.1.3 Aggregation of nodes using Dimo's method: This method works on the principle of replacing a group of nodes by a single equivalent node, illustrated in Fig. 2.15. The author in [87] introduced this method by considering an aggregated node set {A} and assuming the presence of fictitious branches to the aggregated node set. The branch admittances to each node is chosen in such a way as to make the terminal voltage of all the branches equal. Subsequently, the terminal equipotential nodes are connected with a fictitious auxiliary node. The voltage at this fictitious node is zero, hence a negative admittance is added to the node which is given by

$$Y_{fa} = -\frac{S_a^*}{V_a^2}, \qquad \text{where } S_a = \sum_{i \in \{A\}} S_i, \tag{2.50}$$

and where f is the fictitious node and Y_{fa} is the negative admittance between node f and node a which is the equivalent node replacing the aggregated node set {A}. Eq.

(2.50) makes the voltage V_a at the equivalent node equal to the weighted average of the voltages at aggregated nodes V_i for $i \in \{A\}$. This weighted average is determined as shown in (2.51).

$$V_a = \frac{S_a}{I_a} = \frac{\sum_{i\in\{A\}} S_i}{\sum_{i\in\{A\}} \left(\frac{S_i}{V_i}\right)^*}. \tag{2.51}$$

This method produces a large number of fictitious branches and also the aggregation

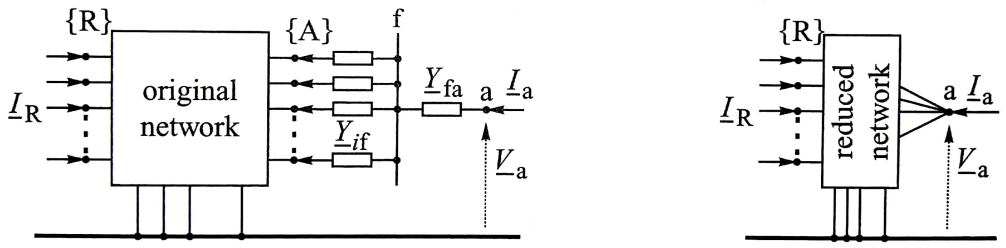

(a) Network with fictitious branches **(b)** Network after elimination/aggregation

Fig. 2.15: Node aggregation using Dimo's Method [4]

introduces a branch with negative impedance, these parameters if exist in a network after reduction may cause convergence problems. These discrepancies were eliminated by Zhukov's method [4].

2.2.8.1.4 Aggregation of nodes using Zhukov's method: This method of aggregation considers impact of voltage angle at the equivalent node which is a function of power injection at the aggregated node i and the inertia coefficient of the unit placed at aggregated node i. In this method, there is no change in admittances of the network branches hence it is not required to introduce fictitious branches as was the case in previous method. However, it does introduce fictitious shunt branches at the retained nodes.

As it is convenient to have equivalent branches of low resistances, the voltage angle δ_a at the equivalent node is assumed to be equal to the weighted average of voltage angles

at the aggregated nodes. This gives a following relation,

$$\delta_a = \frac{\sum_{i\in\{A\}} S_i\delta_i}{\sum_{i\in\{A\}} S_i}, \tag{2.52}$$

or

$$\delta'_a = \frac{\sum_{i\in\{A\}} M_i\delta'_i}{\sum_{i\in\{A\}} M_i}, \tag{2.53}$$

where S_i is the apparent power injection at the aggregated node i and $M_i = \frac{T_{mi}S_{ni}}{\omega_s}$ is the inertia coefficient of the unit installed at aggregated node i. Further since it introduces the shunt branches between the retained nodes, the diagonal element of Y_{RR} which is the sum of all the series and shunt branch admittances is given by

$$Y_{ii} = y_{i0} + \sum_{j\in\{R\}} y_{ij} + \sum_{k\in\{A\}} y_{ik} \quad \text{, for } i \in \{\text{R}\}, \tag{2.54}$$

where y_{i0} is the sum of admittances of all shunt branches connected to i and y_{ij} is the admittance of a branch linking nodes i and j. Hence it can be seen that Zhukov's method introduces some equivalent shunt admittances at the retained nodes {R}.

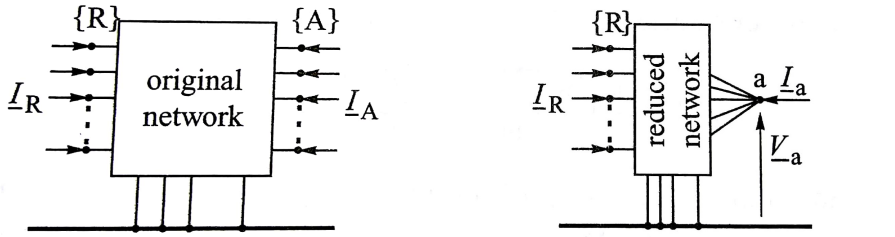

(a) Network before elimination **(b)** Network after aggregation

Fig. 2.16: Node aggregation using Zhukov's method [4]

2.2.8.1.5 Coherency: The prime reason for the dependence of admittances on voltage angle is due to the voltage transformation ratio $\vartheta = \frac{V_i}{V_a}$ between the aggregated nodes $i \in \{A\}$ and the equivalent node a. For any two nodes $i, j \in \{A\}$, the equivalent network obtained for an initial state is valid for other states only if the transformation ratio can

be assumed to remain constant, this is given by

$$\frac{V_i(t)}{V_j(t)} e^{j[\delta_i(t)-\delta_i(t)]} = \text{constant}, \qquad \text{for } i,j \in \{\text{A}\} \tag{2.55}$$

Nodes satisfying the condition in (2.55) are referred to as electrically coherent nodes. If the voltage magnitudes of the aggregated nodes are considered to be constant, the above condition simplifies to

$$\delta_i(t) - \delta_j(t) = \delta_{ij}, \qquad \text{for } i,j \in \{\text{A}\}, \tag{2.56}$$

For generator nodes the coherency condition can be expressed in a similar fashion as shown in (2.57).

$$\delta'_{ij}(t) = \delta'_i(t) - \delta'_j(t), \qquad \text{for } i,j \in \{\text{A}\}, \tag{2.57}$$

where δ_i refers to the rotor angle of the generator connected to node i.

In an operating condition, two generators are said to be coherent if their angular difference is constant within a certain tolerance limit, ϵ, over a certain time interval. As discussed earlier, the coherency-based technique which is based on the property of equal acceleration for coherent machines and focuses on the dynamic equivalence of a network. For the two machines i and j,

$$|\delta_{ij} - \delta^0_{ij}| \leq \epsilon,$$

where δ_{ij} and δ^0_{ij} are the angular differences between the machines at nodes i and j at any time and at initial time respectively. Then the coherency factor can be defined as

$$CF = \frac{max|\delta_{ij}|}{|\delta^s_{ij}|}, \tag{2.58}$$

For a machine i, the dynamic equation is

$$M_i \Delta\ddot{\delta}_i = \Delta P_{m,i} - \Delta P_{G,i}. \tag{2.59}$$

After simplifying, the relation is of the form

$$[M][\Delta\ddot{\delta}] = [M]^{-1}[Y][\Delta\delta]. \tag{2.60}$$

Here $[M]^{-1}[Y]$ is the Jacobian matrix J. This method compares only the elements of the Jacobian matrix to identify the coherent group. A normalized quantity β is defined such that

$$\beta = \frac{|j_{ij} - j_{ji}|}{\max(j_{ij}, j_{ji})}. \tag{2.61}$$

The term $|j_{ij} - j_{ji}|$ can be taken as a measure to estimate the relative variation between $\Delta\delta_i$ and $\Delta\delta_j$. When the moments of inertias M_i and M_y are equal, then $\beta = 0$, which means that the machines are perfectly coherent.

Also, from the DC model in matrix form, the network power flow can be simplified and represented as

$$P = [B]\delta,$$

where P is the power vector of net injection where each element represents the individual power injection. $[B]$ is the susceptance matrix and δ is the vector of phase angles of the respective buses.

Hence, it can be clearly seen that the sensitivity is given by the elements of the Jacobian matrix J and the coherency is observed on the basis of factors such as moment of inertias of the machines as well as on the network admittance.

2.2.8.2 Equivalent model of external subsystem

The process of forming an equivalent model of the external subsystem involves the reduction of the number of nodes. The number of load nodes are either completely eliminated or aggregated to equivalent nodes while generator nodes are aggregated into small groups represented by equivalent nodes based on the coherency of the generators connected to those nodes. The elimination/aggregation is done using the methods described in previous section. In summary, there are certain assumptions that are needed to create dynamic equivalent model which are as follows:

1 Elimination of the load nodes in the external subsystem.

2 Identification of coherent groups of generators in the external subsystem.

3 Aggregation of the coherent groups.

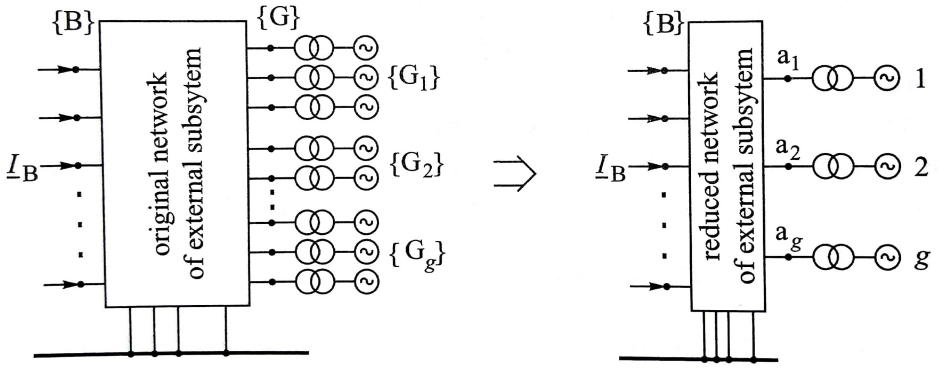

Fig. 2.17: Model reduction of the external system

Fig. 2.17 shows the aggregation of coherent group of generator nodes and illustrates the whole process of forming an equivalent model of the external subsystem.

2.2.9 Remarks

Distance from a power systems perspective is discussed on the basis of various parameters and sensitivities of those parameters with respect to the varying operating conditions. As discussed, EMD is a concept of evaluating the electro-mechanical disturbance propagation between generators which considers the dynamic properties of the machines and their behavior during transient period. Their dynamic behavior with respect to other generators in the network give a relative measure of proximity as described in (2.9) and (2.10), and also defines the coherency of the generators using the coherency factor in (2.12) and EMD measure in (2.17) and (2.18). Coherency of buses is also investigated on the basis of voltage interactions between different buses of the system which reactive power controlled and is shown in (2.23). From the steady-state

operation perspective, the representation of proximity of loads from the generation units on the basis of reactive power supply is discussed using (2.26). Proximity of load nodes from the generator nodes is also shown using relative electrical distance in (2.27) but the basis of this measure is the sensible allocation of transmission charges across the network. Apart from these measures, GSFs and AEDs presents unique measure of impact of a bus on a tie-line, these are shown in (2.29) and (2.30). Further electromagnetic transient perspective of the system is based on structure variables and the initial status of the network. For each element, an equivalent network is setup on the basis of steady state operating conditions. Load modeling on the basis of static and dynamic models are also based on the initial operating conditions and uses an exponential model.

The reduction of dynamic model of power system highlights the significance of electrical distance in order for reduction/aggregation of nodes in the network and hence the structure of the network. Further, the coherency of various generators can be seen as a relation between the angular difference of the machines and electrical distance between them. This ensures the recognition of coherent generators that can be aggregated together to be represented by a single unit.

The electrical distances as seen from power systems perspective are classified in Table 2.2 highlighting significant properties and applications.

Table 2.2: Classification of electrical distance estimation from a power systems perspective

	Electro-Mechanical Distance Perspective	Voltage Interaction Perspective	Steady State Perspective
Measure/ Index	Reflection distance, Coherency Factor, EMD, C-EMD	Voltage Interaction	RPSC, RED, GSF, AED
Similarities	1. Gives the sensitivity index of a network 2. The proximity of the buses across the network is based on various operating parameters and not entirely on the network structure		
Differences	Takes into account the dynamical effect of a generator apart from the electrical perspective when a network is subject to any disturbance	Based on the voltage changes dependent on the controllable reactive power in the area	Defines the proximity of buses relative to other elements in the network in a steady state operation condition
Applications	The development of dynamic electro-mechanical equivalents had been applied to transient stability programs	This finds its application in determining optimum location of installing voltage control facilities to allow better control of voltage profile and segregating areas voltage-control areas by controlling the prices of reactive power services	Most of the electrical distance concepts are used to aggregate the network and reduce the computational load in making decisions on a day-to-day basis such market analysis, generation redispatch, load shedding etc.

CHAPTER 3

Introduction to structural analysis from networks perspective

3.1 Introduction to structural analysis

A main part of the analytical foundation of power system analyses is based on electric circuit theories such as Kirchhoff's current law (KCL) and Kirchhoff's voltage law (KVL). Using these laws, many models have been built including those for individual components as well as the network ones for power systems that involves different components. Also, electric circuit theories and concepts have been used to develop various analytical and numerical methods to address planning and operational issues such as those associated with steady-state, electro-dynamics, electromagnetic transients and economics. These models are electric circuit-based mathematical representations of the power systems and their components. The variables used include state variables, control variables and structure related variables that are used together to describe the characteristics of the components and systems.

Although the individual components models (even high order dynamic models) are much simplified ones, due to the dimension of power systems, particularly bulk power transmission systems, a power system model could be quite complicated and high dimensional. Moreover, because of the non-linearity of the components, a system model normally is complex and could be ill-defined. Therefore, the model is not only time-consuming to analyze, it is very likely to fail to represent some important characteristics of the system. Given the requirements from optimal objectives of planning or operation, as well as changing operating conditions in real-time, the complexity and the curse of dimensionality may present a great challenge to power system analysis, particularity those related to the dynamic and transient issues in real-time power system control and

operation. Furthermore, many power system components such as transformers exhibit non-linear electromagnetic behavior which influence system dynamics and transient disturbances [88]. It is believed that true power system behavior can be better modeled by increasing the level of model details and the order, thus the main efforts of power system analysis will heavily rely on developing advanced solvers to deal with the model complications.

The power system analysis using the complex network theory focuses on two major aspects of power grids, one is network structure and the other is weight of connecting edges. The weight of an edge corresponding to a line in a power grid network is normally represented by the impedance of the line. This representation gives vital information regarding the structure but it may not reflect all the details of the model as some of the variables such as control, load levels and generation outputs are not considered. Using complex network theory has been somewhat controversial and not fully understood in power system analysis. Nevertheless, recent studies including those mentioned above have shown that it might be a promising approach for power system analysis particularly for understanding overall behavior of power system network such as cascading failures and for instances when there is a requirement for quick analysis involving fast computation.

Structural analysis can be seen as one of the network approaches but it is different from the existing approaches as per the following aspects:

1 Identification of critical components based on key information related to changing states of power systems in real-time operations;

2 Ability to analyze dynamic issues in real-time operations;

3 Modifications to electrical distance definition from different perspectives.

These aspects allow the system to be represented in a more appropriate way and hence allow for a better analysis under various circumstances. One of these aspects, namely

electrical distance, has proven to be of great importance especially the manner in which it is defined which can have major impact on structural representation of a power system. In addition, network dynamics play a significant role in representation of the operating power system network. It is important to use the original topology in structural representation when dealing with dynamics of the system. Any reduction in network topology including load buses can result in approximation of the assessment of dynamics in system network. However, the structural analysis from networks perspective discussed in this thesis present an underlying similarity in the analysis of systems which is also explained from port-Hamiltonian formalism.

3.2 Network dynamics described by network models

Network dynamics of a system can be explained on the basis of different perspective based models such as steady-state, electromagnetic transient, and electro-mechanical dynamic models. The structural respresentation of such models are highlighted in this chapter.

One such study of dynamics of power systems is presented in [89] which deals with the preservation of network topology in dynamic and transient stability analyses. The authors highlight the disadvantage of reduction in network topology and its impact on stability assessment. Like the rest of the highlighted methodologies, the authors in this study considers the model of the power system based on the basic load flow equations that preserves the information related to the load connected to the buses without having to assume them as impedance which are absorbed by the transmission network. This is reflected by the non-linear characteristic of the impedance based on the power-angle relationship.

Once the power-angle relationship has been established, the graph of the network is considered to be planar and branches are oriented on the basis of associated reference directions. The direction itself is governed by the angle difference between the two buses

across the transmission line. The model generated through this methodology can be seen as an analogous non-linear resistive network. This model is still simple to analyze but contains the dynamic information of the operation. These considerations ensure the maintenance of system integrity for dynamic analysis.

The structural representation of the dynamic system model can be derived based on the above set of dynamic equations, normally used for construction of energy functions for stability analysis. The energy of the system can described on the basis of Lagrangian and Hamiltonian framework, whereas electrical power system is described based on network topology. Specifically, variables representing the dynamical behavior of the system in (3.1) can also be explained from the structure perspective. The impact of inertia constant, H, on the behavior of the system shows that it is part of the structure while mechanical power, P_m, also has an impact but it remains constant. Also from (3.2), it can be observed that electrical power, P_e, is defined by structure elements such as conductance, G_{ij}, and susceptance, B_{ij}. Hence it becomes evident that these variables are part of the structure and can thus be used for structural representation of the dynamical system.

$$\frac{2H}{\omega_s}\frac{d^2\theta_m}{dt^2} = P_m - P_e, \tag{3.1}$$

where H is the inertia constant, θ_m is the angular position of the rotor with respect to a stationary axis, P_m is the mechanical power and P_e is electrical power. Here the electrical power, P_e, represents the net real power at bus i and can be defined as shown in (3.2).

$$P_i = V_i \sum_{j=1}^{n} V_j(G_{ij}\cos(\delta_i - \delta_j) + B_{ij}\sin(\delta_i - \delta_j)), \tag{3.2}$$

$$Q_i = V_i \sum_{j=1}^{n} V_j(G_{ij}\sin(\delta_i - \delta_j) - B_{ij}\cos(\delta_i - \delta_j)), \tag{3.3}$$

where P_i and Q_i represent the net active power and reactive power injected at bus i respectively, G_{ij} is the real part of the element in the bus admittance matrix corresponding to the i^{th} row and j^{th} column, B_{ij} is the imaginary part of the element in the admittance matrix corresponding to the i^{th} row and j^{th} column.

3.3 Explanation of structural analysis using port-Hamiltonian formalism

The physical systems have historically been analyzed on the basis of Lagrangian and Hamiltonian framework, whereas analysis of complex physical systems such as electrical power system requires a network point of view. The framework of port-Hamiltonian systems combines the original framework by associating it with the network structure. The port-Hamiltonian systems are open dynamical systems which can interact with their environment through ports and are a representation of the energy in a particular network [90]. The electric network can be formulated as a port-Hamiltonian system. In order to formulate such system, let us discuss the representation of classical Hamiltonian equations in the form of port-Hamiltonian system.

The port-Hamiltonian systems are a representation of energy exchange of a system with the surroundings. Such systems can be described by standard Hamiltonian equations and can be used in various energy exchange scenarios.

Standard Hamiltonian equations for a system in general form are given as

$$\dot{q} = \frac{\partial H}{\partial p}(q,p), \tag{3.4}$$

$$\dot{p} = -\frac{\partial H}{\partial q}(q,p) + B(q)f, \quad f \in \mathbb{R}^m, \tag{3.5}$$

where the Hamiltonian $H(q,p)$ is the total energy of the system, $q = (q_1, \cdots, q_k)^T$ are generalized configuration coordinates for the mechanical system with k degrees of freedom, $p = (p_1, \cdots, p_k)^T$ is the vector of generalized momenta, and $B(q)f$ denotes the generalized forces resulting from the input $f \in \mathbb{R}^m$. The state space of the above system with local coordinates (q,p) is called the phase space. The conservation of energy defines

the output of system as $e = \dot{q}$, hence output equation (1.2) can be redefined as

$$e = B^T(q)\frac{\partial H}{\partial p}(q,p) = B^T(q)\dot{q}, \quad e \in \mathbb{R}^m. \tag{3.6}$$

A further generalization is to consider systems which are described in local coordinates as

$$\dot{x} = J(x)\frac{\partial H}{\partial x}(x) + g(x)f, \quad f \in \mathbb{R}^m \tag{3.7}$$

$$e = g^T(x)\frac{\partial H}{\partial x}(x), \quad e \in \mathbb{R}^m \tag{3.8}$$

where $J(x)$ is an $n \times n$ matrix with entries depending smoothly on x,

For a network with n_L inductors and n_C capacitors, the network topology of the system is summarized in the so-called interconnection matrix $D \in \mathbb{R}^{n_C \times n_L}$ that has entries in {-1, 0, 1} and describes the interconnection of the inductors and capacitors. In particular, we associate with each capacitor a node (bus) and with each inductor an edge (branch) and define the matrix D as the incidence matrix with entries

$$d_{ij} = \begin{cases} 0 & \text{if node } i \text{ is not connected to branch } j, \\ 1 & \text{if current in branch } j \text{ is directed away from node } i, \\ -1 & \text{if current in branch } j \text{ is directed towards node } i. \end{cases} \tag{3.9}$$

It is worth noting that the incidence matrix in power systems is defined as the transpose of the matrix D. The total electric energy in the network is given by the Hamiltonian

$$\begin{aligned} H(q,\varphi) &= \sum_{i=1}^{n_C} \frac{q_i^2}{2C_i} + \sum_{j=1}^{n_L} \frac{\varphi_i^2}{2L_i}, \\ &= \frac{1}{2}\begin{bmatrix} q^T & \varphi^T \end{bmatrix}\begin{bmatrix} C^{-1} & 0 \\ 0 & L^{-1} \end{bmatrix}\begin{bmatrix} q \\ \varphi \end{bmatrix}, \end{aligned} \tag{3.10}$$

where C_i is the capacitance of the i^{th} capacitor, L_j is the inductance of the j^{th} inductor

and $C = diag(C_1 \cdots C_{n_C})$ and $L = diag(L_1 \cdots L_{n_L})$. $q(t) \in \mathbb{R}^{n_C}$ and $\varphi(t) \in \mathbb{R}^{n_L}$ are vectors of capacitor charges and inductor fluxes at time t respectively.

Defining the skew symmetric matrix J by

$$J = \begin{bmatrix} 0 & D \\ -D^T & 0 \end{bmatrix}.$$

Then the electric dynamics of the network can be represented in the Hamiltonian form

$$\begin{bmatrix} \dot{q} \\ \dot{\varphi} \end{bmatrix} = J \nabla H(q, \varphi),$$

where $\nabla H(q, \varphi) = \begin{bmatrix} C^{-1}q \\ L^{-1}\varphi \end{bmatrix}$ is the gradient of $H(q, \varphi)$. Consequently,

$$\begin{bmatrix} \dot{q} \\ \dot{\varphi} \end{bmatrix} = \begin{bmatrix} 0 & DL^{-1} \\ D^T C^{-1} & 0 \end{bmatrix} \begin{bmatrix} q \\ \varphi \end{bmatrix}. \tag{3.11}$$

The system is non dissipative and the total energy is conserved, i.e.

$$H(q(t), \varphi(t)) = H(q(0), \varphi(0)),$$

for all times $t \geq 0$.

If we add resistive elements to the network the equations are modified to take the form

$$\begin{bmatrix} \dot{q} \\ \dot{\varphi} \end{bmatrix} = (J - R) \nabla H(q, \varphi),$$

where the positive semidefinite matrix R is obtained from the resistive elements and the system interconnections. In this case the total energy satisfies

$$H(q(t), \varphi(t)) = H(q(0), \varphi(0)) - \int_0^t \nabla H^T(q(s), \varphi(s)) R \nabla H(q(s), \varphi(s)) ds.$$

It can be noted that $H(q(t), \varphi(t))$ is decreasing as a function of time, i.e. energy is dissipated.

To add dynamic loads and disturbances to the network, let us add voltage sources that are connected in series with inductors and current sources that connected in series with capacitors. Then the system equations become

$$\begin{bmatrix} \dot{q} \\ \dot{\varphi} \end{bmatrix} = (J - R)\nabla H(q, \varphi) + B \begin{bmatrix} v(t) \\ i(t) \end{bmatrix}, \tag{3.12}$$

where $v(t) \in \mathbb{R}^{m_v}$ and $i(t) \in \mathbb{R}^{m_i}$ are vectors of voltage and current source and $B \in \mathbb{R}^{(n_C+n_L)\times(m_v+m_i)}$. Note that $m_v \leq n_L$ and $m_i \leq n_C$. If currents are defined through voltage sources and the voltages across current sources as output $y(t)$, it can be shown as

$$y(t) = \begin{bmatrix} i^v(t) \\ v^i(t) \end{bmatrix} = B^T \nabla H(q(t), \varphi(t).$$

In this case the total energy satisfies

$$H(q(t), \varphi(t)) = H(q(0), \varphi(0)) - \int_0^t \nabla H^T(q(s), \varphi(s)) R \nabla H(q(s), \varphi(s)) ds + \int_0^t (v^T(s) i^v(s) + i^T(s) v^i(s)) ds. \tag{3.13}$$

Here in (3.13), the net Hamiltonian energy at time t is defined as the change in energy from the initial state due to the internal energy dissipation and the interaction with the environment in the presence of control sources in the network. Therefore, the Hamiltonian system can be represented as a Dirac structure with different ports representing different energy flow. The Dirac structure is shown in Fig. 3.1.

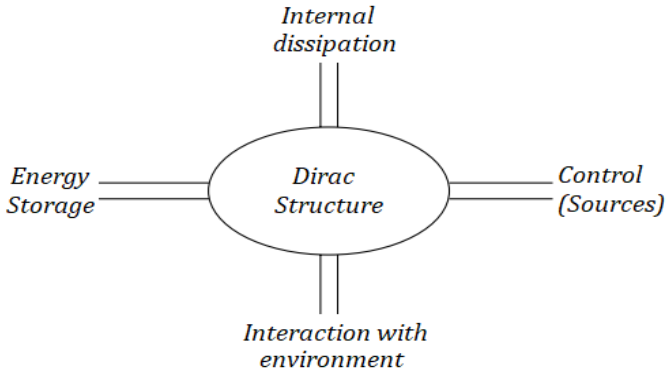

Fig. 3.1: Dirac structure

Considering the autonomous equation (3.11) and defining the change of coordinates, we get

$$\begin{bmatrix} q \\ \varphi \end{bmatrix} = \begin{bmatrix} \sqrt{C} & 0 \\ 0 & \sqrt{L} \end{bmatrix} \begin{bmatrix} \hat{q} \\ \hat{\varphi} \end{bmatrix}.$$

Here $\sqrt{C}$ is the diagonal matrix with $\sqrt{C_i}$ on the diagonal. Then it is straightforward to see that

$$\begin{bmatrix} \dot{\hat{q}} \\ \dot{\hat{\varphi}} \end{bmatrix} = \begin{bmatrix} 0 & \hat{D} \\ -\hat{D}^T & 0 \end{bmatrix} \begin{bmatrix} \hat{q} \\ \hat{\varphi} \end{bmatrix},$$

where $\hat{D} = (\sqrt{C})^{-1} D (\sqrt{L})^{-1}$. The matrix $\hat{D}$ has entries that are either zero or have the form $\frac{\pm 1}{\sqrt{C_i L_j}}$ in entry (i, j). The Hamiltonian now has the form

$$H(\hat{q}, \hat{\varphi}) = \frac{1}{2}(\|\hat{q}\|^2 + \|\hat{\varphi}\|^2)$$

The matrix

$$\hat{A} = \begin{bmatrix} 0 & \hat{D} \\ -\hat{D}^T & 0 \end{bmatrix}$$

is skew symmetric and has all eigenvalues on the imaginary axis and a full set of eigenvectors. Let $\lambda = i\theta$ be a non-zero eigenvalue of $\hat{A}$ with eigenvector $v = \begin{bmatrix} v_1 \\ v_2 \end{bmatrix}$. Then

$$\hat{D} v_2 = \lambda v_1,$$

$$-\hat{D}^T v_1 = \lambda v_2.$$

From these equations,

$$\hat{D}\hat{D}^T v_1 = -\lambda^2 v_1 = \theta^2 v_1,$$

and

$$v = \begin{bmatrix} v_1 \\ v_2 \end{bmatrix} = \begin{bmatrix} v_1 \\ -\frac{1}{\lambda}\hat{D}^T v_1 \end{bmatrix} = \begin{bmatrix} I \\ \frac{i}{\theta}\hat{D}^T \end{bmatrix} v_1.$$

If $n_C \neq n_L$ matrix $\hat{A}$ will have eigenvalues at zero. If $n_C < n_L$ the matrix $\hat{D}$ has

non-trivial null space and if $v_2 \in N(\hat{D})$ the vector $v = \begin{bmatrix} 0 \\ v_2 \end{bmatrix}$ is an eigen vector.

Similarly, if $n_C > n_L$ the matrix $\hat{D}^T$ has non-trivial nullspace and if $v_1 \in N(\hat{D}^T)$ the vector $v = \begin{bmatrix} v_1 \\ v_2 \end{bmatrix}$ is an eigen vector. Let $v = \begin{bmatrix} v^1 & \cdots & v^{n_C+n_L} \end{bmatrix}$ be an orthogonal matrix of eigen vectors of $\hat{A}$. Then

$$\hat{A} = V \Lambda V^*,$$

where $\Lambda = diag(\lambda_1, \cdots, \lambda_{n_C+n_L})$ and * denotes the complex conjugate transpose. Let $2m$ be the number of non-zero eigenvalues of $\hat{A}$. Then

$$\begin{aligned} e^{\hat{A}t} &= V e^{\Lambda t} V^*, \\ &= \sum_{j=0}^{n_C+n_L} e^{\lambda_j t} v^j (v^j)^*, \\ &= \sum_{j=0}^{2m} e^{\lambda_j t} v^j (v^j)^* + \sum_{j=2m+1}^{n_C+n_L} v^j (v^j)^*, \\ &= \sum_{j=0}^{m} (e^{i\theta_j t} v^j (v^j)^* + e^{-i\theta_j t} v^{-j} (v^{-j})^*) + \sum_{j=2m+1}^{n_C+n_L} v^j (v^j)^*, \\ &= \sum_{j=0}^{m} \begin{bmatrix} v_1^j & 0 \\ 0 & \frac{1}{\theta_j} \hat{D}^T v_1^j \end{bmatrix} \begin{bmatrix} \cos\ \theta_j t & \sin\ \theta_j t \\ -\sin\ \theta_j t & \cos\ \theta_j t \end{bmatrix} \begin{bmatrix} v_1^j & 0 \\ 0 & \frac{1}{\theta_j} \hat{D}^T v_1^j \end{bmatrix}^T + \sum_{j=2m+1}^{n_C+n_L} v^j (v^j)^*. \end{aligned} \tag{3.14}$$

The natural frequencies of the system are given by the square roots of the non-zero eigenvalues of the matrix $\hat{D}\hat{D}^T$.

Now considering the non-autonomous system with current and/or voltage source inputs, it has the following form in $\begin{bmatrix} \hat{q} \\ \hat{\varphi} \end{bmatrix}$ coordinates which is given by the state equations

$$\begin{bmatrix} \dot{\hat{q}} \\ \dot{\hat{\varphi}} \end{bmatrix} = \begin{bmatrix} 0 & \hat{D} \\ -\hat{D}^T & 0 \end{bmatrix} \begin{bmatrix} \hat{q} \\ \hat{\varphi} \end{bmatrix} + \hat{B} \begin{bmatrix} v \\ i \end{bmatrix}, \tag{3.15}$$

with output

$$y(t) = \begin{bmatrix} i^v \\ v^i \end{bmatrix} = \hat{B}^T \nabla H(\hat{q}, \hat{\varphi}).$$

A power system in steady state is driven by coherent synchronous generators at a fixed frequency. In particular, the inputs and loads (dynamic and resistive) are such that in steady state (3.13) can be modified as shown below.

$$-\int_0^t \nabla H^T(q(s), \varphi(s)) R \nabla H(q(s), \varphi(s)) ds + \int_0^t (v^T(s) i^v(s) + i^T(s) v^i(s)) ds = 0.$$

Thus the energy of the system is constant. Consider the dynamical equation with only current sources $i(t)$. The resistance matrix is assumed to affect only the lines/branches and not the bus/node shunt capacitances. In this case the system equations are

$$\begin{aligned} \begin{bmatrix} \dot{q} \\ \dot{\varphi} \end{bmatrix} &= \left(\begin{bmatrix} 0 & D \\ -D^T & 0 \end{bmatrix} - \begin{bmatrix} 0 & 0 \\ 0 & R_2 \end{bmatrix} \right) \begin{bmatrix} C^{-1} & 0 \\ 0 & L^{-1} \end{bmatrix} \begin{bmatrix} q \\ \varphi \end{bmatrix} + \begin{bmatrix} 0 & B_{12} \\ -B_{21} & 0 \end{bmatrix} \begin{bmatrix} 0 \\ i(t) \end{bmatrix}, \\ &= \begin{bmatrix} 0 & DL^{-1} \\ D^T C^{-1} & R_2 L^{-1} \end{bmatrix} \begin{bmatrix} q \\ \varphi \end{bmatrix} + \begin{bmatrix} B_{12} i(t) \\ 0 \end{bmatrix}. \end{aligned} \tag{3.16}$$

The steady state sinusoidal input currents are given by

$$i_j(t) = I_j^{max} cos(\omega t + \theta_j) = \mathrm{Re}(I_j e^{j\omega t}),$$

where $I_j = I_j^{max} e^{j\theta_j}, j = 1, \cdots, m_i$. Also, charge across the capacitors and flux in the inductors are given by

$$q(t) = \mathrm{Re} \begin{bmatrix} q_1 e^{j\delta_1} & & \\ \vdots & & e^{j\omega t} \\ q_{n_c} e^{j\delta_{n_c}} & & \end{bmatrix} = \mathrm{Re}(e^{j\delta} q e^{j\omega t}) = \mathrm{Re}(Q e^{j\omega t}),$$

$$\varphi(t) = \mathrm{Re}(e^{j\alpha} \varphi e^{j\omega t}) = \mathrm{Re}(\Phi e^{j\omega t}),$$

where $e^{j\delta} = diag(e_1^{j\delta}, \cdots, e_{n_C}^{j\delta})$ and $q = \begin{bmatrix} q \\ \vdots \\ q_{n_C} \end{bmatrix}$.

From (3.16), we get

$$j\omega \begin{bmatrix} Q \\ \Phi \end{bmatrix} = \begin{bmatrix} 0 & DL^{-1} \\ D^T C^{-1} & R_2 L^{-1} \end{bmatrix} \begin{bmatrix} Q \\ \Phi \end{bmatrix} + \begin{bmatrix} B_{12} I \\ 0 \end{bmatrix}.$$

Since $X_L = \omega L$ and $X_C = (\omega C)^{-1}$, it yields

$$\begin{bmatrix} Q \\ \Phi \end{bmatrix} = \begin{bmatrix} 0 & -jDX_L^{-1} \\ jD^T X_C & jR_2 X_L^{-1} \end{bmatrix} \begin{bmatrix} Q \\ \Phi \end{bmatrix} + \begin{bmatrix} \frac{-j}{\omega} B_{12} I \\ 0 \end{bmatrix}.$$

Further for k^{th} bus/node with a complex power injection given by S_k^{in}, the power can be defined as shown below.

$$\begin{aligned} S_k^{in} &= (I^{in})_k^* V_k = (B_{12} I)_k^* V_k = (B_{12} I^*)_k V_k, \\ &= \Big(\sum_{l=1}^{m_i} B_{12}^{kl} I_l^* \Big) V_k, \\ &= \Big(\sum_{l=1}^{m_i} B_{12}^{kl} I_l^{max} e^{-j\theta_l} \Big) v_k e^{j\delta_k}, \\ &= \sum_{l=1}^{m_i} B_{12}^{kl} I_l^{max} e^{j(\delta_k - \theta_l)}, \\ &= \sum_{l=1}^{m_i} B_{12}^{kl} I_l^{max} cos(\delta_k - \theta_l) + j \sum_{l=1}^{m_i} B_{12}^{kl} I_l^{max} sin(\delta_k - \theta_l), \\ &= P_k^{in} + jQ_k^{in}. \end{aligned}$$

For a system in steady state, the net real and reactive power as well as the bus voltage magnitudes and angles can be known for all generator and load buses from the load flow analysis. This implies that the net power for buses with no external generator or load is zero and the voltage magnitude and angle can be determined from the steady state equations. In particular, let N_{C_i} be the subset of buses that are connected to a generator or load. Clearly, N_{C_i} has m_i elements and for any $k \in N_{C_i}$, the k^{th} row of B_{12} is non-zero. For $k \in N_{C_i}$, the balance equations are

$$S_k^{in} = (I^{in})_k^* \bar{V_k} = P_k^{in} + jQ_k^{in} = \bar{P_k} + j\bar{Q_k},$$

where $\bar{V_k}$, $\bar{P_k}$ and $\bar{Q_k}$, $k \in N_{C_i}$ are supplied by the load flow analysis. Assume that each

generator and/or load is connected to exactly one bus. Then for each $k \in N_{C_i}$ there exists an l_k such that $B_{12}^{kl_k} \neq 0$ and $B_{12}^{kl_k} \neq 0$, $l \neq l_k$. Consequently,

$$P_k^{in} = \bar{v_k} B_{12}^{kl_k} I_{l_k}^{max} cos(\bar{\delta_k} - \theta_{l_k}) = \bar{P_k},$$

$$Q_k^{in} = \bar{v_k} B_{12}^{kl_k} I_{l_k}^{max} sin(\bar{\delta_k} - \theta_{l_k}) = \bar{Q_k}.$$

These are $2m_i$ equations for the $2m_i$ unknowns $I_{l_k}^{max}$ and θ_{l_k}, $k \in N_{C_i}$ and that completely specify the current source at all source nodes. From the above relations of real and reactive powers, we get

$$tan(\bar{\delta_k} - \theta_{l_k}) = \frac{\bar{Q_k}}{\bar{P_k}},$$
$$(I_{l_k}^{max})^2 = \frac{\bar{P_k^2} + \bar{Q_k^2}}{(\bar{v_k} B_{12}^{kl_k})^2}.$$

For a nominal system, selection of the generator and load sources to be modeled as current sources of fixed frequency, magnitudes and phase angles are given by the above relationship. It can be noted that this model does not allow any dynamics in the system frequency, i.e. the generator swing dynamics are not included. This shows that port-Hamiltonian system can be used as a representation of steady-state power system with interaction related to the energy transfer.

Explanation of matrix $\hat{D}\hat{D}^T$

Let the matrix D have entries d_{ij}. Then $\hat{D}$ has entries $\frac{d_{ij}}{\sqrt{C_i L_j}}$ and

$$\begin{aligned}(\hat{D}\hat{D}^T)_{kl} &= \sum_{m=1}^{n_L} \hat{D}_{km}\hat{D}_{ml}^T \\ &= \sum_{m=1}^{n_L} \hat{D}_{km}\hat{D}_{lm} \\ &= \sum_{m=1}^{n_L} \frac{d_{km}}{\sqrt{C_k L_m}} \frac{d_{lm}}{\sqrt{C_l L_m}} \\ &= \frac{1}{\sqrt{C_k C_l}} \sum_{m=1}^{n_L} \frac{d_{km} d_{km}}{L_m}\end{aligned}$$

The kl entry is non-zero if some branch is connected to both nodes k and l. Clearly,

the diagonal entries of $\hat{D}\hat{D}^T$ are non-zero as long as D does not have a zero row (i.e. every node is connected to at least one branch). It can be noted that a non-zero entry $(\hat{D}\hat{D}^T)_{kl}$ has the form $\frac{1}{CL}$ where C is the geometric average of the capacitances of nodes k and l and $\frac{1}{L}$ is the average of the inverse of branch inductances that connect nodes k and l. Assuming that at most one branch connects any two nodes then a non-zero kl entry has the form

$$(\hat{D}\hat{D}^T)_{kl} = \frac{1}{\sqrt{C_k C_l}} \sum_{m=1}^{n_L} \frac{d_{k\hat{m}} d_{l\hat{m}}}{L_{\hat{m}}}$$

where $\hat{m}$ is the branch that connects k and l and $k \neq l$. When $k = l$

$$(\hat{D}\hat{D}^T)_{kl} = \frac{1}{\sqrt{C_k C_l}} \sum_{m=1}^{n_L} \frac{d_{km}^2}{L_m}$$

Note that for the matrix $\hat{D}\hat{D}^T$,

$$(\hat{D}\hat{D}^T)_{kk} - \sum_{l \neq k} (\hat{D}\hat{D}^T)_{kl} \neq 0$$

and consequently $\hat{D}\hat{D}^T$ is not a graph Laplacian matrix. However, if we let $x = \sqrt{C}1$, where 1 is the vector of all ones, then we have

$$\hat{D}\hat{D}^T x = \hat{D}\hat{D}^T \sqrt{C}1 \tag{3.17}$$

$$= (\sqrt{C})^{-1} D (\sqrt{L})^{-1} (\sqrt{L})^{-1} D^T 1 = 0 \tag{3.18}$$

since each row of D^T has exactly one element $+1$, one element -1, and the rest 0. The matrix $\sqrt{C}\hat{D}\hat{D}^T\sqrt{C} = DL^{-1}D^T$ is the Laplacian matrix corresponding to the weighted graph of the electric network with branch/line weights $\frac{1}{L_i}$. The Laplacian matrix here corresponds to the structure representation of the power system which highlights the dependency of various parameters in the system on network connections or structure.

3.4 Remarks

This chapter describes network dynamics using models based on different perspectives such as steady-state, electromagnetic transient, and electro-mechanical dynamic mod-

els. The chapter uses port-Hamiltonian formalism to view the system as open-dynamical systems that can interact with the surrounding environment. Such formulation allows the system to include the dynamics in Hamiltonian form which makes it easier to separate the state variables from the structure parameters. Consequently, the structure matrix J highlights the underlying similarity in different networks with the elements varying with the components present in the system. The study primarily highlights the underlying similarity of different types of networks and the possibility of applying structural analysis to such networks. The analysis in this chapter is further used in presenting the electric circuit foundation of structural analysis in Chapter 5.

CHAPTER 4

Investigation of electrical distance in power system analysis

The analysis of distance from different perspectives for networks and operating power systems is done by evaluation of different scenarios from a networks perspective which essentially gives the sensitivity of different network parameters. This chapter extracts the specific distance calculations with the classification from different perspectives.

4.1 Electrical distance calculations

4.1.1 General description

4.1.1.1 Steady state condition

Electrical distance metric in steady state operating conditions can be defined as an intuitive measure where the distance between two nodes is the equivalent Thevenin impedance between them which is the parallel combination of all impedance paths connecting them.

1 *Thevenin impedance*:

Electrical Distance can be calculated directly from the system's Z_{bus} matrix, which is simply the matrix inverse of the system's Y_{bus} matrix, which describes the fundamental topology of the electrical system connections, corresponding to the Laplacian matrix for general networks. As defined in (2.31), the electrical distance between two buses a and i is given by

$$Z_{ai}^{th} = Z_{aa} + Z_{ai} - 2Z_{ii}, \tag{4.1}$$

where Z_{ai} denotes the element in the a^{th} row and i^{th} column of the Z_{bus} matrix and is the mutual impedance between buses a and i.

While Thevenin impedance defines the distance between two buses, average electrical distance in [66] defined in (2.30) gives a perspective of electrical distance from a bus to a tie-line.

$$d_{ab,i} = \frac{|Z_{th,ai} - Z_{th,bi}|}{2}. \tag{4.2}$$

Equation (2.30) comprises of Thevenin impedances, which are elements from the Laplacian matrix which defines the structure of the system. Note that the Z^{th} distance is independent of system loading and can be calculated without power flow techniques. Crucially, it properly accounts for all the available current paths between two nodes. In networks, the impedance between nodes is approximated by summing impedances along the topologically shortest path.

2 *Power injection sensitivity*:

With power transfer being a significant part of any power system, it becomes imperative to analyze the impact of power injection and withdrawal with respect to the associated distance. Based on the load flow model, the GSF of tie-line ab with respect to bus i, introduced in [63] and discussed in Chapter 2 in (2.29), is given by

$$g_{ab,i} = \frac{\bar{X}_{a,i} - \bar{X}_{b,i}}{x_{ab}}, \tag{4.3}$$

where $\bar{X}_{a,i}$ and $\bar{X}_{b,i}$ are the elements of inverse susceptance matrix and x_{ab} is the reactance of line ab. The power injection at a bus has an impact on power flow in a tie-line which can be observed as sensitivity of power flow in a tie-line. There is a correlation between the impact and the electrical distance between the bus and the tie-line which is given by (2.29). The correlation refers to the increase in impact on line flows when a line and a bus are electrically closer to each other and hence an increase in impact on line flows can be seen as a decrease in net

impedance between the two.

3 *Load points*:

Another method that specifically considers the location of load points with respect to generation nodes is mentioned in [57]. For a system, (2.28) defines the relation between the currents and voltages at respective generator and load nodes as

$$\begin{bmatrix} I_G \\ I_L \end{bmatrix} = \begin{bmatrix} Y_{GG} & Y_{GL} \\ Y_{LG} & Y_{LL} \end{bmatrix} \begin{bmatrix} V_G \\ V_L \end{bmatrix}, \tag{4.4}$$

where I_G, I_L and V_G, V_L represent complex current and voltage vectors at the generator nodes and load nodes respectively. The matrix is the admittance matrix rearranged in the order of generation and load nodes. The location of load nodes with respect to the generator nodes is given by $[F_{LG}] = -[Y_{LL}]^{-1}[Y_{LG}]$. This gives a voltage relation perspective between load and generator nodes and thus voltage stability index is also defined which gives a relation of voltage level with respect to the loading in the system.

4 *Shunt-reactive power handling*:

A similar measure but with respect to the reactive power handling capability is defined in [52] where an index is proposed that load buses can obtain from generation units in a power system by using the reactive power capacities of generation units and the electrical distances between load buses and generation units. This is given by (2.24) in the form,

$$\begin{bmatrix} \Delta Q_G \\ \Delta Q_D \end{bmatrix} = - \begin{bmatrix} B_{GG} & B_{GD} \\ B_{DG} & B_{DD} \end{bmatrix} \begin{bmatrix} \Delta V_G \\ \Delta V_D \end{bmatrix}.$$

This equation gives a relation between the reactive power change (ΔQ_G and ΔQ_D) and the voltage change (ΔV_G and ΔV_D) at generation and load nodes respectively. Hence there is a direct correlation between these operating parameters, however these reactive power and voltage vectors are correlated through susceptance matrix

which defines the system structurally. Hence the structure also has an impact on the reactive support capabilities of generation units. From the susceptance matrix, the distance relation shown in (2.26) can be seen as similar to the electrical distance in a system with current and voltage relation, this relation can also be defined the distance as the ratio of reactive power change at generator and load nodes.

For steady state analysis of power system network, the following are the major impact variables in terms of electrical distance:

- *Impedance*;
- *Power injection with respect to the reference bus*;
- *Reactive power.*

4.1.1.2 Electro-mechanical dynamics

The concept of electro-mechanical distance measure reflects the interaction between machines during a disturbance occurrence in the system. In order to take into account the electro-mechanical effect of machines apart from electrical parameters, it is important to define the impact of machines with linear differential equations.

1 *Line admittances*:

For an electro-dynamical system, the electrical distance comprises of two elements; admittance distance which is the maximum of magnitudes of transfer admittance between two generators, and reflection distance which accounts for the dynamical effect of a generator onto the other generators. The admittance distance $Y_d(k)$ of generator $k \in \Omega$ with respect to a group of generators $i \in \Phi$ is

$$Y_d(k) = \max |Y_{ki}|, \tag{4.5}$$

where Y_{ki} represents the magnitude of the transfer admittance between generator k and generator i.

2 *Power-angle sensitivity*:

The definition of electrical distance directly takes into account the structure of the network by utilizing the admittance matrix, but the electrical distance from the electro-mechanical dynamical perspective must also utilize the dynamic behavior of machines which is captured by reflection distance between the machines and is presented in (4.6) and (4.7).

$$R_d(k) = \max_{f\in\phi}\Big\{\max_{i\in\phi}\frac{\Delta P_{ri}}{M_i}\Big\}, \qquad k \in \Omega, \tag{4.6}$$

where

$$\Delta P_{ri} = \frac{\partial P_{ik}}{\partial \delta_k}\Delta\delta_k. \tag{4.7}$$

In the formulation, reflection distance is a function of sensitivity of the electrical power of generator i with respect to the angle change in generator k and the angular momentum M_i of generator i which is a key in determining the impact of any change in angle of a generator in the network. In (4.6), the change in power ΔP_{ri} is limited by the change in angle of another generator. Further, the distance is defined as the ratio of change in power to angular momentum of the generator which gives a similar impact as seen with admittance in electrical networks.

The measure of maximum angular movement between two machines during a transient period is the EMD between the two machines [44]. The EMD is the measure of electro-mechanical interaction between the pair of machines. This interaction is defined by the Euclidean norm of change in power with respect to the angles.

3 *Inertia*:

Two generators with constant angular difference are said to be coherent and for these machines, the coherency factor given by (2.58) is

$$CF = \frac{max|\delta_{ij}|}{|\delta^s_{ij}|}. \tag{4.8}$$

Here the dynamics are a function of the Jacobian matrix J mentioned in 4.9 as $J = [M]^{-1}[Y]$.

$$[M][\Delta\ddot{\delta}] = [M]^{-1}[Y][\Delta\delta]. \tag{4.9}$$

From such electro-mehcanical dynamic perspective the sensitivity is clearly governed by the elements of Jacobian matrix J and is dependent on the moment of inertias and the admittance across the structure of the network.

For electro-mechanical analysis of power system network, the following are the impact variables in terms of electrical distance are the electrical variables as well as dynamical varibles related to physical movement of the generator:

- *Impedance*;
- *Power-angle*;
- *Inertia*.

4.1.1.3 Voltage interaction

The voltage variations in different buses i, j of the system defines the magnitude of interaction between them and hence the electrical distance. From Chapter 2, it is clear that the voltage variations ΔV_i, ΔV_j of the buses i, j respectively are related as

$$\Delta V_i = \alpha_{ij}\Delta V_j, \tag{4.10}$$

where $\alpha_{ij} = (\delta V_i/\delta Q_j)/(\delta V_j/\delta Q_j)$ represents normalized voltage attenuation on bus i with respect to the perturbation at bus j. The ratios $\delta V_i/\delta Q_j$ and $\delta V_j/\delta Q_j$ are elements of sensitivity matrix of the system.

Further the electrical distance between the buses is defined in (2.23) as

$$D_{ij} = D_{ji} = -log(\alpha_{ij} \cdot \alpha_{ji}). \tag{4.11}$$

Here, it can be seen that the electrical distance is the ratio of voltage attenuations due to the impact of buses onto the other buses. The voltage attenuation are dependent on the elements of Jacobian matrix or sensitivity matrix of the system.

4.1.1.4 Electromagnetic transients

The network defined for electromagnetic transient states consists of line elements such as resistances, capacitances and inductances. Although lossless lines are also defined. In a transient state, the resistance is independent of changing variables such as frequency thus the resistance can be used as it is. However, with changing frequency, the reactances of inductors and capacitors change and it is recommended to represent these elements with a constant equivalent resistance. The equivalent resistance in both the cases is represented in (4.12).

$$R = \frac{2L}{\Delta t}, \text{ and } R = \frac{\Delta t}{2C}. \tag{4.12}$$

The electrical distance here in such operating conditions can be determined by considering the initial state condition and thus representing the network elements by equivalent resistance.

4.1.2 Characterization of impact variable

4.1.2.1 Circuit-based variables

1 *Actual variables:*

The impact variables for a system operating in steady-state condition are the variables that exhibit the true state of the system. These variables include components of impedance such as resistance and inductor-or capacitor-based reactances. In transient conditions, the frequency of the system changes which may not have any impact on the resistance as it is independent of the operating frequency. However, any change in frequency brings a greater impact on the reactances, X_L or X_C

based on inductor or capacitor respectively, although the value of inductor (L) or capacitor (C) does not change.

2 *Approximate Variables:*

During a short-circuit, the steady-state reactance (X_d) is temporarily reduced due to the interaction of the magnetic flux between the damper windings and the armature windings in a generator. The complex magnetic flux interactions created by the small resistances and inductances (self and mutual) between the various elements (damper windings, field windings and rotor body) during a transient condition ultimately act to dramatically and suddenly reduce the machine's reactance. This reactance reduction is temporary, but its sudden drop allows much higher instantaneous short-circuit currents to form during the first few cycles of a fault. The reduced reactance is classified as transient reactance (X'_d) and sub-transient reactance (X''_d).

4.1.2.2 Mechanical-based variables

The impact variables for a system with electro-mechanical dynamics are power-angle and inertia and generator swing equations describe the dynamics of synchronous machines driven by the relationship between mechanical system (i.e. governor/turbine) and electric system. As mentioned in Chapter 2, the equation of motion of the machine rotor is given by

$$J\frac{d^2\theta}{dt^2} = T_m - T_e, \tag{4.13}$$

where J is the total moment of inertia of the rotor mass, T_m is the mechanical torque supplied by the prime mover, T_e is the electrical torque output of the alternator and θ is the angular position of the rotor. In steady state, the machine angular speed is equal to the synchronous speed and we get (3.1).

$$\frac{2H}{\omega_s}\frac{d^2\theta}{dt^2} = P_m - P_e. \tag{4.14}$$

Equation (4.14) describes the behavior of the rotor dynamics and hence is known as the swing equation. The angle δ is the angle of the internal emf of the generator and it dictates the amount of power that can be transferred. This angle is also called the load angle.

4.2 Interpretation of electrical distance

The interpretation of electrical distance in different settings and perspectives is shown in Fig. 4.1.

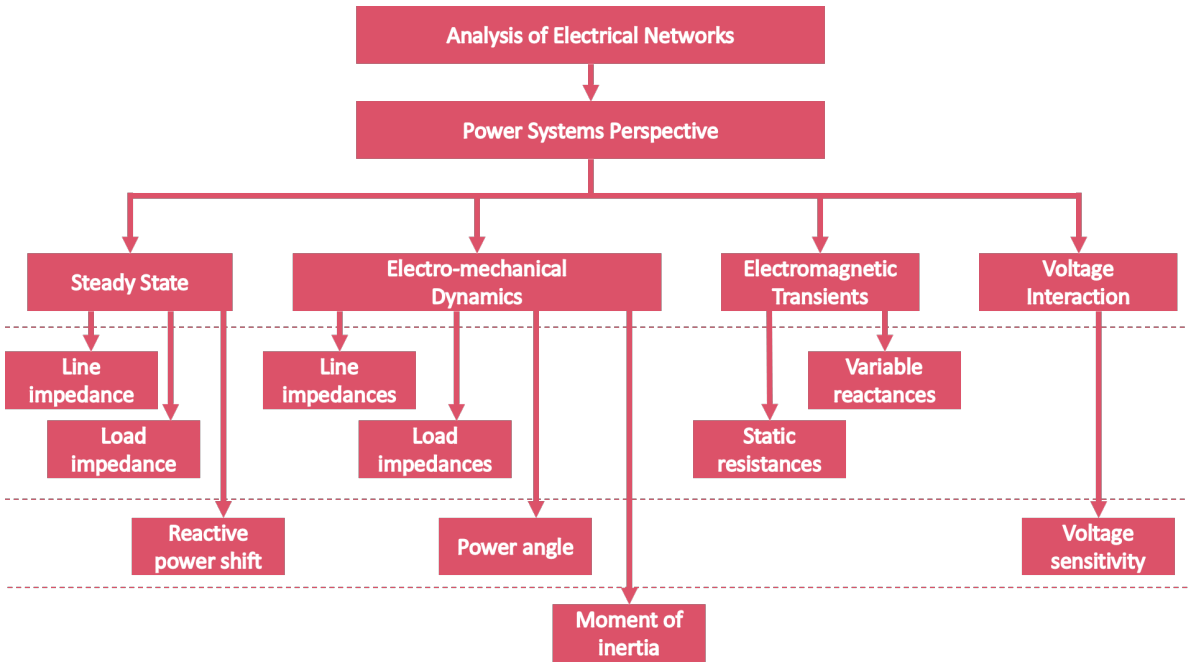

Fig. 4.1: Interpretation of electrical distance

4.3 Remarks

The distance as seen from a networks perspective has been broadly divided into categories defining the proximity of a bus on the basis of topology of the network and on the

basis of actual resistance distance. Further the distance measure from power systems perspective is investigated in order to understand the structure of the network on the basis of impact of various operating conditions on parameters defining the network. In the wake of such analysis, we analyze electro-mechanical distance perspective of a power system which takes into account the dynamical effect of a generator due to any change in another generator with in the proximity when a network is subject to any disturbance which is demonstrated in (2.9), (2.12), (2.17) and (2.18). Each definition of electrical distance represents the coherency of generators which can be simply seen as the power angle sensitivity of one generator with respect to the other. This in turn defines the structure of the network and enables us to identify the valid proximity of impact of each generator.

Electrical distance between different buses can be defined on the basis of voltage control capability of the buses in a network by controlling the reactive power. The rate of change of voltage with respect to reactive power, shown in (2.22), is the inverse of power flow Jacobian matrix and can be approximated by the impedance matrix which defines the structure of the network in terms of electrical distance from a networks perspective which is defined in (2.8). Distance from the steady-state operation perspective, in a similar fashion, can be concluded as the sensitivity with respect to various parameters in the operating system. Hence this can be correlated to the topological perspective of a network which employs electrical distance on the basis of network structure.

Electromagnetic transients studies often require detailed modeling of complex transmission networks. EMT models are based on structure variables as obtained during steady state operation and are taken as initial status of the network. Since transients require a step-by-step procedure starting at the initial condition and solving for the state at a certain time. This requires various parameters to be defined in a steady state form using respective equivalent networks. The system is represented as linear algebraic equations in (2.37). The nodal conductance matrix is the same as the nodal admittance matrix

in steady state analysis which strikes a similarity to the admittance matrix defined in the networks perspective as electrical distance measure for the nodes. Thus for EMT models, it becomes imperative to make the process iterative as the time progresses but uses the same concept of electrical distance as used in steady-state perspective.

As far as transient studies are concerned, there has always been a need for a correct representation of electrical loads in studies. Load characteristics affect the dynamic behavior of a power system, thus can have significant effects on the rates of acceleration or deceleration of individual generators during the fault, and therefore, on eventual stability of the system. Voltage dependency is shown to affect the real and reactive power in (2.39) and (2.40) such that the sensitivity associated with the operating variables provide a case to differentiate the operating nodes with a perspective of effective distance from a generation point. A study made in [91] shows cases in which decreasing the sensitivity of load to voltage in one area increased the tie-line power limit when the area was exporting power, but decreased it when the area was importing power [92]. Stability limits often decrease when active power changes from constant-impedance type toward constant-power type, especially in the cases where loads are at major load centers remote from generation. The impact of frequency decreases as the impedance increases between the generators. This shows a relation between the characteristics of electrical loads and the correlation with the structure of the network and associated electrical distance.

The reduction of dynamic models of power systems is based on the concept of electrical distance. This is achieved by elimination of nodes on the basis of impact on the network. The reduction/aggregation is done in such a way that currents and nodal voltages at the retained nodes remain unaltered. Further, the sparse matrix technique in (2.49) is used to reduce the complexity which utilizes the admittance matrix to assess the impact of each node. The reduction is based on the sensitivity of angular difference of the machines and electrical distance between them. This ensures the identification of

coherent generators that can be aggregated together to be represented by a single unit and hence resulting in efficient aggregation. This highlights the significance of electrical distance in reducing the network and even aggregating the coherent generators.

It is seen that port-Hamiltonian system framework is an open dynamical system and is a representation of the energy in a particular network. From the analysis of the matrix $\hat{D}\hat{D}^T$, it is obtained that matrix $DL^{-1}D^T$ is the Laplacian matrix corresponding to the weighted graph of the network. The elements of the Laplacian matrix serve as a parameter to define the electrical distance of the network nodes in terms of the graph energy of the underlying network.

The study of the existing power system analysis techniques done from a different perspective sheds light on the dependency of parameters sensitivities on the structure of the network and measures associated with it. Analyzing the power system from different perspective gives an insight on different sensitivities and associated relation to the concept of electrical distance. Specifically, EMT studies and modeling of load under transients require a completely different perspective of electrical distance which may not be very obvious. In conclusion, the concept of electrical distance can be correlated with sensitivity of different parameters under varying operating conditions of a power system.

CHAPTER 5

Electric circuit foundation of structural analysis for power systems from a network perspective

In this chapter, analytical foundations of structural analysis is provided by reviewing power system representation from various perspectives, such as steady-state, electromagnetic transient and electro-mechanical dynamic perspectives. Though from an electric circuit theory perspective, these models may differ with change in applications, they demonstrate an embedded consistency from structure perspective. Such formulation is based on port-Hamiltonian approach which represents the energy flow and has been discussed in Chapter 3. Further this chapter also highlights the significance of connection information and link strength in laying the foundation of structural analysis for power systems.

5.1 Background and related work

In this chapter, the analytical foundation of structural analysis based on the characteristics of power systems and some principles of network science is put forth. One of the important factors in structural analysis is the concept of link strength in power grids which is a new quantitative measure of grid connectivity developed based on electrical distances. It is known and has been highlighted in Chapter 2 that there are many definitions of electrical distance mentioned in the literature, [63, 64, 66, 93, 52, 2, 44, 48, 67, 68, 69, 71], but here the electrical distance is chosen with some modifications.

Specifically, [5] redefines, starting from the concept of complex networks, an electrical betweenness metric which considers several of specific features of power systems such as power transfer distribution and direction of power flow. It also accounts for vulnerability

assessment of power grid. This is shown through a study of vulnerability of a network when the network is attacked by removing critical components identified by electrical betweenness metric. Figure 5.1 shows the changes in voltages of 300-bus power systems under random line failures and intentional line attacks. The study highlights the understanding that consideration of electrical properties of power grids in topological assessments can be quite significant [5].

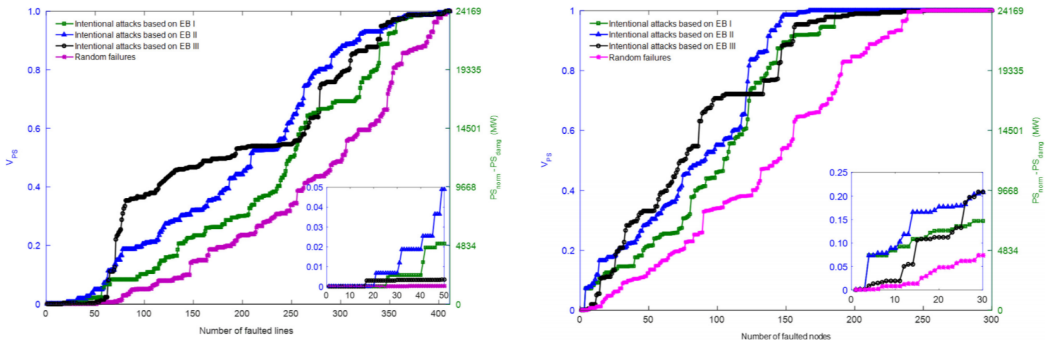

Fig. 5.1: Criticality of lines. [5]

In another study [6], authors show the significance of graph energy interlinks in topology of the power grid, which is formed under the specific reliability principles of power system engineering. Using the reliability principles and graph energy interlinks, a graph of the backbone of power grid is created which is found to be consistent when overlayed on the geographical maps. One such example is shown in Fig. 5.2. The study highlights the underlying consistency of grid reliability principles with that of modified graph energy-based method and generates a graph that can represent the topology of real power grid.

These studies can be pointed out as ad-hoc work related to the structural analyses; however this chapter is focused on providing the underlying foundation of the structural analysis on the basis of power system characteristics. To summarize, the use of electrical distance is preferred instead of the weight of edge in the analysis for better representation and accommodations of different studies and description of the network characteristics. This chapter investigates the electrical distance measure from power systems perspective

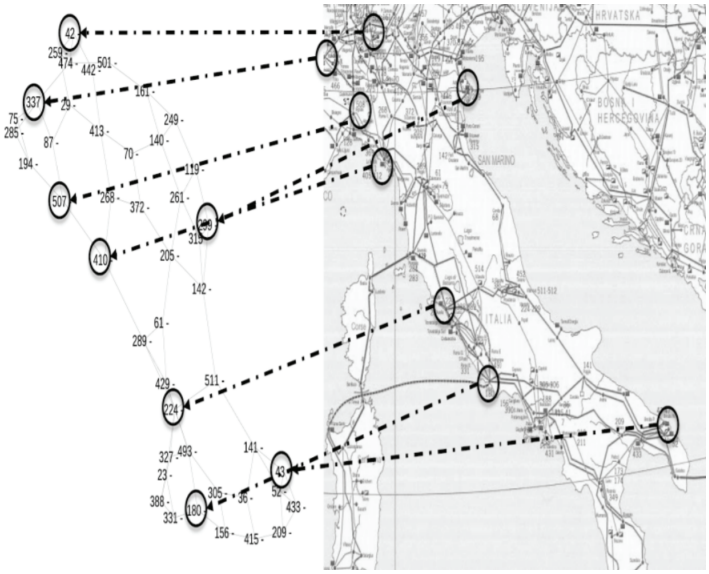

Fig. 5.2: Generated graph interconnection and respective map. [6]

in order to understand the structure of the network on the basis of impact of various operating conditions on parameters defining the network.

5.2 Analysis of structure feature of major types of models

The chapter further overviews major types of models for power system representation from structure perspective on the basis of network topology. Further in this section, the structure feature of these models are analyzed and common structure representation is suggested.

5.2.1 Steady-state models

The steady-state models have been studied on the basis of different distance equivalent measures. For example, distance measures presented in [63, 64, 66, 93, 52] are used by power system utilities for quick analysis of their respective networks. These existing models are essentially based on a typical model form which is discussed below.

5.2.1.1 Typical model form

The analysis of an electrical circuit is governed by laws such as KCL and KVL. The steady-state models of a power system can be represented by algebraic system of equations as shown in (5.1).

$$I = Y \cdot V, \tag{5.1}$$

where I stands for the currents flowing into the network, V for the voltages at the nodes, and Y for the node admittance. Power flow analysis is one of the most common steady-state analysis methods which is used to determine the real and reactive load outputs and verify that steady-state voltages are maintained within limits. Equations (3.2) and (3.3) in Chapter 3 represent the power flow analysis.

$$P_i = V_i \sum_{j=1}^{n} V_j (G_{ij} \cos(\delta_i - \delta_j) + B_{ij} \sin(\delta_i - \delta_j)) \tag{5.2}$$

$$Q_i = V_i \sum_{j=1}^{n} V_j (G_{ij} \sin(\delta_i - \delta_j) - B_{ij} \cos(\delta_i - \delta_j)) \tag{5.3}$$

where P_i and Q_i represent the net active power and reactive power injected at bus i respectively, G_{ij} is the real part of the element in the bus admittance matrix corresponding to the i^{th} row and j^{th} column, B_{ij} is the imaginary part of the element in the admittance matrix corresponding to the i^{th} row and j^{th} column.

5.2.1.2 Structural representation

The structural representation of an electric circuit can be made using an impedance matrix, also known as Z_{bus} matrix, or an admittance matrix, also known as Y_{bus} matrix.

Z_{bus} matrix is the open circuit impedance matrix in circuit theory with the diagonal and off-diagonal elements of the matrix known as the driving point and transfer impedance, respectively. The formation of a bus impedance matrix requires either matrix inversion or the use of involved algorithms. Y_{bus} matrix is the short circuit admittance matrix or

the nodal admittance matrix, with the diagonal and off-diagonal elements of the matrix known as the driving point and transfer admittance, respectively. A sample of Z_{bus} and Y_{bus} matrices is shown below:

$$Z_{bus} = \begin{bmatrix} z_{11} & z_{12} & \cdots & z_{1n} \\ z_{21} & z_{22} & \cdots & z_{2n} \\ \vdots & \vdots & \ddots & \vdots \\ z_{n1} & z_{n2} & \cdots & z_{nn} \end{bmatrix}; Y_{bus} = \begin{bmatrix} y_{11} & y_{12} & \cdots & y_{1n} \\ y_{21} & y_{22} & \cdots & y_{2n} \\ \vdots & \vdots & \ddots & \vdots \\ y_{n1} & y_{n2} & \cdots & y_{nn} \end{bmatrix}$$

where $y_{ij} = 0$, if i and j are not adjacent. Admittance matrix shown above is inversely related to the impedance matrix.

5.2.2 Electromagnetic transient models

The power system model from electromagnetic transients (EMT) perspective is based on the electromagnetic behavior of various power system elements when exposed to frequent switching. Although the process is iterative as the time progresses, it uses the same concept of electrical distance as used in steady-state perspective. In the assessment of the time response of electromagnetic transients, authors in [67] formulated a method of solving networks by nodal admittance matrix which was pursued later in [68, 69, 71].

5.2.2.1 Typical model form

The EMT models are characterized based on the structure variables such as reactance, resistances, loads, generator constants, etc. and their equivalent representation illustrating the main electromagnetic behavior of switching operation.

The EMT model of a generator is represented with an ideal sine-wave source behind the transient impedance to describe the dynamic behavior in high frequency range as shown in Fig. 5.3(a). Based on the switching transient study, the slow mechanical behavior of the machine is not considered. Similarly, the constant load which is essentially parallel

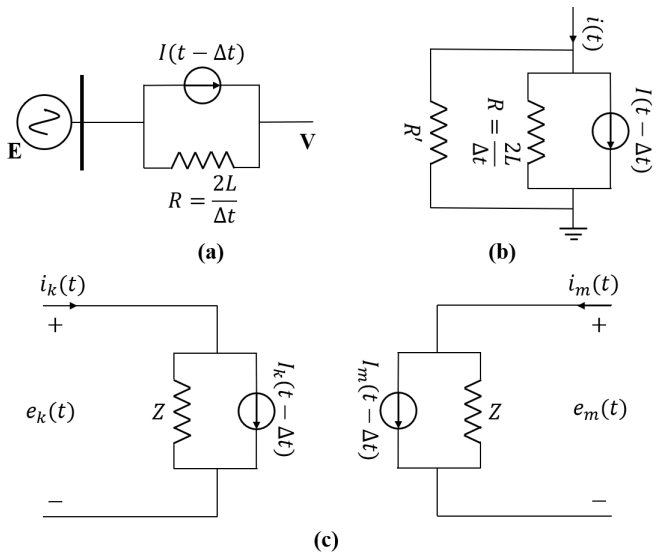

Fig. 5.3: EMT-based equivalent models for (a) a generator; (b) a constant impedance load; (c) a transmission line

R-L branches is shown in Fig. 5.3(b), where L is represented by the electromagnetic behavior of branch switching. Further, the transmission lines can be represented to give an accurate evaluation for switching phenomena. Fig. 5.3(c) represents the equivalent model for the long transmission line in the EMT analysis.

5.2.2.2 Structural representation

When the transient behavior of a circuit is under consideration, the equations representing the circuit are generally integro-differential. They can then be transformed into one scalar differential equation of second or higher order. However, these equations when expressed in matrix form result in a first-order vector differential equation as shown in (5.4).

$$\dot{\mathbf{x}} = f(\mathbf{x}, \mathbf{w}, t) \tag{5.4}$$

where $\mathbf{x}$ is a vector of unknown variables called state variables, $\mathbf{w}$ represents the set of inputs and t is the time. The set of first-order differential equations written in such a form is called the state equation and the vector $\mathbf{x}$ represents the state of the

network. The basic advantages in using the state equations in this form are as follows: 1) there is an enormous amount of mathematical knowledge for solving such equations while the equations by themselves can be derived from formal topological properties of the circuit, using the matrix approach; 2) it can be easily and naturally extended to nonlinear and time-varying or switched networks and is, in fact, the approach most often used in characterizing such networks; and 3) it is easily programmed for and solved by computers.

5.2.3 Electro-dynamic models

This chapter also analyzes the electro-dynamic perspective of power system operation which takes into account the dynamical effect of generators which can be simply seen as the sensitivity of one generator with respect to the other and which enables us to identify the valid proximity of impact of each generator [2, 44, 48].

5.2.3.1 Typical model form

The ability to predict the system behavior in time domain for power system analysis involves solution of a system of differential algebraic equations (DAEs) defining the very power system. DAEs depict a collection of variables of interest and some of their derivatives. Specifically, differential equations describe the dynamical effect on a generator or any other dynamic control devices due to electro-mechanical change in the system while algebraic equations describe the changes in variables of electrical power network in the electromagnetic transient process. Additionally, it also accounts for other subsystems and dynamical elements in the system that may have a significant impact. This is illustrated in the schematic shown in Fig. 5.4, which gives the differential algebraic representation of a power system.

The dynamics of physical systems can be described by a system of differential equations

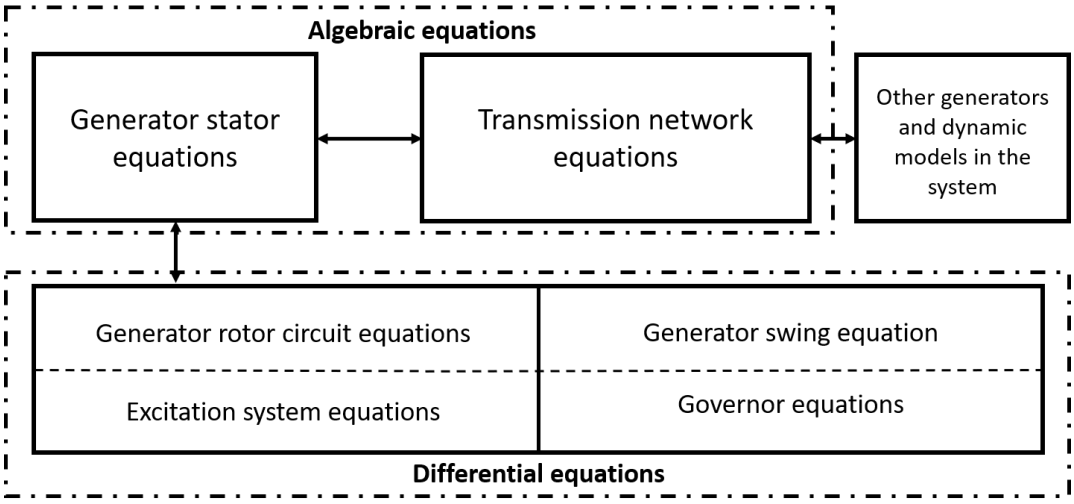

Fig. 5.4: Power system dynamic modeling.

with the most general form as shown in (5.5).

$$\mathbf{F}(t, \mathbf{y}, \mathbf{y}') = 0, \tag{5.5}$$

where t is the independent variable, $\mathbf{y} = \mathbf{y}(t)$ is a vector of m components and $\mathbf{F}$ are, in general, m nonlinear functions of t, $\mathbf{y}$ and $\mathbf{y}'$. In a somewhat similar manner, the most basic and interesting representation of dynamic behavior of a machine in a power system is the relationship between its mechanical system and the electrical system given by swing equation shown in (5.6).

$$\frac{2H}{\omega_s}\frac{d^2\theta_m}{dt^2} = P_m - P_e, \tag{5.6}$$

where H is the inertia constant, θ_m is the angular position of the rotor with respect to a stationary axis, P_m is the mechanical power and P_e is electrical power. Here the electrical power, P_e, represents the net real power at bus i and can be defined as shown in (5.2).

$$P_e = V_i \sum_{j=1}^{n} V_j (G_{ij}\cos(\delta_i - \delta_j) + B_{ij}\sin(\delta_i - \delta_j)) \tag{5.7}$$

5.2.3.2 Structural Representation

The structural representation of the dynamic system model can be derived based on the above set of dynamic equations, normally used for construction of energy functions for stability analysis. The energy is described on the basis of Lagrangian and Hamiltonian framework, whereas electrical power system is described based on network topology. Specifically, variables representing the dynamical behavior of the system in (5.6) can also be explained from the structure perspective. The impact of inertia constant, H, on the behavior of the system shows that it is part of the structure while mechanical power, P_m, also has an impact but it remains constant. Also from (5.7), it can be observed that electrical power, P_e, is defined by structure elements such as conductance, G_{ij}, and susceptance, B_{ij}. Hence it becomes evident that these variables are part of the structure and can thus be used for structural representation of the dynamical system.

5.2.4 A port-Hamiltonian basis for power system models

The analysis of power system models from different perspectives allow us to obtain respective structure representations. Such analyses are required for hassle-free and quick decision making. However, as a requirement for such analyses, these network representations involves many approximations. Therefore, a power system representation is required that retains more information and hence presents a better representation of the original system. It is known that port-Hamiltonian approach may involve DAEs in its formulation and hence is one of the best representations of the dynamic power system [94].

The framework of port-Hamiltonian systems combines the original framework by associating it with the network structure. The port-Hamiltonian systems are open dynamical systems which can interact with their environment through ports and are a representation of the energy in a particular network. Therefore, an electrical network can be formulated as a port-Hamiltonian system. In order to formulate such systems, classical

Hamiltonian equations are represented in the form of port-Hamiltonian system. These equations are shown in Chapter 3 in (3.4) and (3.5).

The total electric energy in the network is given by the Hamiltonian

$$\begin{aligned} H(q,\varphi) &= \sum_{i=1}^{n_C} \frac{q_i^2}{2C_i} + \sum_{j=1}^{n_L} \frac{\varphi_i^2}{2L_i} \\ &= \frac{1}{2} \begin{bmatrix} q^T & \varphi^T \end{bmatrix} \begin{bmatrix} C^{-1} & 0 \\ 0 & L^{-1} \end{bmatrix} \begin{bmatrix} q \\ \varphi \end{bmatrix} \end{aligned} \tag{5.8}$$

where C_i is the capacitance of the i^{th} capacitor, L_j is the inductance of the j^{th} inductor and $C = diag(C_1 \cdots C_{n_C})$ and $L = diag(L_1 \cdots L_{n_L})$. $q(t) \in \mathbb{R}^{n_C}$ and $\varphi(t) \in \mathbb{R}^{n_L}$ are vectors of capacitor charges and inductor fluxes at time t respectively. The dynamics of the electrical network can be represented in Hamiltonian form as

$$\begin{bmatrix} \dot{q} \\ \dot{\varphi} \end{bmatrix} = \begin{bmatrix} 0 & DL^{-1} \\ D^T C^{-1} & 0 \end{bmatrix} \begin{bmatrix} q \\ \varphi \end{bmatrix} \tag{5.9}$$

In this representation, the net Hamiltonian energy at time t is defined as the change in energy from the initial state due to the internal energy dissipation and the interaction with the environment in the presence of control sources in the network.

Similar to the port-Hamiltonian approach, the structure of power system based on probability-based representation of power flow is discussed in [95]. The power flow and voltage phase angles of interconnected buses in a power system are clearly described by the circuit equations and their significance is well known to the power system community. [95] presents a generic way to describe the power flow in terms of bus voltage phase angles from a probabilistic perspective. The associated probability-based representation of power flow, shown in (5.10), takes the form similar to port-Hamiltonian systems

representation.

$$\mathbf{\Theta}^*_{-t} = \sum_{u=0}^{\infty} \left(\mathbf{M}^T_{-t,-t}\right)^u \mathbf{D}^{-1}_{-t,-t}\mathbf{P}^*_{-t} \tag{5.10}$$

where the term $\mathbf{D}^{-1}_{-t,-t}\mathbf{P}^*_{-t}$ gives the initial probability distribution, $\mathbf{M}^T_{-t,-t}$ describes the transition probabilities and $\mathbf{\Theta}_{-t}$ is the equilibrium distribution. These transition probabilities depend on the connecting strength between vertices and weighted adjacency matrix. The elements in the weighted adjacency matrix and connecting strength between vertices mainly depend on transmission line susceptances in the power network.

5.3 Overview to analysis of structure

The structural analysis of physical power grids from network perspective involves conversion of the power grid into a general graph and extraction of the main topological information about vertices and edges in the graph, such as degree, degree distribution, fuzziness, and other network properties to characterize the corresponding topological connection. Further, this information is used to identify the critical components in the system from different perspectives including the strength of the links associated. The characteristics of the analytical foundation of structural analysis can be summarized by the following three perspectives:

5.3.1 Decoupling of state variables and structure

The structural analysis of power systems using port-Hamiltonian approach yields the representation of the dynamics as shown in (5.9). The system representation can be seen as decoupled subsystems since the variables become independent of each other. In this case, the Hamiltonian matrix acts as the decoupling matrix. As a result the state variables are no longer dependent on the structure parameters and hence the analysis becomes much more simpler. This is different from typical models that are used in

power system analysis since it is very difficult to separate the state variables from the structure parameters.

5.3.2 Two types of information from structure

The second perspective provides an assessment of power system network from structure perspective reveals following relevant information as explained below:

5.3.2.1 Connection information

The structure representation revealed by topological properties of a power system network gives important information related to the connections of adjacent buses or nodes through the links between them and is represented by incidence and Laplacian matrices.

1 *Incidence matrix:* For a power system network, consider an equivalent graph, G, with n vertices or nodes and m edges or links. The all-vertex incidence matrix, $A_G = [a_{ij}]$, of G has n rows and m columns. The element, a_{ij}, of A_G can be defined as follows:

$$a_{ij} = \begin{cases} 1, & \text{if } j^{th} \text{ edge is incident on } i^{th} \text{ vertex,} \\ 0, & \text{otherwise.} \end{cases} \tag{5.11}$$

2 *Laplacian matrix:* Let $G = (V, E)$ be a weighted undirected graph with vertex set, $V(G) = \{v_1, v_2, \ldots, v_n\}$, and edge set, $E(G)$. Let w_{ij} denote the weight of edge (i, j).

Note that $(i,j)^{th}$ element, l_{ij}, of the Laplacian matrix, L, can be written as:

$$l_{ij} = \begin{cases} -w_{ij}, & \text{if } i \neq j \text{ and } v_i \text{ and } v_j \text{ are adjacent;} \\ 0, & \text{if } i \neq j \text{ and } v_i \text{ and } v_j \text{ are not adjacent;} \\ \text{sum of the weights of the edges incident on } i, & \text{if } i = j. \end{cases} \tag{5.12}$$

So, the Laplacian matrix, L, can also be written as

$$L = A_G W A_G^t, \tag{5.13}$$

where W is the diagonal matrix with the diagonal entries representing the weights on the edges.

One very important aspect apart from the connection information that the analysis highlights is the link strength between the buses which is defined by the corresponding weight for each link in the system and can be utilized to obtain a critical measure known as electrical distance.

5.3.2.2 Electrical distance and link strength

Given the complexity of the structure of power grids, the interest in its study from a complex networks perspective is ever growing. This requires a study of not only its topology, but also its electrical structure. Electrical distance measure can be used to understand the electrical structure of a given power grid. This measure has been used in a number of power systems problems [38, 51, 96]. The equivalent electrical distance measure between two nodes corresponds to the link strength between them. There are number of variant measures of electrical distance for a power network, which are discussed in previous sections, but the simplest is the absolute value of the inverse of

the system admittance matrix.

$$\mathbf{D} = [\mathbf{Y}_{bus}^{-1}], \tag{5.14}$$

where $\mathbf{Y}_{bus}$ represents the admittance matrix of the network and $\mathbf{D}$ is the electrical distance matrix and gives a measure of sensitivity of voltage and current changes for every pair of nodes.

One of the prominent definitions of electrical distance measure is defined by Thevenin impedance. Given two nodes in a network, r and s, this measure, $Z_{th,rs}$, includes the parallel combination of all the impedance paths between r and s. It is defined as the Thevenin impedance between the two nodes [28], which can be calculated as

$$Z_{th,rs} = Z_{rr} - 2Z_{rs} + Z_{ss}, \tag{5.15}$$

where Z_{rs} is the element at r^{th} row and s^{th} column in the bus impedance matrix. This serves as the basis for the measure average electrical distance (AED) introduced in [66].

In addition, the assessment of power systems from a structure perspective also allows identification of critical components on the basis of associated link strength. The link strength parameter or weight associated with a link is primarily utilized in complex networks approach for network analysis.

5.3.3 Complex networks approach

The basis of complex network approach in this setting is the behavior of large power networks that is similar to the complex systems in different fields [97, 98, 99, 100].

A graph can be visually represented as a collection of nodes joined by links. If the nodes are joined by non-directional links, the graph is known as undirected graph, which is shown in Fig. 5.5(a). If the links in the graph contains information related to the

direction, the graph is then known as directed graph. This is shown in Fig. 5.5(b). In the weighted graph, shown in Fig. 5.5(c), the values $w_{i,j}$ reported on each link indicate the weights of the links which gives the valuable information related to the strength of each link.

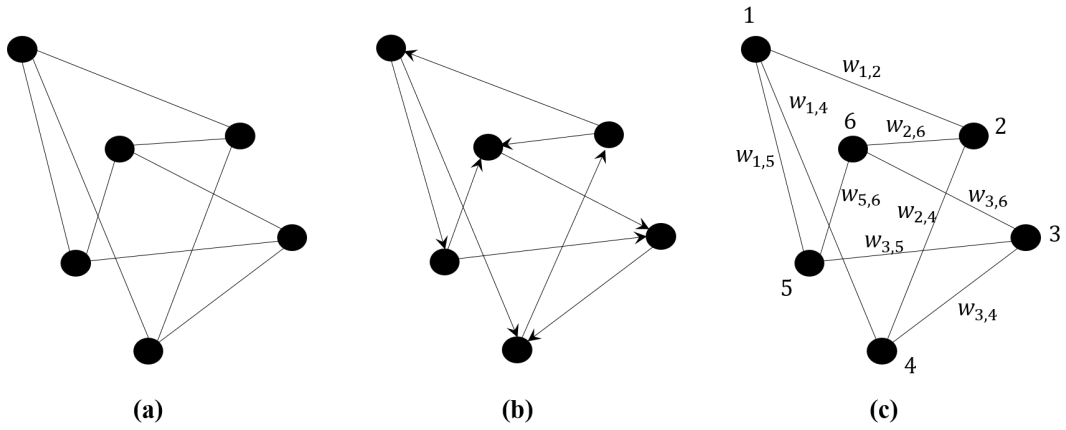

Fig. 5.5: Graphical representation of (a) an undirected graph; (b) directed graph; (c) weighted graph

The connection information illustrated in Fig. 5.5 can very well explain the information obtained from structural analysis of a power system. Moreover, the connection of the nodes, electrical distance and link strength can be used to determine the structure of any power network.

5.3.4 Example of Structural Analysis

Complex network metrics for the assessment of networked systems have been recently applied to power systems [12, 13]. The optimal restoration of a real-time power system following a disruption can be a complex process. In [101], the authors present an integrated tool based on approximate dynamic programming with solution space reduction methodology. The main theoretical foundations of the methodology and the key algorithms used in this integrated tool include the knowledge of power system engineering, methods in complex networks science, concepts of graph theory, and dynamic programming in operation research. This tool, developed on the basic foundation of structural

analysis, addresses the concerns related to the curses of dimensionality and simplifies the solution space and thus can be applied to various complex real-time operation settings.

5.4 Remarks

This chapter provided the description of the analytical foundation of structural analysis. It also summarizes the analysis of major types of power system models and show the structure description from different perspectives such as steady-state, electromagnetic transient and electro-dynamic perspectives.

The work presented in this chapter provides the possibility of applying structural analysis to all the networks since they are intrinsically identical and can be represented using port-Hamiltonian models. Using port-Hamiltonian approach, we were able to separate the state variables from the structure parameters. The port representation of each component in the power system can be combined resulting in a larger unifying port system. The structure matrix, J, represents the connection information and does not include the state change of the system. Any change in the operating conditions impart a change in the structure connection of the system but the overall representation of structure matrix is consistent. Thus presenting a consistent methodology for different system operating conditions. The study in this chapter provided the key features of structural analysis which are decoupling, connection information, electrical distance and link strength.

The study of the existing power system analysis techniques done from a different perspective sheds light on the dependency of parameters sensitivities on the structure of the network and measures associated with it. The concept of electrical distance can be correlated with sensitivity of different parameters under varying operating conditions of a power system. This chapter highlights the point that analysis of the characteristics of different models from a structure perspective is important to bridge the gap between complex networks and power system analysis. This chapter also lays an analytical foundation of structural analysis from network perspective thereby simplifying the solution

space and providing solution to various complex real-time operation settings. One such structural analysis-based tool is discussed in the next chapter.

CHAPTER 6

Practical application in power system restoration

Optimal restoration of a real-time power system following a disruption can be a complex process. In view of that and with an increase in frequency and severity of power system outages across the U.S. and their impact on consumers and utilities, North American Electric Reliability Corporation (NERC) elevated the standard of compliance for power system restoration [102, 103]. While several utilities have proposed solutions addressing the elevated standards based on dynamic programming, they could not address the issues for large scale power systems and real-time operations including those using steady-state and transient analysis due to the curses of dimensionality. As laid out in Chapter 5, the foundation of structural analysis is used in a system restoration tool which is based on approximate dynamic programming (ADP) integrated with solution space reduction methodology. The main theoretical foundations of the methodology and the key algorithms used in this restoration process include the knowledge of power system engineering, methods in complex network science, concepts of graph theory, and dynamic programming in operation research. This method addresses the concerns related to the curses of dimensionality and simplifies the solution space and thus can be applied to various complex real-time operation settings.

6.1 Background and related work

The consideration of power system restoration is that the system restoration should be achieved optimally according to different objectives such as maximizing generation capacity and quickly re-energizing major transmission corridors in order to minimize the impact of blackout and recover the load. This makes it a multi-objective and

multi-stage non-linear integer programming problem [104]. For such a problem, several approaches have been proposed, which can be categorized as: heuristics-based methods [105, 106, 107, 108] which require more time to solve this combinatorial optimization problem and may not be adequate for real-time operation; expert systems (ES) [109, 110, 111, 112] require specialized software which make the process time-consuming for the operators. Additionally, mathematical programming (MP) [113], soft computing [114] and combinations of above approaches [115, 116, 117] are some approaches that may not be considered reliable in terms of solution accuracy at specific and crucial times.

6.2 NERC requirements for system restoration

Due to the concerns related to increasing frequency and severity of power outages in an interconnected power system network, North American Electric Reliability Corporation (NERC) elevated the standard of compliance for restoration by adopting revised Emergency Operations and Preparedness (EOP) reliability standards [102, 103]. The critical importance of having advanced analytics and techniques that can be applied to real-world restoration planning and real-time decision support has been recognized and is becoming more significant for the power community.

The revisions carried out by NERC are deemed important for reliability of the North American bulk power system. The NERC standards EOP-005-2 [102] and EOP-006-2 [103] proposed to have a definite procedure for Blackstart and required Generator Operators (GOP) to meet the requirements for the Transmission Operators (TOP). Thus, the operators must be able to identify the Blackstart capabilities so that generation utilization can be maximized and an optimal start-up sequence can be initiated. On the hind sight, most power system operators rely on off-line restoration plans that only deal with certain contingencies and outages. The power network planners and operators have found it challenging to address NERC's elevated standards regarding restoration

at planning stage, let alone meet the demands in real time. This issue has become more serious as recent changes in generation mix have prompted operators to reassess Blackstart needs. Even though NERC has revised the standards to provide enhanced reliability, it still remains a long standing challenge to meet these standards for the power industry.

6.3 Efforts to meet NERC requirements

In order to overcome the challenge for power system operators to meet the NERC standard regarding restoration, several methods have been proposed to provide optimal solutions [118, 119]. Most of the proposed solutions are limited to a theoretical discussion with very few extending the findings and applying them to a practical real-time situation. Out of those, two major efforts in this area are carried out by Power System Engineering Research Center (PSERC) and Electric Power Research Institute (EPRI).

1 *PSERC's methodology:* PSERC's effort follows a practical approach with an adaptive strategy procedure for power system restoration [115]. The procedure is governed by a strategy module which centrally controls four major operation modules: (1) Generation Capability Optimization; (2) Transmission Path Search; (3) Constraint Checking; (4) Distribution System Restoration. The restoration process with central strategy module is illustrated in Fig. 6.1.

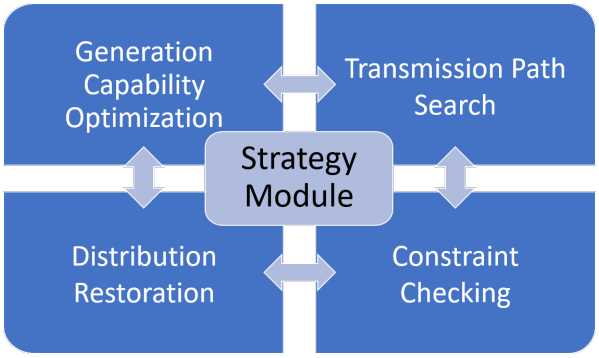

Fig. 6.1: Illustration of PSERC's restoration process

In this methodology, PSERC adopted a goal oriented restoration process involving a different problem formulation for each of the modules. The overall objective is to maximize the total number of transmission lines energized along with the feeders for all the time intervals and in addition allowing the increase of overall system generation capacity for start-up power requirements as shown below in (6.1).

$$\begin{aligned} \max \quad & \sum_{t=1}^{N_T} \left[\sum_{l=1}^{N_L} (\omega_l^t \cdot L_l^t) + \sum_{i=1}^{N_B} (\omega_i^t \cdot P_i^t) \right]. \qquad (6.1) \\ s.t. \quad & \text{Critical Min. \& Max. Time Intervals} \\ & \text{Start-up Power Requirement} \\ & \text{Flow capacity of transmission lines.} \end{aligned}$$

where N_T is the total number of time intervals, N_L is the total number of transmission lines, N_B is the total number of buses and for the time interval t, transmission line l and bus i, ω represents the respective weighting factors, L is the status of lines and P is the active power. The objective function in (6.1) is subject to physical constraints such as flow capacity of transmission lines, generation limits with other start-up power requirements. In addition, the model also considers the minimization of de-energized load for the start-up period.

2 *EPRI's methodology:* EPRI developed tools to provide decision support to system restoration planning citing that the system reliability is directly affected by the efficiency of system restoration [120, 121]. On-line restoration process after a blackout requires the operators to adapt to actual outage scenarios and available resources. In order to cater to the on-line restoration process, EPRI developed two tools:

(a) *System Restoration Navigation (SRN)*: This was intended to be used for offline planning at the initial stage and further on for dispatcher training and

online decision support for power system restoration;

(b) *Optimal Blackstart Capability (OBC)*: This was designed to assist system restoration planners in evaluating system Blackstart capabilities and determining the optimal locations and amounts for additional Blackstart resources.

The methodologies proposed by PSERC and EPRI, although designed to address the elevated system restoration requirements, could not address the issue for large-scale power systems and the changing dynamics of real-time operation. The methods are subject to the limitations of dynamic programming (DP) which have been highlighted and addressed upon in this study.

In this chapter the key ideas and associated algorithms are introduced that have made a significant breakthrough in development of system restoration technique. They have not only been used in improving the effort and time of planning but has also made the real-time application very possible. The proposed method is based on Approximate Dynamic Programming (ADP) which addresses the key limitations of DP and uses the structural analysis to reduce the solution space. This allows the proposed method to create a feasible restoration plan of a large-scale power system along with completions of sophisticated simulation tests including steady state AC power flow analysis, frequency dynamic stability analysis and electromagnetic transients analysis in a significantly shorter duration of time when compared to other existing platforms. Currently, the work is being used to integrate the solver engine and automated techniques into a software package that are designed for off-line system restoration planning. Also based on this study, the work is to be extended further so that it can be used for real-time applications.

6.4 Approximate dynamic programming-based technique

The advanced system restoration technique has taken an unconventional approach which is based on dynamic programming (DP). The DP approach allows recursive optimization that includes backward induction process and provides a systemic way to address a multi-stage non-linear integer programming problem. However, DP still faces the challenge of the curse of dimensionality which can be addressed by using ADP approach.

6.4.1 Limitations of dynamic programming

The inherent nature of non-linear integer programming problems presents three curses of dimensionality which challenge the development of this technology. These three curses of dimensionality are:

1 Size of *state space*;

2 Size of *action space* or *feasible region*;

3 Size of *outcome space*.

These curses act as major limitations to any dynamic programming model since the number of variables and stages increases rapidly and with that the number of calculations required and hence the computational effort. It is due to these curses of dimensionality that PSERC and EPRI could only address small scale problems, possibly localized and could not address large scale real-time problems. Consequently, EPRI's tool has been used for training and restoration drills while PSERC's model works as a research grade solution. Moreover, both the tools only concern steady state stability.

6.4.2 Approximate dynamic programming

The limitations of DP due to the curses of dimensionality cause the model to fall short when dealing with real-time problems. In order to overcome such limitations, ADP-

based modeling framework offers strategies for tackling the curses of dimensionality in large, multi-period, stochastic optimization problems.

As the algorithm steps forward in time, it may take many iterations before the costs incurred in later time periods are correctly transferred to the earlier time periods. To overcome this, the ADP algorithm can also be used with a double pass approach consisting of a forward pass and a backward pass. In the forward pass, decisions simulated moving forward in time, remembering the trajectory of states, decisions, and outcomes. Then it is followed by a backward pass strategy that determines a decision, given the available information at the current state, updating the value functions moving backwards in time using the trajectory information [122].

For ADP, the principle of optimality is determining a sequence of optimal decisions or choices at each stage which is defined by a policy or decision function. This sequence of sub-problems is solved recursively as a natural form of the Bellman equation as shown in (6.2).

$$V_t(S_t) = \max_{x \in \mathcal{X}} \Big[C_t(S_t, x_t) + \mathbb{E}\{V_{t+1}(S_{t+1}|S_t, x_t)\} \Big], \tag{6.2}$$

where each possible state S_t maps to a decision x_t for each stage at time t in the planning horizon. The state space $\mathcal{S}$ determines the evaluation of value function $V_t(S_t)$ for all states within a reasonable time along with the addition of decision space $\mathcal{X}$.

6.5 Proposed ADP with solution space reduction

Different from the perspectives provided by the existing theories of power system analysis and techniques of optimizations, the solution space reduction technology developed is based on graph theory and advanced complex network techniques. The technique is useful in identification of critical components in a weighted network, and it also highlights

the relation between global performance of power grids and localized interactions, and successfully addresses the long-standing real-world power system problem. In addition to the complex networks techniques, we use additional information about the strength of the links to incorporate the electromagnetic properties, transient behavior and laws of physics underlying the power grid.

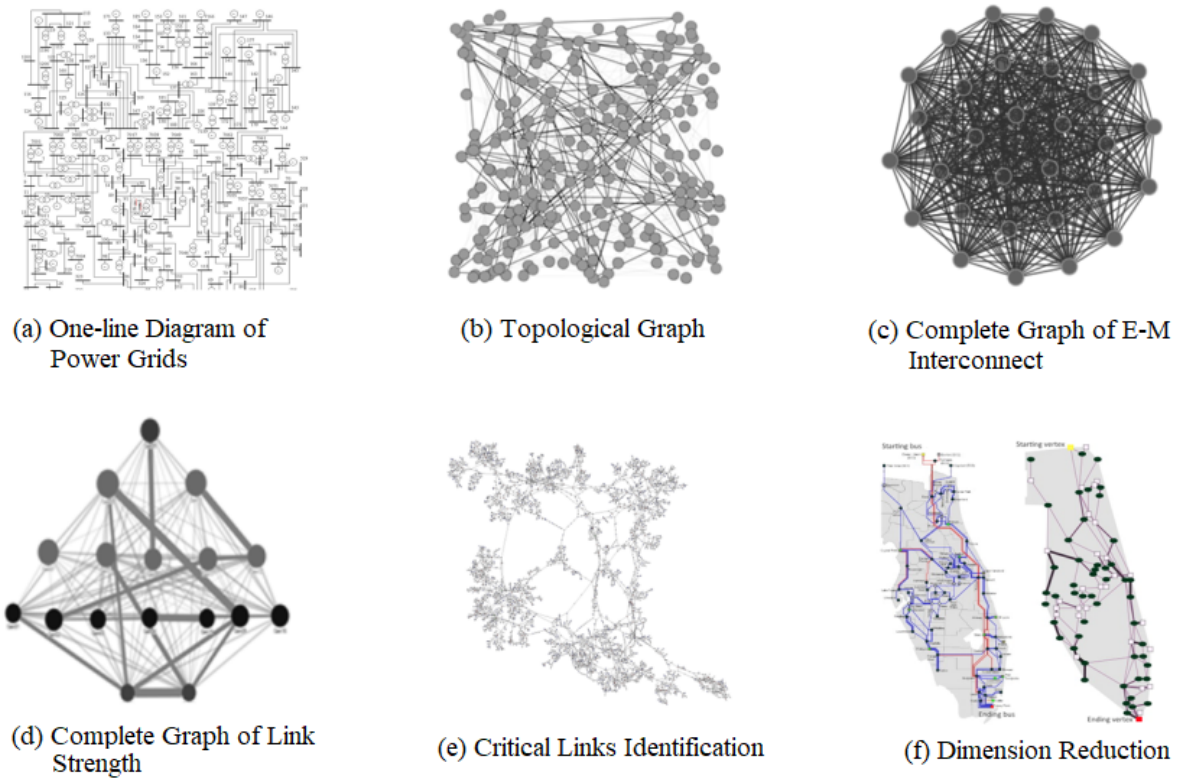

Fig. 6.2: Illustration of solution space reduction [7]

The solution space reduction technology shown in Fig. 6.2 is based on four key algorithms:

1 Topological representation;

2 Complete graph and link strength determination;

3 Structural analysis and criticality identification;

4 Reduced solution space.

These key algorithms are discussed here in detail:

1 *Topological representation:* The first algorithm considers a power system network, shown in 6.2(a), and produces a corresponding topological graph representation to allow structural and criticality analyses.

Research in network science has shown that there are important relationships between network structure of the power grids and its performance related to reliability and risks. Thus we can represent the connection of the power grids with a graph, and thus can further analyze the performance of the power grids for identification of risks and mitigation of reliability issues. A power transmission system can be represented as a graph of edges and vertices, in which the edges are electrical transmission branches including lines and transformers, while vertices are the nodes where electrical power can be injected, withdrawn or redistributed, accordingly known as generation nodes, load nodes, and transfer nodes. Each line in a power network has its own maximum power flow capability, which is the maximum amount of power flow that the line can sustain. Although there are various levels of voltages for transmission branches and nodes, they are all electric-magnetically interconnected. In per unit measure, the electric distances are normalized to represent the strengths of links between all interconnected components. The power grids usually contain over thousands of buses and links which can be represented by vertices and edges respectively as shown in Fig. 6.2(b). In order to utilize the complex networks techniques and graph theory methods, it is necessary to convert the physical topology of the power grid in its graph representation by vertex-edge diagrams, which represent the buses as vertices and the connections between those buses as edges connecting two buses Fig. 6.2(a) and 6.2(b);

2 *Complete graph and link strength determination:* Once the original power system model is converted to its abstract graph representation, we try to incorporate several essential features of power grids in graph modeling, particularly those

related to the electromagnetic nature of edge that links all the interconnected vertices and the strength of the link. After incorporating these essential features, we can use the additional information or insights in criticality analysis to localize the problem and break the issue of the curse of dimensionality.

The second algorithm generates a complete graph representing electromagnetic links between all the nodes, shown in Fig. 6.2(c), and estimates link strength or weights of the edges/links in the complete graph for a given problem, illustrated in Fig. 6.2(d).

In graph theory, a complete graph is referred to as a simple undirected graph in which every pair of distinct vertices is connected by a unique edge. A complete digraph is a directed graph in which every pair of distinct vertices is connected by a pair of unique edges (one in each direction). Therefore, once the topological graph representation of the power grids is obtained i.e. the one shown in Fig. 6.2(b), we need to convert it to a complete graph representation as shown in Fig. 6.2(c).

From a connection perspective, all nodes in a complete graph are identical as shown in Fig. 6.2(c). The only factor that differentiate different types of complete graph is the property of edge that links each pair of vertices. In the context of complex networks, the property of edge can be seen as the weight of the link, while in the context of power grids, it can be seen the strength of electromagnetic link between components interconnected either synchronously or asynchronously. Due to the difference in link weights in finite identical complete graphs, there could be infinite number of graphs distinctively different from each other that may change the performance of power grids. Thus a simple representation of link strength can be used as the "link-weight" of edge. Based on the algorithms described in the previous subsections, it is clear that, for a given operating condition, the link strength depends on both topology of power grid as well as the electric

variables include those related to the buses such as voltage magnitude, voltage angle, real power injection, reactive power injection, real load, reactive load, shunts, transformers, etc; and those related to the transmission lines such as resistance, reactance, impedance, real power flow, reactive power flow, real losses, reactive losses, etc.

The quantification of the strengths of different types of electromagnetic links is based on the steady state-based electric distance measure for different risk and reliability problems. Fig. 6.2(d) illustrates the link strength in a layered format which is another layout of complete graph, and allows separations of edges based on link strength of edge.

3 *Structural analysis and criticality identification:* Identification of critical components or weak areas in power grids are challenging issues, yet critical to the operation of power grids. In the control center of almost every power grid, a list of critical components are identified and frequently updated by operating support group, the status of critical components are monitored, and if certain threshold values are exceeded, then actions must be taken promptly. The third algorithm uses criticality and structural analyses to find the winning probabilities of possible solutions and determine the categories of granularity as illustrated in Fig. 6.2(e), in which various critical components can be distinguished.

The most significant part of the reduction process is the criticality identification based on the weighted graph. This involves algorithms primarily based on planarity test of the weighted structure to characterize the set of planar graphs; and planarization which involves removal of a certain number of vertices so that the graph becomes planar ensuring a minimal impact on the criticality of the graph. This is shown in Fig. 6.3.

Planarity test algorithms typically take advantage of theorems in graph theory that characterize the set of planar graphs in terms that are independent of graph

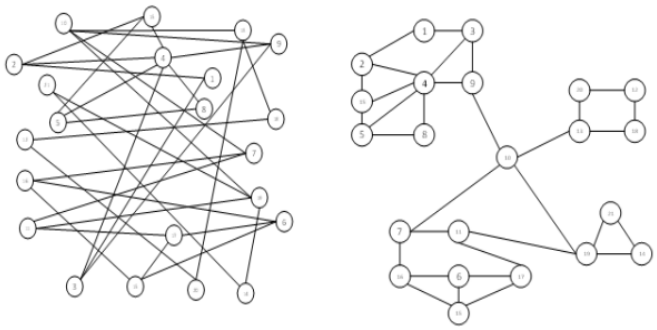

Fig. 6.3: Critical components identification

drawings. The planarization represents the procedure of identification and temporary removal of a number of vertices so that the graph becomes planar. This is different from the objective of planarization in computer science which is to recreate the layout of a planar graph in such a way that there is no visual edge crossing. In order to preserve most of the properties of the original graph, a computational algorithm is developed to remove a minimum set of vertices to ensure a minimal impact on the criticality of graph.

The utilizations of weights and planarization successfully uncover the information about the hierarchy of power grids and criticality of connected vertices and edges. Fast and proper usage of system information and complex network method can help identify which areas of the system are critical for system restoration. Comparing the original topological graph shown in Fig. 6.2(b), the network in Fig. 6.2(e) is no longer just a graphic or topological layout that rearranges the edges and vertices, it is capable to solve the criticality of the corresponding components of power grids which could largely characterize the performance of power grids in many power system analyses. Although many analyses require to be much detailed, the structural information is always a part of it. Analyses identified based on structural information may be the same which can be applied to many studies. Even though the list of critical elements may not be complete, identification of these critical elements can greatly reduce the dimension of the problems which is adequate to support system restoration decisions, at least for reasoning purposes

or computational applications, like system restoration issues associated with the challenge of the curses of dimensionality of system restoration.

4 *Reduced solution space:* Above algorithms for identification of critical components represent a significant innovation in techniques that address the key challenges in system restoration analyses. The complex networks methods and power system analysis techniques are used coherently to pinpoint the criticality of power grids based on the topological structure of graph and electric properties of power grids. This provides useful information about the structural characteristics of power grid and critical components. In system restoration analyses, this information can be used by the system operators to prioritize buses or zones based on their importance, categorize the transmission lines or corridors based on the restoration strategies, respond to the realities aftermath of blackout or large-scale brownout. Moreover, the algorithms are flexible and can be easily embedded so that they can be adapted to any optimization framework.

   The fourth algorithm solves the optimization problem in the reduced solutions space by either avoiding lower winning probability options or selecting high winning probability options based on link strength information. This results in a condensed solution space with critical components, as illustrated in Fig. 6.2(f).

The advanced algorithm with reduced solution space can carry out all stability analyses to allow feasibility studies, as illustrated using a flowchart in Fig. 6.4 and it can be applied to most optimization problems with different objective functions. The aforementioned algorithms and structural analysis have been integrated to address the real-world restoration problems and incorporated into an analytical tool.

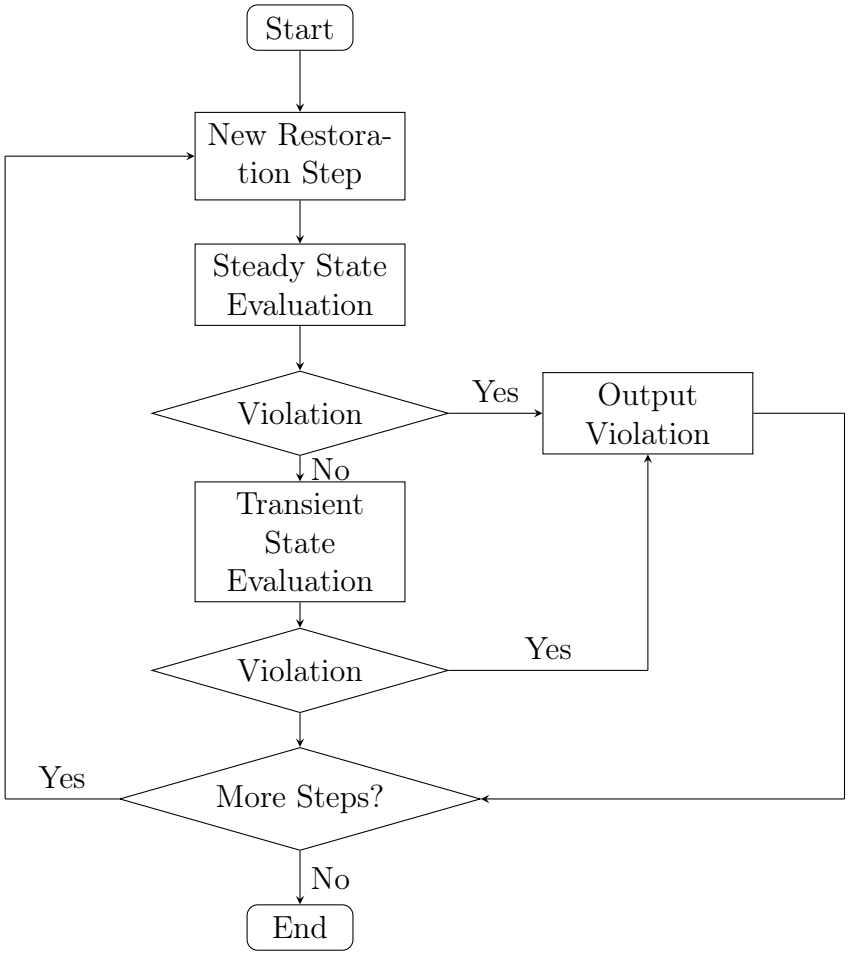

Fig. 6.4: Restoration process involving transient state evaluation.

6.6 Integrated tool for system restoration

The development of the integrated tool with a number of integrated automated analytics allows it to be NERC compliant with standard power system models. This tool still follows the standard model of restoration and the optimization problem presented here is similar to the existing models involving automated modeling, path searching, simulation and feasibility studies. However it simplifies the analysis with the application of ADP-based formulation with involvement of complex networks science and graph theory-based solution space reduction technique. Further, the solution is based on an algorithm which uses an optimal strategy to obtain restoration path by dividing the problem into various sub-problems.

Further, the model can be utilized for real-time scenarios due to its capability to carry out steady-state, transient and dynamic stability analyses as opposed to only steady-state analysis in the existing models. Such a model formulation of optimal decision in each backward induction step is similar to the Bellman equation as shown in (6.3) below.

$$V(X_0) = \sup_{(U_t)_{t=0}^{N_T}} \left[\sum_{t=0}^{N_T} \left(\sum_{j=1}^{N_G} G_j(U_j) + \sum_{i=1}^{N_D} D_i(U_i) + \sum_{k=1}^{N_L} L_k(U_k) - f_c(U_c) \right) \right], \tag{6.3}$$

where

$$\begin{aligned}
U_t &= \{u_{g,j}^t, u_{d,j}^t, u_{l,k}^t, P_{g,j}^t, V_{set}^j, P_i^t, Q_i^t, Q_{shunt,s}^t\}, \\
U_j &= \{X_t, u_{g,j}^t, t, \omega_j^g, P_{g,j}^{min}, P_{g,j}^{max}, T^{min}, T^{max}, j, P_{g,j}^t, R_j, V_{set}^j\}, \\
U_i &= \{X_t, u_{d,i}^t, t, \omega_i^d, P_i^{min}, P_i^{max}, P_i^t, Q_i^{min}, Q_i^{max}, Q_i^t\}, \\
U_k &= \{X_t, u_{l,k}^t, t, \omega_k^l\}, \ and \ U_c = \{N_{GS}^t, N_{DS}^t, N_{LS}^t, t\}.
\end{aligned}$$

where P, Q represent the active and reactive power respectively, associated with the generators in the network, G_j represents the set of generation output, D_i represents the set of loads, L_k is the set of status of transmission lines, f_c is the set of operating frequencies, R_j is the ramping rate of generator j, u is the decision variable for various sub-problems and ω represents the weight associated with various elements in the system. The above objective function is subject to constraints similar to those of the PSERC model in (6.1).

In order to obtain a solution to the Bellman's type equation in (6.3), the following algorithm is used to select the most probable/optimal set of elements and state path at each stage of restoration:

Step 1: The problem in (6.3) is divided into a set of overlapping sub-problems;

Step 2: An optimal strategy, $\pi^* = \arg\max_\pi V^\pi(x_0)$, is constructed which is used to generate the choice at the current restoration stage, such that the solution space is reduced on the basis of the importance of the state sequence and an optimal path of restoration;

Step 3: This strategy, π^*, is used to find the sub-problem solutions at all stages for the overall optimal solution of the original problem described by (6.3).

Since the essence of ADP is to replace the true value function with the statistical approximation, based on the algorithm mentioned above, the problem function in (6.3) can be framed as an objective function for each sub-problem as shown in (6.4).

$$\begin{aligned} V(X_s) = {}^{sup}_{(U_t)_{t=s}^{N_T}} \Bigg[\sum_{t=s}^{N_T} \Bigg(\sum_{j=1}^{N_G} G_j(X_t, U_t) \\ + \sum_{i=1}^{N_P} D_i(X_t, U_t) + \sum_{k=1}^{N_L} L_k(X_t, U_t) - f_c(U_t) \Bigg) \Bigg], \end{aligned} \tag{6.4}$$

where X_s and U_s represent the state at stage s and the decision that optimizes the value of the subsequent stages, respectively. Equation (6.4) can be rewritten in Bellman equation form as shown in (6.5).

$$V(X_s) = {}^{sup}_{U_s} \Big(T(X_s, U_s) + V(X_{s+1}) \Big), \tag{6.5}$$

where $T(X_s, U_s)$ represents the elements of (6.4) for $t = s$. The dimensionality of the problem can be reduced if the important states of transition function, $S(X_t, U_t) = X_{t+1}$, to the global optimal value can be percepted and quantified by an associated weight a_s^{ij}. Hence the optimal decision can also be obtained based on the weights. Further, with the assumption of a perception function based on weights, the Bellman equation in (6.5) can be approximated as

$$V(X_s) = \overset{sup}{U_s}\Big(F\{V(X_s)\} \cdot T(X_s, U_s) + V(X_{s+1})\Big), \tag{6.6}$$

where $F\{V(X_s)\} = a_s^{ij}$ is the assumed perception function with $i \in X_s, j \in X_{s+1}$.

The reduction in dimensionality as a result of approximation on the basis of assumed perception function makes the process of restoration explicit. This improves the quality of the restoration path without concerning associated voltage violations. The advantages of using solution space reduction based on approximation is illustrated in the next section using an IEEE 118-bus test system and further validated using 2000-bus synthetic test system.

6.7 Illustration of system restoration

This section demonstrates the restoration process using the integrated tool on IEEE 118-bus test system [1] and a bigger 2000-bus synthetic test grid system [123]. The capability of the tool is highlighted by specifying a Blackstart unit in these systems and carrying out feasible restoration plan. The feasibility of the restoration plan is validated based on steady-state analysis, transient analysis and frequency dynamics of the system.

6.7.1 IEEE 118-bus system

The restoration process is demonstrated on IEEE 118-bus system which is illustrated in Fig. 6.5. In this system, there are 54 generator units and 99 load units with a peak demand of 4242 MW. For this study, the generator at bus 12 can be assumed to be the Blackstart unit and for demonstration of restoration process, the location of nuclear generator station is assumed to be located at bus 77.

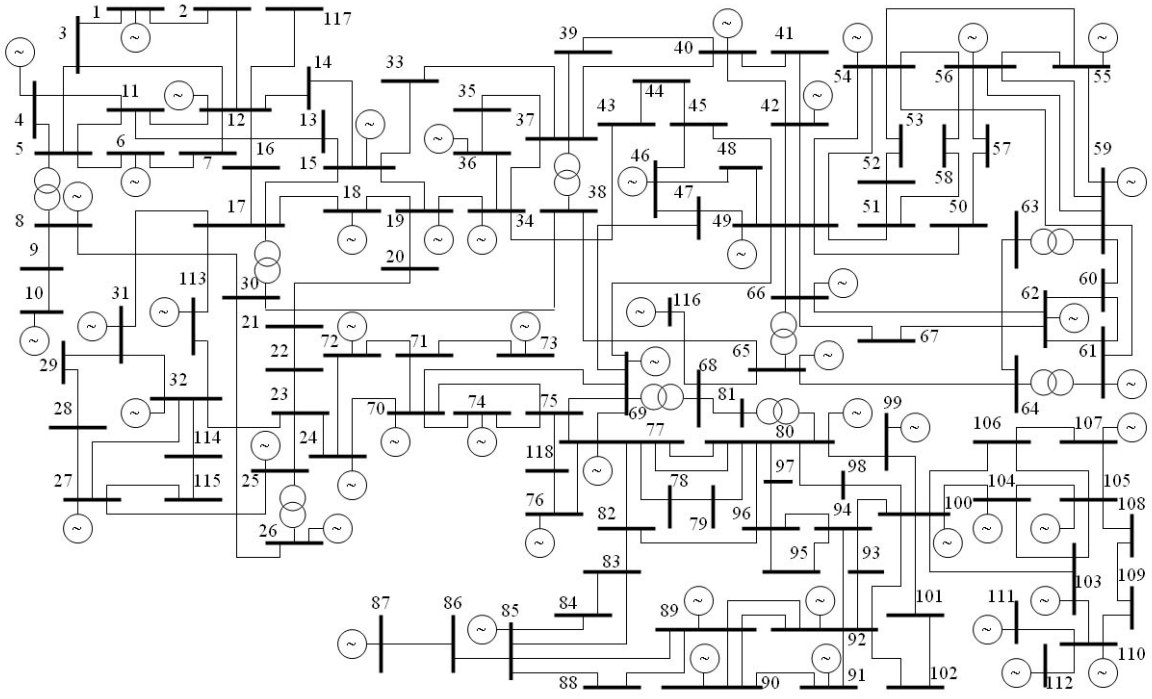

Fig. 6.5: IEEE 118 bus system. [1]

6.7.1.1 Generation restoration

One of the critical requirements after a system blackout is the assurance of reliable shutdowns of nuclear generators. Therefore it is imperative to have a feasible restoration plan for expeditious restoration of off-site AC power sources to the nuclear station.

Keeping this as the priority, a restoration scenario is simulated using different restoration plans devised using the proposed tool. The tool is used to create a critical restoration path from the Blackstart unit at Bus 12 to the nuclear station assumed to be located at bus 77 in the test system. Three different plans are tested to restore the system:

1 Restoration Plan I generally renders priority to the final outcome without focusing on the criticality of the path;

2 Restoration Plan II is based on the simple distance rule;

3 Restoration Plan III uses an alternative restoration path based on the ADP algorithm with solution space reduction.

Plan I and Plan II show steady-state and transient violations for different cases while Plan III avoids such steady-state and transient violations based on alternative restoration path as shown in Table 6.1.

Table 6.1: Restoration Plan III

Sequence No.	Bus No.	Bus (From)	Bus (To)	Type	Bus (From)	Bus (To)	Output (MW)
1	12	Txxxxxxh	Txxxxxxh	Gen			47
2	12	Txxxxxxh	Sxxxxxxd	Branch	12	11	
3	11	Sxxxxxxd	Sxxxxxxd	Load			70
4	11	Sxxxxxxd	Oxxxe	Branch	12	11	
5	12	Txxxxxxh	NxE	Branch	12	16	
6	16	NxE	NxE	Load			25
7	16	NxE	Sxxxxxxn	Branch	16	17	
8	17	Sxxxxxxn	Sxxxxxxn	Load			11
9	17	Sxxxxxxn	Dxxxxxk	Branch	17	31	
10	31	Dxxxxxk	Dxxxxxk	Load			21.5
11	31	Dxxxxxk	Dxxxxxxe	Branch	31	32	
12	32	Dxxxxxxe	Dxxxxxxe	Load			7.37
13	32	Dxxxxxxe	Cxxxxxxr	Branch	32	33	
14	23	Cxxxxxxr	Cxxxxxxr	Load			7
15	23	Cxxxxxxr	Txxxxxn	Branch	23	24	
16	24	Txxxxxn	Txxxxxn	Load			13
17	24	Txxxxxn	Pxxxxxxh	Branch	24	70	
18	70	Pxxxxxxh	Pxxxxxxh	Load			8.25
19	70	Pxxxxxxh	Sxxxxxxt	Branch	70	75	
20	75	Sxxxxxxt	Sxxxxxxt	Load			2.94
21	75	Sxxxxxxt	Txxxxr	Branch	75	77	
22	77	Txxxxr	Txxxxr	Load			3.81

6.7.1.2 Ideal restoration plan

As discussed earlier, Restoration Plan I prioritizes restoration of off-site power sources to the nuclear power station without any specific rules, hence it may be seen as a pure vanilla case. The restoration path starts with energization of Blackstart unit at bus 12 and after 27 sequences, the off-site power sources to the nuclear power station at bus 77 is restored. This restoration plan shows no steady-state violations, however, when subject to worst-case switching transients, it may show transient voltage violations at certain locations in the path. Restoration Plan II on the other hand follows most existing restoration plans in utilities which are manually created by operators based on the simple distance rule, which selects restoration paths using minimum distance.

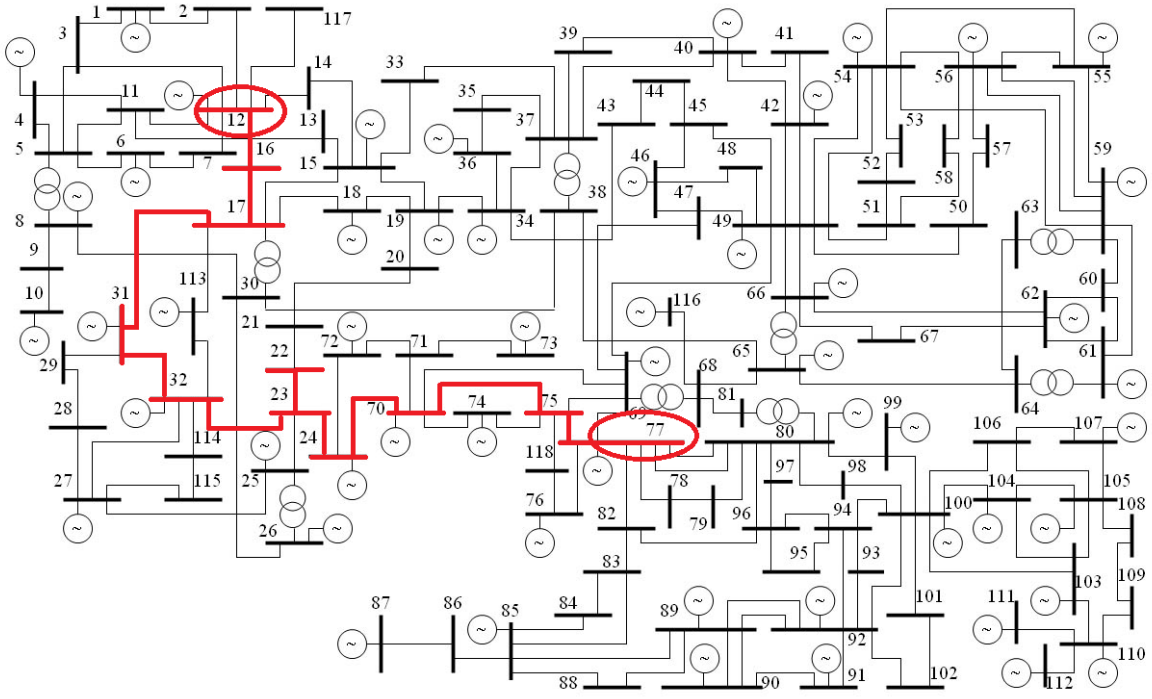

Fig. 6.6: Restoration Plan III on IEEE 118-bus system

Although this rule may work in several simple cases, it does not guarantee feasibility for all complicated systems. For example, in the test case restoration plans created by simple distance rule generate a quick path with only 10 sequences but it also shows voltage violations which may cause instability issues. Hence, considering the real-time dynamics of a power system Plan I and Plan II may not be feasible.

Table 6.2: Comparison of restoration plans

Restoration Plans	Blackstart Unit	Restored Bus	No. of Sequences	Steady-state Violations	Transient Violations
Restoration Plan I	12	77	27	No	Yes
Restoration Plan II	12	77	10	Yes	-
Restoration Plan III	12	77	22	No	No

The integrated tool is then used to create an alternative Restoration Plan III which utilizes the ADP algorithm with backward induction along with solution space reduction. This plan reduces the dimensionality of the problem and using the perception function, it can reach an optimal decision by avoiding use of any risky branches in the

restoration path that can cause transient over-voltage violations. This plan, shown in Fig. 6.6, takes 22 sequences to successfully restore bus 77 in the test system. This makes Restoration Plan III more robust and ideal for real-time scenarios. The comparison of the three plans based on voltage violations is illustrated in Table 6.2.

6.7.2 2000-bus synthetic test system

Next, the proposed integrated tool is further validated and the restoration process is demonstrated on a bigger and more complex 2000-bus synthetic test grid system which is overlayed on the geographic footprint of the state of Texas, USA served by Electrical Reliability Council of Texas (ERCOT) [123]. The system on the Texas map is shown in Fig. 6.7. In this system eight major geographic areas are identified which comprise of a total 1500 substations. The system is considered to operate at two nominal voltages, 345 kV and 115 kV.

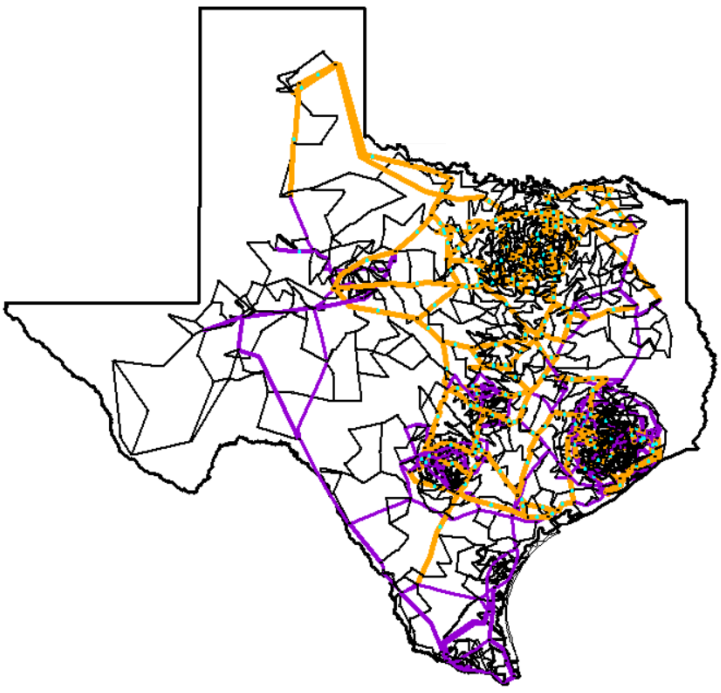

Fig. 6.7: 2000-bus synthetic grid test case [8]

6.7.2.1 Generation restoration

In the system, let us consider the generator at Bus 5262 located in Zone 1 as the Blackstart unit and assume a nuclear generator station in Zone 1 at Bus 6216. A restoration plan is devised for the nuclear generator station using Restoration Plan III which is based on the proposed ADP algorithm with solution space reduction. It is shown in case of the IEEE 118-bus system in Section 6.7.1, the Restoration Plan III does not exhibit any steady-state and transient violations and thus prove to be better than Restoration Plan I and Restoration Plan II.

The restoration plan for the nuclear generator starting from the Blackstart unit at Bus 5262 utilizes 369 sequences to reach the target generator at Bus 6216. The restoration plan model based on solution space reduction takes approximately 4 minutes to simulate and is illustrated in Table 6.3. The restoration plan is also illustrated on the county map of the power system with Blackstart unit in Somervell county as shown in Fig. 6.8.

Table 6.3: Restoration plan for 2000-bus synthetic test system

Sequence No.	Bus No.	Bus (From)	Bus (To)	Type	Bus (From)	Bus (To)	Output (MW)
1	5262	Gxxxxe3	Gxxxxe3	Gen			390.249
2	5263	Gxxxxe4	Gxxxxe1	Transf	5263	5260	
3	5317	Gxxxx10	Gxxxx20	Branch	5317	5401	
4	5401	Gxxxx20	Gxxxx21	Transf	5401	5402	
5	5402	Gxxxx21	Gxxxx21	Load			65.97
6	5405	Sxxxxxxl1	Bxxxxxd0	Branch	5045	5120	
7	5120	Bxxxxxd0	Bxxxxxd1	Transf	5120	5121	
8	5121	Bxxxxxd1	Bxxxxxd1	Load			76.66
9	5317	Gxxxy1	Wx20	Branch	5317	5388	
10	5388	Wx20	Wx21	Transf	5388	5389	
11	5389	Wx21	Wx21	Load			87.46
⋮							
361	6214	Mxxx8	Mxxx8	Gen			14.89
362	6215	Mxxx9	Mxxx4	Transf	6215	6210	
363	6210	Mxxx4	Mxxx5	Transf	6210	6211	
364	6211	Mxxx5	Mxxx6	Transf	6211	6212	
365	6212	Mxxx6	Hxxxx1	Branch	6212	6020	
366	6020	Hxxxx1	Hxxxx1	Load			16.53
366	6215	Mxxx9	Mxxx9	Gen			16.53
367	6216	Mxxx10	Mxxx4	Transf	6216	6210	
368	6212	Mxxx6	Kxxx0	Branch	6212	3014	
369	6216	Mxxx10	Mxxx10	Gen			22.002

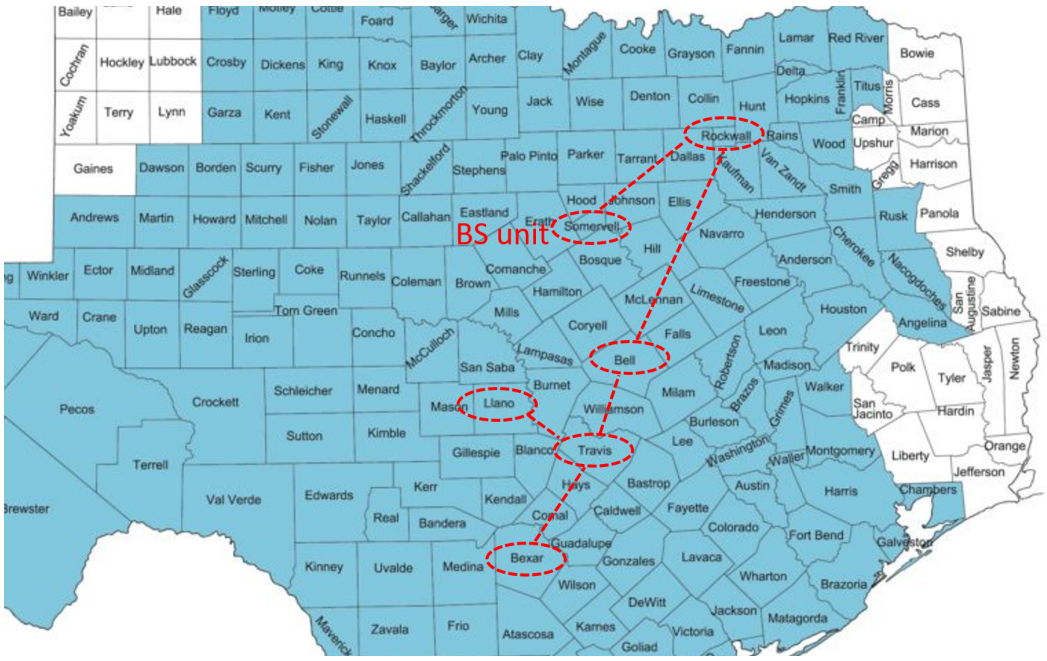

Fig. 6.8: Restoration plan on the county map of a real power interconnection. [9]

6.8 Remarks

The system restoration chapter highlights the key ideas and major algorithms that are based on complex networks science, advanced stochastic optimization techniques and theory, and experience of power engineering to address the system restoration problem in large-scale power systems. The solution has addressed a long standing issue with significant breakthroughs to system restoration technology.

The applications based on the methodology range from creation of new restoration plans to validation of existing restoration plans and non-restoration testing along with the satisfaction related to the computational times for different applications. The creation of restoration model takes less than 5 minutes on a Pentium-4 processor of a laptop computer for an approx. 3000-bus system. Validation and enhancement of over ten comprehensive restoration plan of over 10 TOs only takes about 3 days which includes the time spent in gathering information, communication with restoration plan owner for missing information and corrections.

CHAPTER 7

Extension of electrical distance in network science analysis

7.1 Background and related work

Electrical market analysis involving power exchange is becoming more and more complex due to the size and degree of interconnections in modern power systems for economic, political and environmental reasons [17]. With such inherent complexities and information deficiency, it is difficult for participants to make operational and market decisions at buses that are sensitive to the condition of transmission lines. For these reasons, it is necessary to develop an enhanced method to support decisions, particularly, those sensitive to major and critical transmission lines. The analysis can be computationally challenging, especially, when a full AC implementation approach is used [18]. As compared to the full AC analysis, a simplified analysis of the network can be done by using full network DC power flow model [19]. Although the full AC analysis would be the most accurate approach, the DC approach allows network operators to make informed dispatch decisions thereby saving time and effort required. The enormous size of power system networks makes full network DC analysis computationally taxing. To reduce the computational burden and to simplify the analysis of electricity markets, several network equivalence models have been used [18, 20, 63, 64].

Various approaches for network equivalencing have been presented in [87, 124, 125, 126, 127, 128]. These approaches follow the traditional method of eliminating less important elements from the system on the basis of geographical and electrical parameters. Such elimination results in partitioning of the network into three clusters of buses: a cluster of internal buses, a cluster of external buses, and a cluster of boundary buses that divide the external buses from the internal buses. Due to their trivial impact on the

internal system, remote generators and transmission lines connected to the boundary buses may be eliminated with minor impact on decisions. However, irrespective of the bus demarcation, market analysis of large power system networks requires retaining the desired buyer/seller pairs corresponding to operating zones in order to understand the impact of power flows on transmission lines from the buyer/seller pairs at various buses. Hence, in this study we do not eliminate the external buses but rather focus on the line flows between various operating areas. These line flows are called tie-line flows.

The metric introduced in this chapter is developed for the study and has properties similar to resistance distance which has been widely used since the early days of electrical circuit theory. There are several books on the basics of circuit analysis that deal with resistance distance and topological formula for resistance distance, for example [27]. However, recently this concept gained increased importance in view of its applications in areas outside electrical circuit theory [28, 129, 130, 131, 132, 133, 134].

In recent studies, network equivalencing has been done using generation shift factor (GSF)-based methods [63, 65, 64, 135]. In these methods, buses with similar impact on the interconnecting tie-line flows evaluated using GSFs are grouped together. In order to improve the efficiency and accuracy of bus clustering, [64] uses k-means algorithm based on GSF to cluster the buses. However, GSFs are sensitive to the change in the location of slack generator. Network operators supervising different regions of the interconnection might not be aware of the slack bus change and hence there could be discrepancies in decision making, which can provoke an impact on regional power transactions. Therefore, the main objective is to develop a new clustering method as well as new network equivalent that overcomes the limitation of the GSF-based methods.

7.2 Basic concepts

In addition to the concept of electrical distance and one of its measure, generation shift factor, which has also been discussed in Chapter 2, the basic concept of Laplacian matrix

of a graph is discussed here. The concept of Laplacian matrix of a graph provide an underlying similarity to the connection matrix of a power network and hence can be utilized in power network equivalencing. Therefore, in order to introduce the average electrical distance measure, let us first discuss the following basic concepts:

1 Laplacian matrix of a graph;

2 Foundation of electrical distance;

3 Generation shift factor.

7.2.1 Laplacian matrix of a graph

Consider a graph $G = (V, E)$ with vertex set $V = \{0, 1, \ldots, n\}$. Edge $e \in E$ connecting vertices i and j is denoted by (i, j). It is assumed that there are no loops on any vertices and there are no parallel edges connecting the vertices. In this chapter, the terms, vertices and nodes, as well as links and edges, will be used interchangeably. Let an edge (i, j) be assigned a weight w_{ij}, a positive real number. If there is no edge connecting i and j then $w_{ij} = 0$. Two vertices i and j are adjacent if there is an edge (i, j). A vertex j is incident on vertex i if there is an edge connecting i and j. The degree of a vertex i denoted by $deg(i)$ is the sum of the weights of the edges incident on i.

The Laplacian matrix, $Y = [y_{ij}]$ of G is an $(n + 1) \times (n + 1)$ matrix defined as follows:

$$y_{ij} = \begin{cases} -w_{ij}, & \text{if } i \neq j \\ deg(i), & \text{if } i = j \end{cases} \tag{7.1}$$

As an example, a graph G and its adjacent matrix are shown in Fig. 7.1(a) and 7.1(b). Note that $y_{ij} = y_{ji}$. It can be seen that the sum of all the elements in any row and the sum of all the elements in any column are both equal to zero. So, Y is singular and

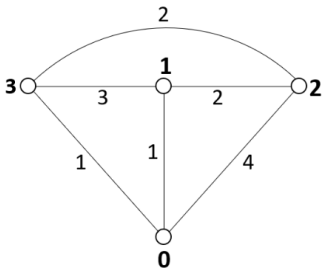

(a)

$$Y = \begin{array}{c} \\ \mathbf{1} \\ \mathbf{2} \\ \mathbf{3} \\ \mathbf{0} \end{array} \begin{array}{c} \begin{array}{cccc} \mathbf{1} & \mathbf{2} & \mathbf{3} & \mathbf{0} \end{array} \\ \begin{bmatrix} 6 & -2 & -3 & -1 \\ -2 & 8 & -2 & -4 \\ -3 & -2 & 6 & -1 \\ -1 & -4 & -1 & 6 \end{bmatrix} \end{array}$$

(b)

$$Y(o) = \begin{array}{c} \\ \mathbf{1} \\ \mathbf{2} \\ \mathbf{3} \end{array} \begin{array}{c} \begin{array}{ccc} \mathbf{1} & \mathbf{2} & \mathbf{3} \end{array} \\ \begin{bmatrix} 6 & -2 & -3 \\ -2 & 8 & -2 \\ -3 & -2 & 6 \end{bmatrix} \end{array}$$

(c)

Fig. 7.1: (a) Graph G with weighted edges; (b) Laplacian matrix of G; (c) Reduced Laplacian matrix, $Y(o)$.

has no inverse. To handle this singularity problem of Y, two different approaches are adopted, namely, the eigenvalue approach and the determinant approach.

In the eigenvalue approach, the pseudo-inverse Y^+ of Y is used. The properties of G are studied in terms of the elements of Y^+. This approach is quite popular among mathematicians. See [136, 137]. In this chapter, the determinant approach is followed which is popular in the electrical engineering community. In this approach, let us first remove a row and the corresponding column from the Laplacian matrix, Y. Let us assume that the vertex labelled o called the datum node or slack node is removed. The resulting matrix denoted by $Y(o)$ is called a reduced Laplacian matrix. The reduced Laplacian matrix $Y(o)$ of Y in Fig. 7.1(b) is shown in Fig. 7.1(c). It can be shown that the matrix $Y(o)$ is non-singular and it has several other properties. See for example, [27].

In this chapter, $Y = [y_{ij}]$ is used to denote the reduced Laplacian of the network.

7.2.2 Foundation of electrical distance

Consider an electrical network N represented by the graph G. The admittance of the edge (i, j) in N serves as the weight w_{ij} in G. Each edge (s, t) in G is associated with two variables, voltage, v_{st} and current i_{st}. See Fig. 7.2. Then by Ohm's law, we get

$$\frac{i_{st}}{v_{st}} = w_{st}, \text{ the admittance of } (s, t). \tag{7.2}$$

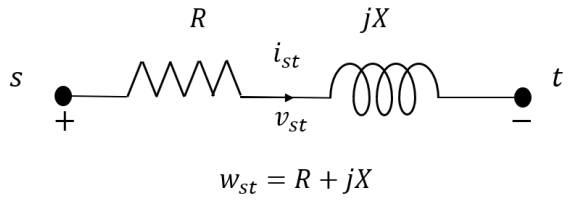

Fig. 7.2: Demonstration of Ohm's law.

In electrical engineering literature, the reduced Laplacian matrix, Y is called the node-to-datum matrix of N with vertex o as the datum vertex. Datum vertex is also known as the slack vertex. Let $Z = [Z_{ij}]$ be the inverse of the reduced Laplacian matrix. This matrix is called Z-bus (Z_{bus}) matrix in power engineering literature. Also, the ground is usually used as the slack vertex.

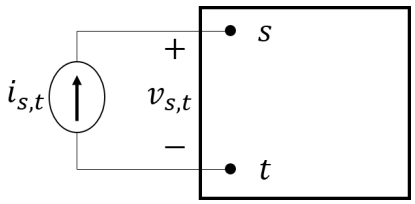

Fig. 7.3: Current source across the nodes (s, t).

Let us now connect a current source of value $i_{s,t}$ across nodes (s, t) as shown in Fig. 7.3. Let $v_{s,t}$ be the voltage across s and t. Then the electrical distance between s and t, denoted as $r_{s,t}$ is defined as

$$r_{s,t} = \frac{v_{s,t}}{i_{s,t}}. \tag{7.3}$$

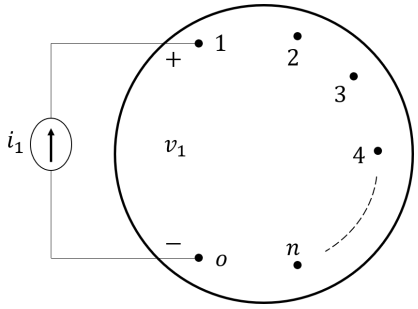

Fig. 7.4: Current source connected across $(0,1),(0,2),\ldots,(0,n)$.

Let us now proceed to show how to evaluate $r_{s,t}$ across all pairs of nodes s and t. Note that definition of $r_{s,t}$ does not require that s and t be connected by edge (s,t) in the network N. Suppose we now connect a current source of value i_s across the vertices o and for each $s \in \{1,2,\ldots,n\}$, as shown in Fig. 7.4. Note that the current flows from node o to node s. Let v_s denote the voltage from node s to node o. Let $V = \begin{bmatrix} v_1 \\ \vdots \\ v_n \end{bmatrix}$ and $I = \begin{bmatrix} i_1 \\ \vdots \\ i_n \end{bmatrix}$, then the matrix Z represents the relation between V and I as

$$\begin{bmatrix} v_1 \\ \vdots \\ v_n \end{bmatrix} = Z \begin{bmatrix} i_1 \\ \vdots \\ i_n \end{bmatrix}. \tag{7.4}$$

So,

$$Z_{ss} = \left.\frac{v_s}{i_s}\right|_{i_j=0, j\neq s}, \tag{7.5}$$

$$Z_{st} = \left.\frac{v_s}{i_s}\right|_{i_j=0, j\neq t}. \tag{7.6}$$

Note that Z_{ij} is a complex number denoted by $(R_{ij} + jX_{ij})$.

It follows from (7.5) that $r_{s,o} = Z_{ss}$, for all s. It can be shown that for all i and j

$$r_{ij} = Z_{ii} + Z_{jj} - 2Z_{ij}. \tag{7.7}$$

In power engineering literature, electrical distance r_{st} is called Thevenin resistance/impedance between the nodes s and t, denoted by $Z_{th,st}$. Thus,

$$Z_{th,st} = r_{st} = Z_{ss} + Z_{tt} - 2Z_{st}. \tag{7.8}$$

Also, in chemistry literature electrical distance is referred to as resistance distance [28].

7.2.3 Generation shift factor

Given a power network with two or more interconnected areas, in power market analysis, a simpler equivalent network is needed which preserves the flows across the lines (edges) connecting different areas. In this context and as previously discussed in Chapter 2, the concept of GSF [63] was introduced and used in determining power network equivalents.

Given a network N represented by graph G. Consider a line connecting two nodes u and v. Suppose we inject a current of unit value at node i i.e. connect a current source of unit value between node i and the slack node o. Then the current that flows through the line (u, v) is called the generation shift factor of i with respect to (u, v), denoted as $g_{uv,i}$. To find a formula for $g_{uv,i}$ consider (7.4). Then,

$$v_u = z_{u1}i_1 + z_{u2}i_2 + \ldots + z_{ui}i_i + \ldots + z_{uu}i_u, \tag{7.9}$$

$$v_v = z_{v1}i_1 + z_{v2}i_2 + \ldots + z_{vi}i_i + \ldots + z_{vv}i_v. \tag{7.10}$$

If $i_j = 0$ for all $j \neq i$ and $i_i = 1$, we get $v_u = z_{ui}$ and $v_v = z_{vi}$. Then the current flowing

through line (u, v) is given by

$$i_{uv} = \frac{z_{ui} - z_{vi}}{c_{uv}}, \tag{7.11}$$

where c_{uv} is the admittance of line (u, v). Thus the GSF of i with respect to (u, v) is

$$g_{uv,i} = \frac{z_{ui} - z_{vi}}{c_{uv}}. \tag{7.12}$$

7.3 Average electrical distance

Average electrical distance (AED) is defined as the electrical distance of a specific bus with respect to a transmission line or a tie-line connecting different operating zones. It can also be viewed as the relative electrical distance of a bus w.r.t. a line. The AED, $d_{uv,i}$, is defined as

$$d_{uv,i} = \left| \frac{Z_{th,ui} - Z_{th,vi}}{2} \right|, \tag{7.13}$$

where $Z_{th,ui}$ is the electrical distance between buses u and i and shown in Fig 7.5.

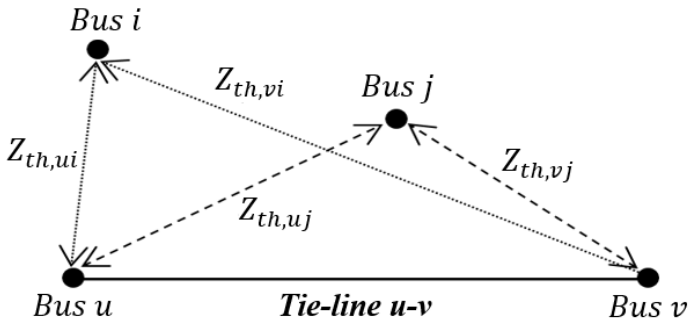

Fig. 7.5: Illustration of average electrical distance.

Using (7.8), we get

$$d_{uv,i} = \left| \frac{(Z_{uu} - 2Z_{ui} + Z_{ii}) - (Z_{vv} - 2Z_{vi} + Z_{ii})}{2} \right|, \tag{7.14}$$

$$= \left| \frac{\bar{Z}_{uu} - \bar{Z}_{vv}}{2} - (\bar{Z}_{ui} - \bar{Z}_{vi}) \right|. \tag{7.15}$$

where Z_{ui} is the corresponding (u, i) element in the bus impedance matrix shown in (7.16).

$$Z = \begin{bmatrix} Z_{11} & \cdots & Z_{1i} & \cdots & Z_{1n} \\ \vdots & \ddots & \vdots & \ddots & \vdots \\ Z_{u1} & \cdots & Z_{ui} & \cdots & Z_{un} \\ \vdots & \ddots & \vdots & \ddots & \vdots \\ Z_{n1} & \cdots & Z_{ni} & \cdots & Z_{nn} \end{bmatrix}. \tag{7.16}$$

In (7.16), the diagonal elements of the impedance matrix represent the Thevenin impedance at each corresponding bus. For real-time analysis, it is required to execute calculations of electrical distance at short intervals which can be achieved through simplification of electrical distances. Since transmission lines usually have a high X/R ratio (see Fig. 7.2), the resistances of the lines can be neglected when compared to the high reactances of lines. Thus, the impedances in (7.14) can be simplified as shown in (7.17).

$$X_{th,ui} = \bar{X}_{uu} - 2\bar{X}_{ui} + \bar{X}_{ii}, \tag{7.17}$$

where elements in $\bar{X} = [\bar{X}_{ij}]$ represent the approximation of elements in Z i.e. $Z_{ij} \approx \bar{X}_{ij}$. Then, AED defined in (7.13) can be rewritten as

$$d_{uv,i} = \left| \frac{X_{th,ui} - X_{th,vi}}{2} \right| = \left| \frac{\bar{X}_{uu} - \bar{X}_{vv}}{2} - (\bar{X}_{ui} - \bar{X}_{vi}) \right|. \tag{7.18}$$

In previous studies [65, 64], GSF-based bus clustering methods have been used to analyse the impact of injections from groups of buses on the power flows of different transmission lines. In these GSF-based methods, buses that have similar contributions to the power flows on lines of interest are grouped together based on GSFs. But GSF does not take

into account the impact of injection on buses u and v. As shown below, AED is indeed a measure that captures the impact of injection at u and v. This important characteristic of AED can be explained by analysing the relationship between AED and GSF. GSFs can be calculated using elements of $\bar{X}$ as shown in (7.19).

$$g_{uv,i} = \frac{\bar{X}_{ui} - \bar{X}_{vi}}{x_{uv}}. \tag{7.19}$$

Similarly, the sum of GSFs of bus u and bus v with respect to tie-line uv is given by

$$g_{uv,u} + g_{uv,v} = \left| \frac{\bar{X}_{uu} - \bar{X}_{vv}}{x_{uv}} \right|. \tag{7.20}$$

Comparing (7.18)-(7.20), it can be seen that $d_{uv,i}$ enhances $g_{uv,i}$ by adding an additional term capturing the impact of injection at buses, u and v, on the power flow across the tie-line, uv.

7.3.1 Calculation of AED

Algorithm given below to determine AED for each bus in the network with respect to the tie-lines of interest includes the following main steps:

Algorithm 1: Calculation of AED

1 *Creation of bus impedance matrix.* According to the system data, bus admittance matrix is first developed. Then, bus impedance matrix, shown in (7.16), is created by calculating the inverse of bus admittance matrix.

2 *Calculation of Thevenin impedance.* Using the elements of bus impedance matrix obtained in Step 1, the thevenin impedance for each pair of buses are calculated according to (7.17).

3 *Calculation of AED.* After calculating the Thevenin impedances, AEDs between buses and tie-lines of interest are calculated using (7.18). The results of AEDs are

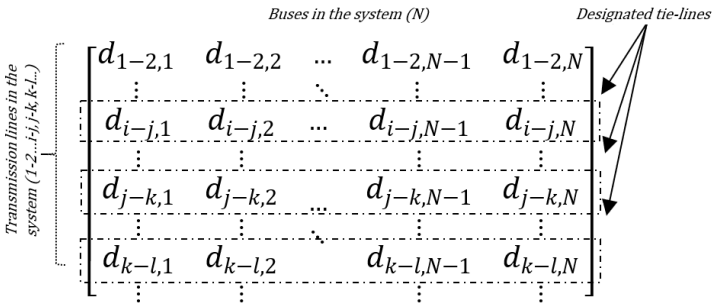

Fig. 7.6: Illustration of AED matrix.

used to create a matrix as shown in Fig. 7.6. In this matrix, each row corresponds to a tie-line and each column corresponds to a bus in the system. Thus, an element in the matrix corresponds to AED from a bus to a tie-line in the system.

■

7.3.2 Implications and relevance for social network analysis

In the graph representation of a social network, link weights are all unity. Different types of metrics/measures are defined to determine certain properties of links or nodes. For example, a measure called PageRank is used to rank the nodes in terms of their importance [138]. As another example, the betweenness measure of a link is used to determine the importance of a link. A link e is considered more important than another link e', if the fraction of the total number of messages that flow through e is greater than that for e'. In view of the connection between random walk and current flow in a resistance network [132], this fraction is in fact equal to the current through the link when a unit current is injected at a node. Taking advantage of this connection in [129], a measure similar to GSF is used to determine the betweenness measures of links. For a detailed discussion of many of these measures, see [139].

The concept of role discovery in networks was first studied in sociology [140, 141]. In this context, roles considered are social roles. Thus role discovery has become an important topic in social network analysis. Recently role discovery has been studied in other

settings such as online social networks, technological networks, biological networks, web graph etc.

In [142], a comprehensive review of literature on role discovery in network has been given. This chapter also discusses the problem of identifying clusters in a network such that all nodes in each cluster are equivalent in some sense. Two types of equivalence are considered: graph-based equivalence and feature-based equivalence. Several challenges that arise in the application of role discovery in non-static network such as dynamic and streaming graphs are also discussed in [142].

A part of this chapter is focused on clustering in a power network and its application in deriving a simplified approximate equivalent network that preserves flows along certain lines. The GSF and AED are measures that are defined for each node with respect to certain lines. If the line weights are set to unity, then these measures in the context of social networks capture the fraction of total messages that flow through a link when messages arrive (or injected) at a node. This may help in extending this work in the field of social network studies. For example, a problem of interest is to determine clusters such that the total flow carried by inter-cluster links is optimized. Once such clusters are identified, simplified approximate equivalent network can be determined as explained in Section 7.7 that can be used to predict the flows across the clusters. Further discussion of these ideas is given in Section 7.8.

7.4 k-means algorithm

k-means algorithm is one of the most popular clustering techniques in unsupervised learning tasks. Given a set of nodes or buses, this algorithm has been efficiently used to partition a network into k clusters [143]. This is based on the optimal placement of centroid for the respective cluster in a network [144].

In this algorithm, initially the network is divided into k clusters with each cluster defined

by a reference bus (centroid). Remaining buses are then partitioned and assigned appropriately to the clusters based on the closeness of each bus to k reference buses. Then cluster adjustments are made with the calculation of new centroids. These centroids act as new reference points for the next partitioning of all the buses. These adjustments naturally produce error whose minimum corresponds to "Voronoi configuration" [145] which result in reference locations at the centroid of the clusters. The error measure or potential function is the sum of all the variances and is given as shown in (7.21).

$$\phi = min \sum_{j=1}^{k} \sum_{i=1}^{n_j} |x_{ij} - \mu_j|^2, \tag{7.21}$$

where k is the total number of clusters; n_j is the number of buses belonging to the j^{th} cluster, x_{ij} represents i^{th} bus in the j^{th} cluster, μ_j is the centroid in the j^{th} cluster and the term $|x_{ij} - \mu_j|$ represents the distance between x_{ij} and μ_j.

The process becomes iterative in order for the clusters to reach a local minimum which is dependent on the initial selection of the reference buses. The k-means algorithm keeps on adjusting the centroids after each partition making it more dynamic to the changes. The k-means algorithm is explained in Algorithm 2.

Algorithm 2: k-means algorithm

1 *Selecting initial cluster centroids.* Cluster formation is initialized by selecting k centroids, i.e., $\mu_1, \mu_2, \cdots, \mu_k$ in the network. These centroids act as initial reference points for the buses to be assigned to an appropriate cluster.

2 *Grouping buses into clusters.* For the selected k centroids, based on the Euclidean distance, a bus is assigned to a cluster which has its centroid closest to the bus.

3 *Recalculating centroid positions.* After all the buses are assigned to respective

clusters, the new centroid of each cluster is recalculated as shown in (7.22).

$$\mu_j = \frac{1}{n_j} \sum_{i=1}^{n_j} x_{ij} \tag{7.22}$$

4 *Evaluating objective function in (7.21).* After all buses are grouped into the clusters in Step 2, the potential function in (7.21) is evaluated.

5 *Iterations of algorithm.* Steps 2-4 are repeated until the centroid of each cluster ceases to change its position with further iterations.

■

7.5 AED-based k-means bus clustering method

In this section, AED-based improved clustering method is discussed that uses k-means algorithm for power system network equivalence. This method uses a simple iterative technique known as Lloyd's algorithm for finding a locally minimal solution [144]. Further it utilizes AED as a measure of distance between the buses in the system. Integration of AED makes k-means algorithm more relevant to the power system network study. This is because AED gives a measure of distance of a bus with respect to a tie-line. This algorithm proves to be sufficiently accurate for the independent analysis done by various utilities on their networks.

7.5.1 AED-based k-means algorithm

With reference to the power system network equivalence, it is preferred to incorporate a measure that can reflect the true distance from a power system network perspective. AED presented in Section 7.3 is one such measure. In the network while determining the clusters, the actual distance term in the variance calculation can be replaced with the AED measure. Specifically, in (7.21) let us replace the location of the bus x_{ij} with

$d(x_{ij})$ which represents the AED of the i^{th} bus in the j^{th} cluster with respect to set of tie-lines and $d(\mu_j)$ represents the AED-based measure of the centroid in the j^{th} cluster with respect to the tie-lines. If the number of tie-lines is greater than 1, $d(x_{ij})$ is replaced with the average of AEDs considered for the given set of tie-lines. The updated potential function is shown in (7.23).

$$\phi = min \sum_{j=1}^{k} \sum_{i=1}^{n_j} |d(x_{ij}) - d(\mu_j)|^2, \tag{7.23}$$

This improves the k-means algorithm when applied in power system setting as compared to general distance used in the classical algorithm.

7.6 AED-based k-means++ bus clustering method

This section introduces AED-based improved k-means++ algorithm which can be used for clustering of large power system networks. In order to introduce the new method, let us discuss the following:

1 k-means++ algorithm;

2 AED-based k-means++ algorithm;

3 Silhouette value analysis.

7.6.1 k-means++ algorithm

Although the results showed improvements as compared to other methods used for clustering power system networks, the AED-based improved k-means clustering method may deliver inconsistent results for large power system networks comprising of a large data set. This is due to the fact that k-means algorithm uses random centroids for initialization and thus achieves different results for each simulation. To address this problem,

a seeding technique was proposed in [146] which selected the first centroid position at random and then initialized the remaining centroids by sampling probabilistically, proportional to the squared distance of the nearest centroid. This made an improvement in the k-means algorithm which helps to achieve a clustering which is $O(logk)$ competitive. This is achieved by considering a potential function that satisfies the following relation for any set of buses,

$$\mathbb{E}[\phi] \leq 8(\ln\, k + 2)\phi^*, \tag{7.24}$$

where ϕ^* is the potential function corresponding to the set of cluster centroids in the network. The resulting augmented k-means algorithm is called k-means++ algorithm.

It can be pointed out that k-means++ algorithm, due to its initialization process, produces starting centroids uniformly distributed for different iterations as compared to k-means algorithm starting centroids. This is illustrated in [147].

7.6.2 AED-based k-means++ algorithm

Different from commonly used k-means++ algorithm, the improved AED-based algorithm groups the buses in a power system into various clusters based on the closeness between buses and the centroid of each cluster in terms of AEDs. The objective of the improved AED-based k-means++ algorithm is also to minimize the same potential function, ϕ, as shown in (7.23).

To achieve the objective described in (7.23) with the initial seeding as shown in (7.24), the improved AED-based algorithm, shown in algorithm 3, includes the following main steps:

Algorithm 3: AED-based k-means++ algorithm

1 *Cluster initialization:* Cluster formation is initialized by selecting one centroid μ_1, chosen uniformly at random in the network. This centroid acts as initial reference

point for the buses to be assigned to an appropriate cluster. Those buses that are closer to μ_1 are later assigned to the same cluster.

2 *Determining cluster centroids.* Given the centroids, $\mu_1, \ldots, \mu_{j-1}$, a new centroid, μ_j, is chosen and each bus, i, is selected with probability

$$\frac{D(i)^2}{\sum_{i=1}^{n} D(i)^2},$$

where $D(i) = \min|d(uv, i) - d(uv, \mu_r)|$, where $r = 1, \ldots, j-1$.

3 Step 2 is repeated until we get all the centroids.

4 *k-means algorithm.* Proceed as with the standard k-means algorithm (Algorithm 2) with AED used as distance measure as discussed in Section 7.5.

■

7.6.3 Silhouette value analysis

An important problem in the application of k-means algorithm is to determine an appropriate value of k. This problem has been extensively studied in mathematical statistics literature [148, 149]. The authors in [150] identified certain best performing methods. In [148], authors determined through extensive simulation studies that all the best performers do quite well in selecting the appropriate number of clusters. This algorithm uses silhouette value analysis proposed in [151] which is also among the best performers.

Silhouette value analysis is a graphical partitioning technique [152] allowing an appreciation of the relative quality of clusters. Here, silhouette value analysis is used to enhance the quality of clusters identified by the improved AED-based k-means++ clustering algorithm. The main steps of the silhouette value analysis that are incorporated into the improved AED-based k-means algorithm are explained below:

Algorithm 4: Silhouette value analysis algorithm

Consider that in a network with k clusters, a bus $i \in \{1, 2, \cdots, n\}$ is assigned to a cluster $j \in \{1, 2, \cdots, k\}$. Let n_j be the number of buses in cluster j and k is the arbitrarily selected number of clusters. Clusters neighboring j are represented by $m \in \{1, 2, \cdots, k-1\}$ such that $m \neq j$; these are all the clusters other than j.

1 *Evaluating closeness between buses in a cluster.* In this step, the average closeness between the buses in cluster j is evaluated by calculating AED measure, ac_{ij}, with respect to the tie-lines in the network. This is shown in (7.25).

$$ac_{ij} = \frac{1}{n} \sum_{\substack{r=1 \\ r \neq i}}^{n_j} |d(uv, i) - d(uv, r)| \tag{7.25}$$

2 *Evaluating closeness between each bus and clusters.* In this step, the minimum of average closeness of a bus i with respect to each cluster $m \neq j$ is evaluated which is given by eb_{im}.

$$eb_{im} = \frac{1}{n_m} \sum_{r=1}^{n_m} |d(uv, i) - d(uv, r)|, \ m = 1, \ldots, k-1; \ m \neq j \tag{7.26}$$

where n_m is the number of buses in cluster m.

3 *Calculating average silhouette coefficient of all the clusters.* The silhouette coefficient of a bus indicates whether its placement is in an appropriate cluster. Silhouette coefficient (s_{im}) of bus i can be calculated as

$$s_{im} = \frac{eb_{im} - ac_{ij}}{\max(ac_{ij}, eb_{im})}, \ m = 1, \ldots, k-1; \ m \neq j \tag{7.27}$$

The average of silhouette coefficients, s_{im}, of buses is evaluated as s_i. The average silhouette coefficient, s_i, of all the buses in the whole network is evaluated to give a perspective of average closeness of all the buses to their neighboring clusters. The coefficient is in a range $[-1, +1]$, where $+1$ indicates that buses are far away from their closest neighboring clusters; while -1 indicates that the buses are closer to

their neighboring clusters.

4 *Selecting value of k based on silhouette value analysis.* Steps 1, 2 and 3 are repeated for different values of k and the one with average silhouette coefficient closest to +1 is selected.

■

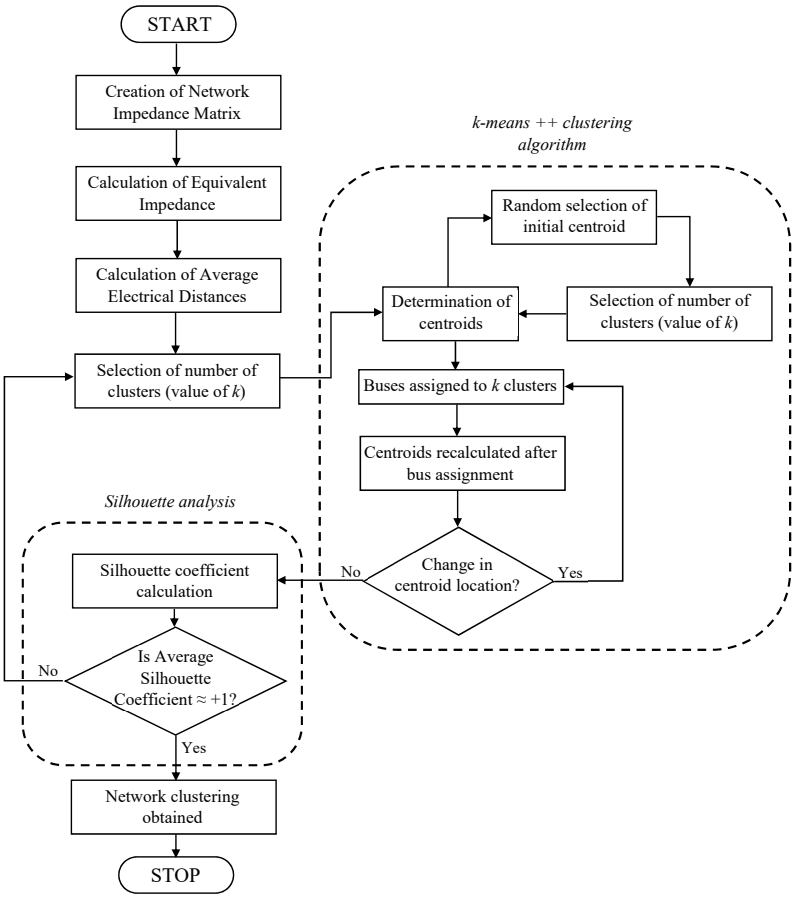

Fig. 7.7: Flowchart for the proposed improved k-means++ based clustering process.

7.6.4 Flowchart

The proposed AED-based bus clustering method integrates the improved AED-based k-means++ algorithm and silhouette value analysis to group buses for network equivalence of large power system networks. The flowchart shown in Fig. 7.7 describes this bus clustering method.

7.7 Power network equivalencing based on AED-based k-means++ clustering method

7.7.1 Power network equivalents based on aggregation of buses in a cluster

The given power system network is divided into various sub-networks governed by local utilities and connected by several tie-lines. Power system operators employ various approximation methods to quickly analyse the behavior of power system. To replicate the scenario, a similar methodology is employed that divides a given sub-network into smaller areas. This allows us to identify the tie-lines connecting the smaller areas. Further the AED-based improved clustering method is then used to identify appropriate clusters within each smaller area from which the equivalent network is obtained. The equivalent network includes each cluster represented by an equivalent bus with a combined generation and load for that cluster connected directly to it. This equivalent bus is connected to the other equivalent buses through the tie-lines. A sample aggregation is illustrated in Fig. 7.8. In Fig. 7.8(a), a part of the network is shown with two identified clusters connected through a tie-line. Each cluster can be approximated by considering a single aggregated bus without any change in relevant information. As a result, a simple approximated network is obtained with each aggregated bus representing its respective cluster. This is shown in Fig. 7.8(b).

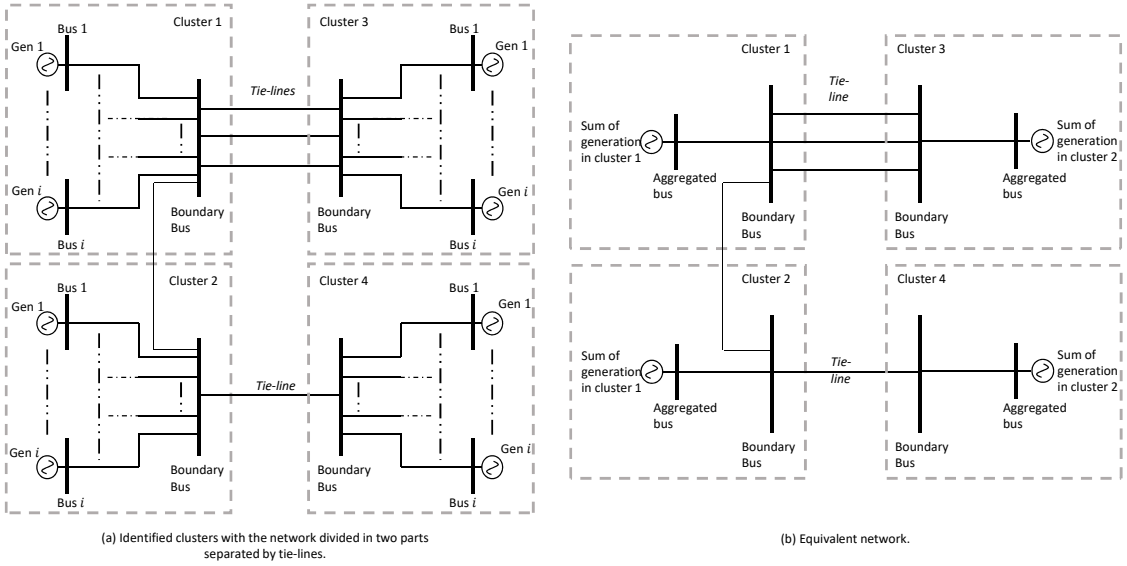

Fig. 7.8: Illustration of equivalent network construction.

7.7.2 Case Studies using Tie-lines

In this section, let us demonstrate the efficacy of the proposed AED-based improved k-means++ clustering method by comparing it with the previous clustering method [93] (Section 7.5) on the IEEE 39-bus system. Then, IEEE 300 bus system is used to show the superiority of the proposed method when compared to the widely used GSF-based clustering method [63, 65, 64, 135].

7.7.2.1 39-bus system

The IEEE 39-bus system is a standard test system composed of 39 buses with 10 generators and 18 loads connected as shown in Fig. 7.9 [153, 154]. The net generation and load capacity is 5266.69 MW and 5222.80 MW, respectively. The system is considered

to be divided into two areas interconnected with four tie-lines in order to analyse the impact of any injection change in generation/load zones on designated transmission line flows. In Fig. 7.9, area 1 comprises of 24 buses while area 2 consists of 15 buses.

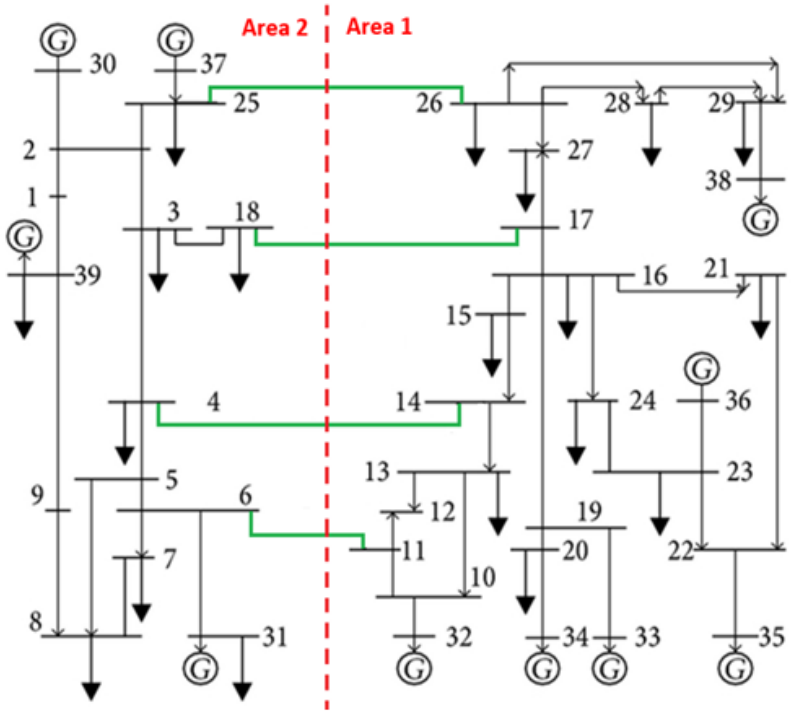

Fig. 7.9: IEEE 39-bus system.

7.7.2.1.1 ***Comparison of AED-and GSF-based clustering methods using single tie-line scenario:*** In the system, the proposed AED-based clustering method is compared with GSF-based clustering method using Single tie-line Scenario in which the two areas in the system are connected only via one of the four tie-lines. In the scenario, let us change the single tie-line connecting two areas to compare the tie-line flows in equivalent network based on the two methods in terms of minimum and maximum flow, and standard deviation.

First, the clusters of the proposed AED-and GSF-based clustering methods are compared. The results are presented in Tables 7.1 and 7.2. Table 7.1 shows the clusters of the GSF-based clustering technique for tie-line 25-26 when slack generator bus is chosen at buses 30 and 39, respectively. Table 7.2 shows the clusters of the AED-based

clustering technique for tie-line 25-26 when slack generator bus is chosen at buses 30 and 39, respectively.

Table 7.1: Identified clusters based on GSF method with slack generator at two different buses for tie-line 25-26.

Tie-Line 25-26 & Tie-Line 17-18			
Slack bus 30		**Slack bus 39**	
Clusters	Buses	Clusters	Buses
SA 11	26,27,28,29,38	SA 11	26,28,29,38
SA 12	16,21,22,23,24,25, 36	SA 12	16,19,20,21,22,23,24, 33,34,35,36
SA 13	19,20,32,33,34	SA 13	10,11,12,13,14,15,32
SA 14	10,11,12,13,14,15, 17,32	SA 14	17,27
SA 21	25,37	SA 21	1,2,3,18,25,30,37
SA 22	1,2,3,4,5,6,7,8,9,18, 30,31,39	SA 22	4,5,6,7,8,9,31,39

It can be observed from Table 7.1 that clusters based on GSF-based clustering method are sensitive to the location change of slack generator. When the location of slack generator buses changes from bus 30 to bus 39, the same cluster has different buses. For example, when the location of slack generator is at bus 30, cluster SA11 consists of 5 buses (i.e., 26, 27, 28, 29 and 38); however, when the location of slack generator is at bus 39, cluster SA11 contains only 4 buses (i.e., 26, 27, 28 and 38).

Table 7.2: Identified clusters based on AED method with slack generator at two different buses for tie-line 25-26.

Tie-Line 25-26 & Tie-Line 17-18			
Slack bus 30		**Slack bus 39**	
Clusters	Buses	Clusters	Buses
SA 11	26,28,29,38	SA 11	26,28,29,38
SA 12	16,19,20,21,22,23,24, 33,34,35,36	SA 12	16,19,20,21,22,23,24, 33,34,35,36
SA 13	10,11,12,13,32	SA 13	10,11,12,13,32
SA 14	14,15,17,27	SA 14	14,15,17,27
SA 21	1,2,25,30,37	SA 21	1,2,25,30,37
SA 22	3,4,5,9,18,39	SA 22	3,4,5,9,18,39
SA 23	6,7,8,31	SA 23	6,7,8,31

It can be seen from Table 7.2 that clusters identified based on AED are independent of the location change of slack generator. When the location of slack generator changes

from bus 30 to bus 39, each cluster has the same buses. For instance, when the location of slack generator is at bus 30, cluster SA11 consists of 4 buses (i.e., 26, 28, 29, and 38); when the location of slack generator is at bus 39, cluster SA11 is also composed of 4 buses (i.e., 26, 28, 29, and 38). In addition, comparing the results of Table 7.1 with those of Table 7.2, the identification results of AED-based method are different from those of GSF-based method. Especially, at the same location of slack generator, the total number of clusters identified based on AED method is different from the one identified based on GSF method; also, buses in each cluster identified based on AED method are different from those identified based on GSF method.

The formation of clusters for the two methods regarding slack bus 39 can be better visualized in Fig. 7.10 with graphical representation of the network. The weighted graphs are constructed based on following rules: 1) each cluster is represented by a vertex; 2) the size of the vertex is based on average of electrical distances between the buses in the cluster; 3) the edges represent the electrical connections between the clusters; 4) dashed edges represent the interconnected tie-lines between the two areas; 5) the thickness of an edge represents the closeness between two clusters determined by the average of electrical distance between the buses of two clusters. Based on the graphs in Fig. 7.10, smaller vertex size in graph representing clusters for AED-based method suggests that buses are close to each other which is not the case with GSF-based method.

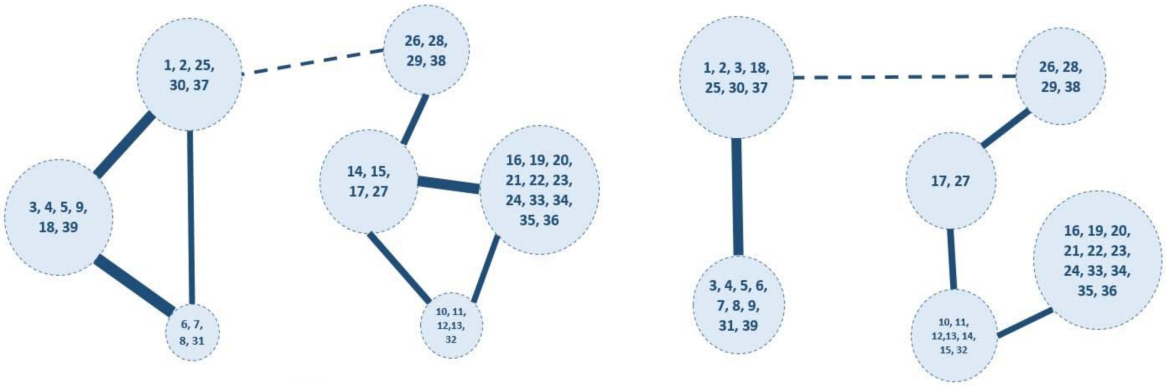

a. Clusters based on AED method

b. Clusters based on GSF method

Fig. 7.10: Weighted graph of identified clusters for slack generator 39 and tie-line 25-26.

As seen from the graphical representation, the clusters identified based on the AED-and GSF-based clustering methods are different. To further compare the identified clusters, the equivalent networks based on clusters identified with each method are created, and the tie-line active power flow is calculated in the equivalent networks. The tie-line flow in the equivalent network is compared with the one in the original network. In the original network, the tie-line flows are calculated using GSFs. In the equivalent networks, tie-line flows are calculated based on average GSFs. After buses in the original network are partitioned into different clusters, the average GSF in a cluster can be obtained by averaging all GSFs of buses in the cluster relative to a designated tie-line. Note that in the study, only one of the four tie-lines connects the two areas in the system. When a single tie-line changes, buses are regrouped to obtain new average GSFs to calculate the flow of new tie-line in equivalent networks. Also, note that the clusters identified based on AED-based method are independent from the location change of slack generator; however, the tie-line flow is sensitive to the location change of slack generator since the tie-line flow is calculated with average GSFs, which depend on the location change of slack generator.

Table 7.3: Comparison of tie-line 25-26 active power flow in reduced networks created based on GSF and AED methods with slack generator at different buses.

		Reduced network based on GSF method		**Reduced network based on AED method**	
Reference Bus	Original Flow (MW)	Flow (MW)	% deviation	Flow (MW)	% deviation
Bus 30	23.269	22.998	1.16	23.310	0.18
Bus 31	23.171	22.839	1.44	23.117	0.23
Bus 32	19.592	18.867	3.70	20.166	2.93
Bus 33	19.158	19.506	1.81	19.726	2.96
Bus 35	19.158	19.749	3.08	19.731	2.99
Bus 37	23.343	23.094	1.07	23.346	0.01

Table 7.3 shows the comparison of active power flows on tie-line TL 25-26 in the original network with those in reduced networks based on AED-and GSF-based clustering method with slack bus at different locations. It can be seen from Table 7.3 that with slack bus location at bus 30, 31, 32, 35, 37, the tieline flow in AED-based reduced

network is closer to the one in the original network than the tie-line flow in GSF-based reduced network; on the other hand, when the slack bus location is at bus 33, the tie-line flow in GSF-based reduced network is closer to the one in the original network than the tie-line flow in AED-based reduced network. Thus, according to the results in Table 7.3, it can be concluded that for majority of slack bus selections AED-based reduced network is better than GSF-based reduced network.

Table 7.4: Comparison of active power flow for different tie-lines in reduced networks based on GSF and AED methods.

	Reduced network based on GSF method				**Reduced network based on AED method**			
Tie-lines	Max flow (MW)	Min flow (MW)	Range (MW)	Std. dev.	Max flow (MW)	Min flow (MW)	Range (MW)	Std. dev.
Line 25-26	23.094	18.867	4.227	1.93	23.346	19.665	3.681	1.76
Line 17-18	23.246	19.967	3.279	1.40	23.450	20.209	3.241	1.39
Line 4-14	23.335	19.788	3.547	1.61	23.496	20.287	3.209	1.51
Line 6-11	23.535	19.736	3.798	1.50	23.514	20.423	3.091	1.46

Further a comparison is made based on the changes of tie-line flow with different locations of slack generator in AED-and GSF-based reduced networks in terms of maximum, minimum, and standard deviation. Table 7.4 shows the maximum, minimum, and standard deviation of active power flows of four tie-lines in AED and GSF-based reduced networks when slack generator changes in 10 different locations. It can be seen from Table 7.4 that AED-based bus clustering method is better than GSF-based bus clustering method. In AED-based reduced network, the change of each tie-line flow is smaller than the one in GSF-based reduced network. The change range is represented with the difference of maximum and minimum power flow. Also, the standard deviation of each tie-line flow is smaller in AED-based reduced network than the one in GSF-based reduced network when slack generator changes in different locations. The smaller deviation in tie-line flows suggests that AED-based bus clustering method gives a more accurate reduced network that can represent the original network.

To further validate the efficacy of the proposed method, the buses in clusters created by the two methods are compared for similarity. In AED-based method, buses are grouped together based on AEDs. The similarity of buses is measured by standard deviation of AEDs. In GSF-based method, buses are aggregated together based on GSFs. The similarity of buses is measured by standard deviation of GSFs. In order to make a comparison between the clusters of reduced networks based on the two methods, the average of standard deviation of AED and GSF is calculated for their respective reduced networks for each tie-line. Fig. 7.11 shows the comparison of average of standard deviation of AED and GSF for each tie-line for the respective network reduction method. In Fig. 7.11, blue bars indicate the average of standard deviation of AEDs in the clusters corresponding to each tie line; orange bars represent the average of standard deviation of GSFs in the clusters corresponding to each tie line. It can be observed from Fig. 7.11 that for each tie-line, buses in clusters created based on AEDs are slightly closer to each other than those in clusters created based on GSFs. This is based on the fact that the average of standard deviations of AEDs in clusters for each tie line is slightly smaller than the average of standard deviations of GSFs in clusters for each tie line. This may validate the results presented in Table 7.3 and Table 7.4 that the tie line flows in the equivalent networks created by AED-based method are more accurate than those in the equivalent networks created by GSF-based method.

7.7.2.1.2 ***Comparison of proposed method with method of Section 7.5 based on two tie-line scenario:*** Further in this study, the two tie-line scenario is used to compare the proposed method with the method of Section 7.5. In this scenario, any two tie-lines out of four are utilized to connect the two areas in the system. Bus 31 is chosen as slack bus. Under this scenario, the clusters are identified using the two methods which are based on average AEDs of each bus with respect to the two tie-lines connected. The two clustering methods follow different algorithms and hence the clusters obtained using the two methods are different as can be observed in Table 7.5.

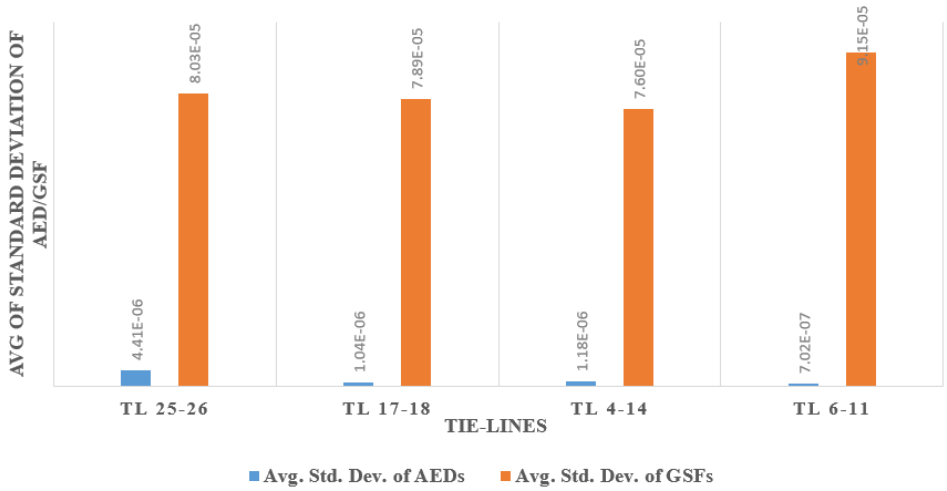

Fig. 7.11: Comparison of average of standard deviations of AEDs and GFSs in clusters for each tie line.

This may affect the accuracy of tie-line flows in equivalent networks when compared to the tie-line flows in the original network. The comparison of accuracy of tie-line flows in the equivalent network is demonstrated using tie-line flow analysis. Further, the quality of clusters in the equivalent networks is also analyzed based on the similarity of buses in each cluster.

Table 7.5: Comparison of clusters identified by two different AED-based clustering methods

Tie-Line 25-26 & Tie-Line 17-18			
Clusters identified by AED-based k-means algorithm (Section 7.5)		**Clusters identified by proposed AED-based improved k-means++ algorithm** (Algorithm 3)	
Clusters	Buses	Clusters	Buses
SA 11	26,28,29,38	SA 11	26,28,29,38
SA 12	27	SA 12	27
SA 13	10,11,12,13,14,15,16,17, 19,20,32,33,34,35,36	SA 13	10,11,12,13,14,15,16,17, 19,20,32,33,34,35,36
SA 21	25,37	SA 21	25,37
SA 22	1,2,30,39	SA 22	1,2,30
SA 23	18	SA 23	39
SA 24	3,4,5,6,7,8,9,31	SA 24	3,18
		SA 25	4,5,6,7,8,9,31

7.7.2.1.3 *Tie-line Flow Analysis* (Algorithm 3 and method of Section 7.5):

The tie-line flow analysis is based on the comparison of accuracy of net tie-line flows in the equivalent networks with those in the original network. The equivalent networks are

created using Algorithm 3 and method of Section 7.5. Different cases with combinations of two tie-lines are studied. In this study, the tie-line flows in the original network are calculated using GSFs and those in the equivalent networks are calculated using average GSFs for each cluster.

Table 7.6 shows the comparison of net tie-line flows under different tie-line combination cases. It can be observed from Table 7.6 that the net tie-line flows in the equivalent networks created using the proposed method are more accurate than those in the equivalent networks created using the AED-based k-means clustering method of Section 7.5. For instance, in cases 1, 4, 5 and 6, the net flows in the tie-lines in equivalent network obtained using AED-based k-means++ method are more accurate as compared to the net flows in equivalent network obtained using AED-based k-means method. For cases 2 and 3, the net flows in the equivalent networks obtained using the two methods are almost similar. Next, a study involving the quality of clusters is presented which explains the tie-line flow analysis on the basis of cluster formations and similarity of buses in each cluster.

Table 7.6: Comparison of net tie-line power flows in the original network and AED-based equivalent networks for 39 bus system

		Original Network	**AED-based Equivalent Networks**			
			AED-based k-means algorithm (Section 7.5)		**AED-based k-means++ algorithm** (Algorithm 3)	
Case No.	**Tie-Line Combination**	Flow (MW)	Flow (MW)	% deviation	Flow (MW)	% deviation
Case 1	TL25-26/ TL17-18	41.30	41.50	0.48%	41.34	0.10%
Case 2	TL25-26/ TL4-14	35.78	35.81	0.09%	35.75	0.09%
Case 3	TL25-26/ TL6-11	41.50	40.50	2.40%	40.49	2.43%
Case 4	TL17-18/ TL4-14	10.67	19.73	84.90%	18.85	76.66%
Case 5	TL17-18/ TL6-11	23.58	40.52	71.82%	32.76	38.93%
Case 6	TL4-14/ TL6-11	32.81	32.67	0.43%	32.77	0.12%

7.7.2.1.4 ***Cluster Quality Analysis*** Here the quality of clusters is analyzed which has been identified using Algorithm 3 and method of Section 7.5. In this study, the cluster quality analysis is carried out in terms of the similarity of buses in clusters. The similarity is measured by the average of standard deviation of the AEDs in each of the clusters identified by the AED-based k-means++ algorithm and the k-means++ algorithm. The standard deviation of the buses in a cluster can be defined as

$$\sigma_j = \sqrt{\frac{1}{n_j}\sum_{i=1}^{n_j}(d_{ij} - \mu_j)^2} \tag{7.28}$$

where σ_j represents the standard deviation of AEDs in j^{th} cluster; d_{ij} indicates the AED of i^{th} bus in j^{th} cluster; μ_j indicates the mean of AEDs in j^{th} cluster. In (7.28), a smaller value of standard deviation indicates that the AEDs of the buses tend to be closer to the mean of the cluster, i.e. the buses are closer to each other.

The analysis of the cluster quality is carried out based on (7.28), the results of which are shown in Fig. 7.12. The figure compares the average of standard deviation of the clusters identified by the AED-based improved k-means++ clustering method with those identified with the previous method. In Fig. 7.12, for each case of combinations of tie-lines, gray bars indicate the average of standard deviations of AEDs for the clusters obtained using AED-based improved k-means++ algorithm; black bars correspond to the average of standard deviations of AEDs for the clusters obtained using previous AED-based algorithm.

It can be observed from Fig. 7.12 that for each set of two tie-lines, the similarity of buses in clusters created using proposed AED-based k-means++ algorithm is clearly more as compared to the buses in clusters created using previous AED-based method. Based on similarity of buses in the clusters, the created equivalent network has net tie-line flows very similar to the original network which can be observed from Table 7.6.

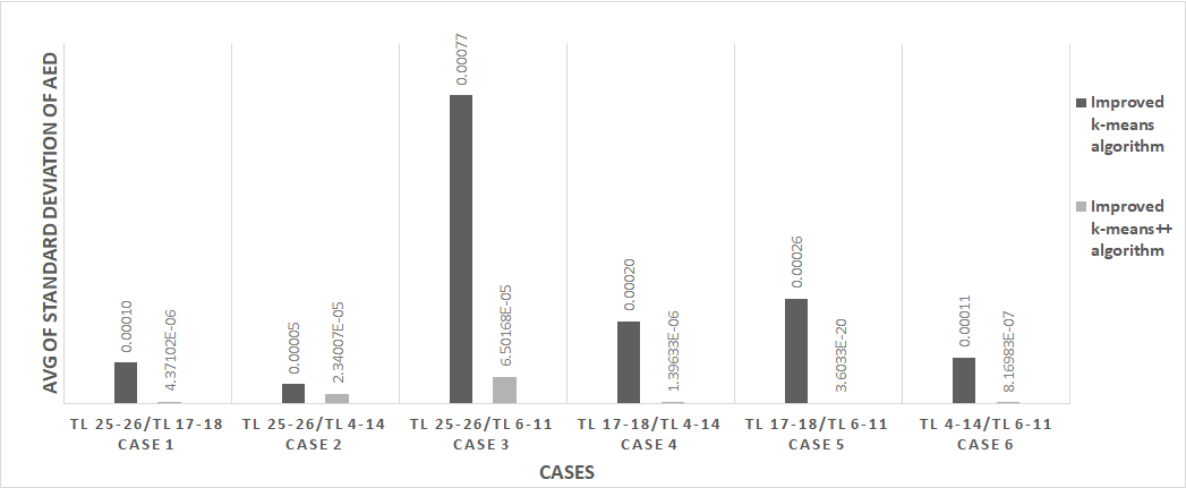

Fig. 7.12: Comparison of averages of standard deviations of AEDs in clusters for different methods for 39-bus system.

Thus, modifying the clustering method by replacing the method of Section 7.5 with the proposed AED-based improved k-means++ algorithm provides much accurate results for network clustering schemes.

7.7.2.2 300-bus system

The IEEE 300-bus system is a test system developed by the IEEE Test Systems Task Force in 1993 [155]. It is composed of 300 buses with 69 generators and 195 loads connected through 409 transmission lines as shown in Fig. 7.13. Similar to IEEE 39-bus system, in order to analyse the impact on designated transmission line flows, the system is divided into two major areas interconnected using four tie-lines. In Fig. 7.13, area 1 comprises of 111 buses with total load of 11824.31 MW; area 2 consists of 189 buses and total load of 11701.54 MW. Bus 7049 is chosen as slack bus.

To demonstrate the efficacy of Algorithm 3, let us compare it with the widely used GSF-based clustering method. Different two tie-line scenarios are used in the 300-bus system and the two methods, based on average AEDs and average GSFs respectively, are used to identify clusters to obtain equivalent networks using k-means++ algorithm. Further, to validate the use of k-means++ algorithm, let us compare Algorithm 3 with the

AED-based method of Section 7.5 that uses k-means algorithm. In this study, different two tie-line scenarios are used in the 300-bus system for clustering. These methods yield different clusters for the same network and in order to compare the two clustering methods, the accuracy of tie-line flows in the equivalent networks is analyzed. Analysis of the quality of clusters in these equivalent networks is done in terms of similarity of buses in each cluster.

7.7.2.2.1 ***Tie-line Flow Analysis*** **(Algorithm 3, method of Section 7.5 and GSF-based clustering method)** This section compares the net tie-line flows in the equivalent networks with those in the original 300-bus network. In order to study the flows, cases with different combinations of two tie-lines connect the areas in the network are considered. The results are shown in Table 7.7 and Table 7.8 with different combinations of two tie-lines. The net tie-line flows in the equivalent networks in Table 7.7 are obtained using average GSFs for cluster identification. It can be observed that for each of the cases, the net tie-line flow in the equivalent network created using the proposed method is more accurate as compared to the tie-line flow in equivalent network created using the GSF-based method that uses k-means++ algorithm. Also, from Table 7.8, it can be observed that the tie-line flows in the AED-based equivalent network using k-means++ algorithm are better as compared to the equivalent network that uses k-means algorithm. Further, cluster quality analysis is done in order to compare the methods based on the similarity of buses in each of the cluster obtained in equivalent networks.

7.7.2.2.2 ***Cluster Quality Analysis*** **(Algorithm 3 and GSF-based clustering method)** This section analyses the quality of clusters identified using the proposed method (Algorithm 3) and GSF-based method in terms of similarity of buses. Here, the similarity of buses refers to the degree of change in AEDs or GSFs in a cluster with respect to a set of tie-lines. The similarity of buses in a cluster is decided using

Table 7.7: Comparison of net tie-line power flows in the original network and those in GSF and AED-based equivalent networks obtained using Algorithm 3 for 300 bus system

		Original Network	**GSF-based equivalent network**		**AED-based equivalent network** (Algorithm 3)	
Case No.	**Tie-Line Combination**	Flow (MW)	Flow (MW)	% deviation	Flow (MW)	% deviation
Case 1	TL19-87/ TL8-14	448.09	375.31	16.24%	392.85	12.33%
Case 2	TL19-87/ TL4-16	1051.79	1019.24	3.09%	1032.31	1.85%
Case 3	TL19-87/ TL62-144	55.34	156.84	183.41%	57.93	4.68%
Case 4	TL8-14/ TL62-144	450.86	391.79	13.10%	487.01	8.02%
Case 5	TL4-16/ TL62-144	994.46	490.70	50.66%	973.19	2.14%

the standard deviation of buses given by (7.28). Based on (7.28), results are obtained as shown in Fig. 7.14. In this figure, for each combination of two tie-lines, grey bars indicate the average of standard deviations of AEDs for the clusters obtained using AED-based improved k-means++ algorithm; black bars correspond to the average of standard deviations of GSFs for the clusters obtained using widely used GSF-based clustering method.

It can be observed from Fig. 7.14 that for each set of two tie-lines, buses in clusters created based on AEDs are more similar than those in clusters created based on GSFs since the average of standard deviations of AEDs in clusters for each set of two tie-lines is smaller than the average of standard deviations of corresponding GSFs. Based on the similarity and closeness of buses in the clusters, the created equivalent network has net tie-line flows very similar to that of the original network. It can be observed from Table 7.7, that the net tie-line flows in the equivalent network of 300-bus system created by bus clustering method using AED-based improved k-means++ algorithm are more accurate than those in the equivalent network created by GSF-based bus clustering method. Similar results comparing AED-based k-means algorithm [93] and the proposed k-means++ algorithm are shown in Table 7.8.

Table 7.8: Comparison of net tie-line power flows in the original network and the AED-based equivalent networks obtained using the Algorithm 3 and method of Section 7.5

		Original Network	**AED-based Equivalent Networks**			
			AED-based k-means algorithm (Section 7.5)		**AED-based k-means++ algorithm** (Algorithm 3)	
Case No.	**Tie-Line Combination**	Flow (MW)	Flow (MW)	% deviation	Flow (MW)	% deviation
Case 1	TL19-87/ TL8-14	448.09	292.39	28.08%	392.85	12.33%
Case 2	TL19-87/ TL4-16	1051.79	978.73	6.95%	1032.31	1.85%
Case 3	TL19-87/ TL62-144	55.34	89.87	62.39%	57.93	4.68%
Case 4	TL8-14/ TL62-144	450.86	324.26	28.08%	487.01	8.02%
Case 5	TL4-16/ TL62-144	994.46	922.42	7.24%	973.19	2.14%

7.8 Remarks

This chapter presents an AED-based improved bus clustering method for network equivalence of large interconnected power systems. The method utilizes AED-based improved k-means++ algorithm for grouping similar buses together to form clusters on the basis of their respective AEDs. The new algorithm is obtained by augmenting the AED-based k-means algorithm to probabilistically initialize the centroids of clusters thereby, as in [137], improving the accuracy of the algorithm. The use of silhouette analysis along with improved k-means++ algorithm has resulted in further maximizing the accuracy of the clusters. The proposed method has been compared with the previous method presented in [93] on the IEEE 39-bus system. It has been shown that when compared to the full network, the net tie-line flows in the equivalent networks created using the proposed method are more accurate than those in the equivalent networks created using the previous AED-based k-means method. Also, the proposed method yields a better cluster quality which shows that the buses in clusters formed using the proposed method are more closely connected than those in the clusters formed using the previous AED-based k-means method.

Moreover, the proposed method has been compared with the widely used GSF-based clustering method [64] on the IEEE 300-bus system. It has been shown that the net tie-line flows in the network with different combinations of tie-lines are more accurate for the equivalent network obtained using the proposed AED-based improved k-means++ clustering method than the one obtained using GSF-based clustering method as well as the one obtained with the AED-based k-means algorithm. Further, the results of the cluster quality analysis show that the buses in the clusters obtained using proposed method are more closely connected. Thus the reduced network obtained using the proposed method gives a better representation of the original network as compared to the widely used GSF-based clustering method.

Section 7.3.2 of this chapter discusses the relevance and implications of this work in the context of social network analysis. This chapter concludes by pointing to an application to what is called the community detection problem in social networks. A community in a social network is a collection of closely related nodes with respect to a closeness measure. For a detailed discussion of the community detection problem, see [139]. Electrical distance is a measure of closeness of two nodes when the links are assigned weights that capture the characteristics of interest. The Kirchhoff index [156, 157, 158] of a cluster is the sum of electrical distances between all pairs of nodes in the cluster. The smaller the Kirchhoff index of a cluster, the closer are the nodes in the cluster. On the other hand, the sum of the AEDs of all the nodes in a cluster is a measure of the total flow across inter-cluster links. Let us call this as inter-cluster Kirchhoff index. Then the smaller the inter-cluster Kirchhoff index of two clusters, the less closely connected are the nodes in the two clusters. A problem of interest is designing a clustering algorithm that determines clusters such that the Kirchhoff index of each cluster and inter-cluster Kirchhoff index of each pair of clusters are within pre-specified limits. The clusters so determined will provide a solution to the community detection problem in social networks. This is a fairly complex problem involving the solution of a bi-criteria optimization problem, Kirchhoff indices of clusters and inter-cluster indices

of pairs of clusters, optimization problem.

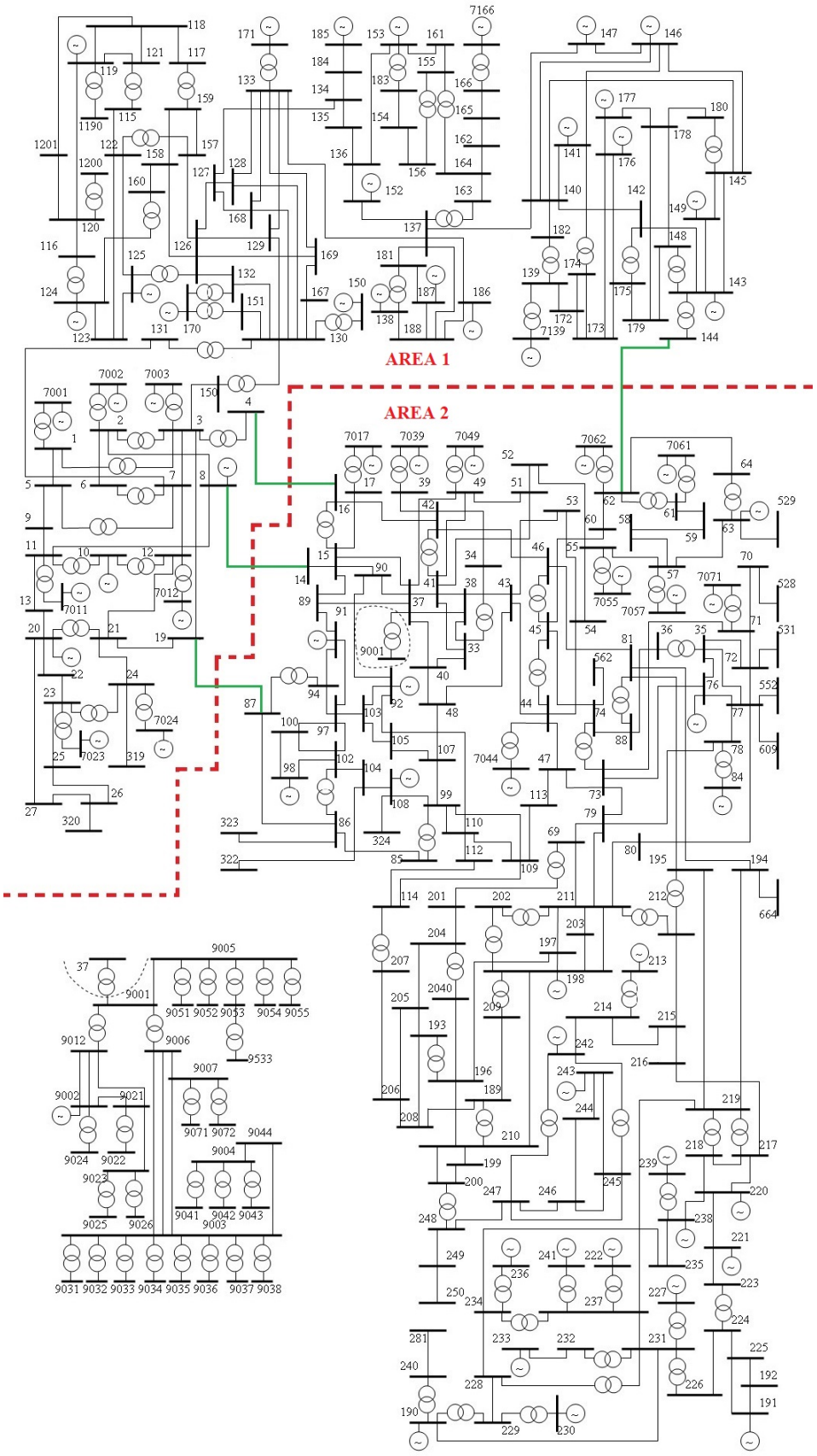

Fig. 7.13: IEEE 300-bus system.

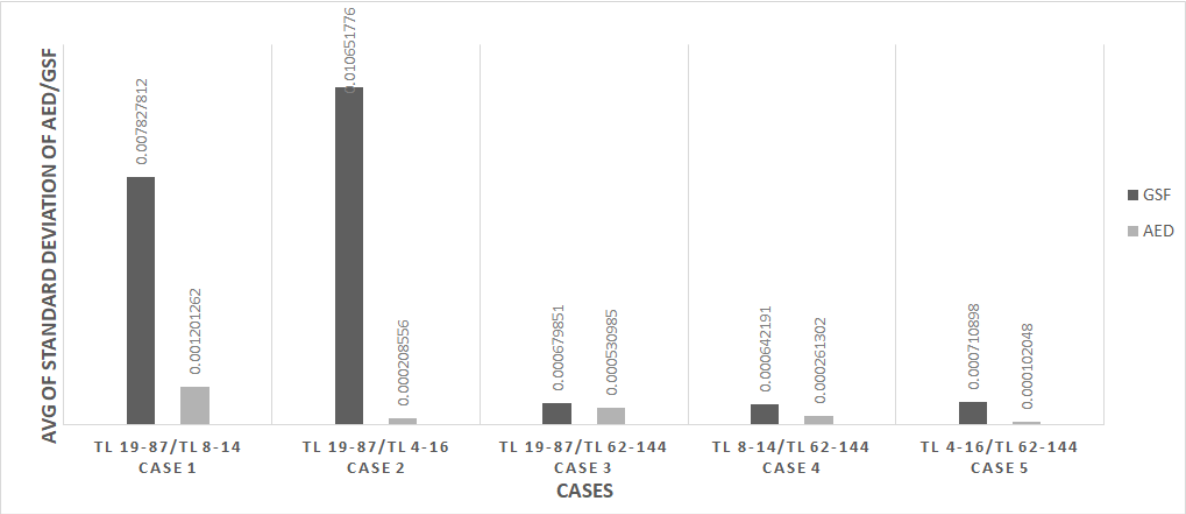

Fig. 7.14: Comparison of averages of standard deviations of AEDs and GSFs in clusters for 300-bus system.

CHAPTER 8

Conclusion and future research directions

8.1 Conclusion

The challenges associated with complexity of power system analysis are addressed in this thesis with proposed measures and associated derived methodologies. The thesis provides the description of the analytical foundation of structural analysis from a networks perspective and highlights key features along with demonstration of the methodology in various application areas of power system.

This thesis extracts the common features through relatively thorough investigation and the results of this investigation provide the analysis of major types of power system models and show the structure description from different perspectives such as steady-state, electromagnetic transient and electro-dynamic perspectives. This investigation provides the possibility of analyzing the power system network on the basis of only structural information. The study provided the key features of structural analysis which are decoupling, connection information, electrical distance and link strength. This highlights the dominating influence of the structure features in the network topology.

The basis of newly developed structural analysis is introduced and described in Chapter 4 and further establishment of electric circuit foundation for structural analysis is described in Chapter 5 using port-Hamiltonian formalism. This shows the underlying similarity of network models which is later reflected in the analysis done in power system restoration.

An application of structural analysis in system restoration planning is shown in Chapter 6. The analysis is completely based on the network topological information extracted from the actual network. The results have addressed the long-standing issue of solving

system restoration problem using conventional techniques. The applications range from creation of new restoration plans to validation of existing restoration plans and non-restoration testing along with the satisfaction related to the computational times for different applications. The restoration plans are generated for IEEE 300-bus system and a large-scale 2000-bus system and the application shows faster simulation times as compared to the restoration plans based on conventional techniques on a similar network.

Application of structural analysis in science area is also presented with the network equivalencing problem in Chapter 7. Specifically the application reduces the complexity of the interconnected network and thus simplifies analyses. This is illustrated with the introduction of electrical distance measure which is based on the network connection information. Further the results of these applications are presented.

The success of the method in addressing these long-term challenging issues can be seen as experimental evidence of the effectiveness of the use of network topology. These applications demonstrate how use of structural analysis from a networks perspective helps in bridging the gap between power systems and complex network science.

8.2 Future research direction

The future research directions opened up by this thesis include the development of real-time dynamic analyses and more sophisticated solutions in the area of power system restoration that may require state estimation details as part of the system structure. Further, this can be used in protection studies since it requires real-time analysis. Another potential area of research opened up by this study is the use of structural analysis based modified short circuit ratio parameter to study the system strength at various points of interconnection for integration of solar PV plants. Further extension of this research would continue to aid in bringing between areas in power systems and complex networks.

List of Abbreviations

EMD	Electro-mechanical distance
C-EMD	Composite electro-mechanical distance
CF	Coherency factor
RPSC	Reactive power support capability
RED	Relative electrical distance
GSF	Generation shift factor
AED	Average electrical distance
EMT	Electromagnetic transient
FACTS	Flexible AC transmission system
SVS	Static VAR system
SVC	Static VAR compensator
TCR	Thyristor-controlled reactor
TSR	Thyristor-switched reactor
TSC	Thyristor-switched capacitors
MSR	Mechanically-switched reactors
MSC	Mechanically-switched capacitors
STATCOM	Static synchronous compensator
VSC	Voltage source converter
UPFC	Unified power flow controller
SSSC	Static synchronous series compensator
NERC	North American Electric Reliability Corporation
DP	Dynamic programming
ADP	Approximate dynamic programming
ES	Expert systems

MP	mathematical programming
EOP	Emergency Operations and Preparedness
GOP	Generator operators
TOP	Transmission operators
PSERC	Power System Engineering Research Center
EPRI	Electric Power Research Institute
SRN	System restoration navigation
OBC	Optimal Blackstart capabilities
ERCOT	Electrical Reliability Council of Texas
TO	Transmission owner

List of Key Symbols

$d_G(u, v)$	Distance between two vertices u, v of a graph G;
$\mu(G)$	Average distance of a graph G of order n;
$R(G)$	Resistance distance of connected undirected graph G;
S_{kl}	Effect of state change at location l due to state change at location k;
e_a	Measure of connectivity distance for node a;
$R_d(k)$	Reflection distance of generator k of set Ω;
ΔP_{ri}	Change in electrical power of a generator i owing to a small change in the angle of generator k;
a_k	Acceleration of generator k at the instant of fault;
CF	Coherency factor for dynamic equivalence of network;
J	Jacobian matrix
H_i	Moment of inertia of machine i;
β	Normalized coherency factor of the machines;
d_{in}	Electro-mechanical distance between the generator i and the reference generator n;
B	Susceptance matrix;
p_{il}	Amplitude of the real mode corresponding to change in rotor angle $\Delta\delta_{in}$;
q_{il}	Amplitude of the complex mode corresponding to change in rotor angle $\Delta\delta_{in}$;
α_{ij}	normalized voltage attenuation on bus i with respect to the perturbation at bus j;
V_i	Voltage magnitude at i^{th} bus;

δ_i	Rotor angle of i^{th} machine with respect to a synchronously rotating frame, electrical radians;
G_{ij}	Real part of the negative of the branch admittance between buses i and j;
G_{ii}	Sum of real parts of all branch admittances connected to i^{th} bus;
B_{ij}	Imaginary part of the negative of the branch admittance between buses i and j;
B_{ii}	Sum of imaginary parts of all branch admittances connected to the i^{th} bus;
I_G	Complex current vector at the generator node;
I_L	Complex current vector at the load node;
V_G	Complex voltage vector at the generator node
V_L	Complex voltage vector at the load node;
d_{ij}	Electrical distance between j^{th} load unit and i^{th} generation unit;
$g_{ab,i}$	Generation shift factor of tie-line ab with respect to bus i;
$\bar{X}_{a,i}$	Element of inverse of susceptance matrix;
x_{ab}	Reactance of tie-line ab;
$d_{ab,i}$	Average electrical distance of bus i from tie-line ab;
$Z_{th,ai}$	Thevenin impedance between bus a and bus i;
$X_{th,ai}$	Thevenin reactance between bus a and bus i;
Z_{bus}	Open circuit impedance matrix;
Y_{bus}	Short circuit admittance matrix or the nodal admittance matrix;
θ_m	Angular position of the rotor with respect to a stationary axis;
P_m	Mechanical power;
P_e	Electrical power;
L'	Inductance of a lossless line;
C'	Capacitance of a lossless line;
Δt	Time delay;

Δf	Frequency deviation $(f - f_0)$;
$i_{FL}\alpha$	Fundamental reactor current;
ϑ	Voltage transformation ratio;
$H(q, p)$	Hamiltonian representation of total energy of the system;
p	Vector of generalized configuration coordinates for mechanical system;
q	Vector of generalized momenta;
$B(q)f$	Generalized forces resulting from input $f \in \mathbb{R}^m$;
$\nabla H(q, \varphi)$	Gradient of $H(q, \varphi)$;
$\mathbf{D}_{-t,-t}^{-1}\mathbf{P}_{-t}^{*}$	Initial probability distribution;
$\mathbf{M}_{-t,-t}^{T}$	Transition probabilities dependent on connection strength;
$\mathbf{\Theta}_{-t}$	Equilibrium distribution;
G	Weighted undirected graph;
$V(G)$	Vertex set of graph G;
$E(G)$	Edge set of graph G;
w_{ij}	Weight of the edge (i, j);
W	Diagonal matrix with the diagonal entries representing the weights on the edges;
L	Laplacian matrix;
$\mathcal{X}$	Decision space;
$\mathcal{S}$	State space;
S_t	Possible state for each stage at time t;
G_j	Set of generation outputs;
D_i	Set of loads;
L_k	Set of status of transmission lines;
f_c	Set of operating frequencies;
R_j	Ramping rate of generator j;
u	Decision variable for the sub-problems;
ω	Weight associated with the elements in the system;

π^*	Optimal strategy used to find the sub-problem solutions at all stages for the overall optimal solution;
X_s	State at stage s;
U_s	Decision that optimizes value of the subsequent stage;
$F\{V(X_s)\}$	Assumed perception function with $i \in X_s, j \in X_{s+1}$
$deg(i)$	Degree of a vertex i;
Y^+	Pseudo-inverse of admittance matrix Y;
$Y(o)$	Reduced Laplacian matrix;
ϕ	Error measure or potential function for determination of clusters;
μ_j	Centroid location;
$d(\mu_j)$	AED-based measure of the centroid in the j^{th} cluster with respect to the tie-lines;
s_{im}	Silhouette coefficient of bus i;
s_i	Average silhouette coefficient;

Bibliography

[1] University of Washington, "118-bus power flow test case," 1993. [Online]. Available: https://www2.ee.washington.edu/research/pstca/pf118/pg_tca118bus.htm

[2] S. Lee and F. Schweppe, "Distance measures and coherency recognition for transient stability equivalents," *IEEE Trans. Power App. Syst.*, vol. 92, no. 5, pp. 1550–1557, 1973.

[3] M. Kent *et al.*, "Dynamic modeling of loads in stability studies," *IEEE Trans on PAS*, vol. 88, pp. 756–763, 1969.

[4] J. Machowski, J. Bialek, and J. Bumby, *Power System Dynamics: Stability and Control*, John Wiley & Sons Ltd., 2008.

[5] D. Wu, F. Ma, M. Javadi, K. Thulasiraman, E. Bompard, and J. N. Jiang, "A study of the impacts of flow direction and electrical constraints on vulnerability assessment of power grid using electrical betweenness measures," *Physica A: Statistical Mechanics and its Applications*, vol. 466, pp. 295 – 309, 2017.

[6] X. Li, M. Javadi, B. Zhao, D. Wu, and J. Jiang, "Evidence of significance of graph energy interlinks in topological form of the power grid," in *2015 5th International Conference on Electric Utility Deregulation and Restructuring and Power Technologies (DRPT)*, Nov 2015, pp. 2596–2602.

[7] Y. Xu, A. Gurfinkel, and P. Rikvold, "Architecture of the florida power grid as a complex network," *Physica A: Statistical Mechanics and its Applications*, vol. 401, pp. 130 – 140, 2014.

[8] Texas A&M Engineering Experiment Station (TEES), "Electric test grid repository," 2015. [Online]. Available: https://electricgrids.engr.tamu.edu/electric-grid-test-cases/activsg2000

[9] T. A. of Counties, "Texas county map." [Online]. Available: https://www.county.org/About-Texas-Counties/Texas-County-Maps

[10] D. Watts and S. Strogatz, "Collective dynamics of 'small-world' networks," *Nature*, vol. 393, no. 6684, pp. 440–442, 1998.

[11] L. Amaral, A. Scala, M. Barthelemy, and H. Stanley, "Classes of small-world networks," in *National Academies of Science*, vol. 97, no. 21, Apr 2000, pp. 11 149–11 152.

[12] R. Albert, I. Albert, and G. Nakarado, "Structural vulnerability of the North American power grid," *Physical Review E*, vol. 69, no. 2, Feb 2004.

[13] P. Crucitti, V. Latora, and M. Marchiori, "A topological analysis of the italian electric power grid," *Physical Review E.*, vol. 338, no. 1, pp. 92–97, 7 2004.

[14] D. Chassin and C. Posse, "Evaluating North American electric grid reliaiblity using the barabasi-albert network model," *Physica A*, vol. 355, pp. 667–677, 2005.

[15] U.S. Department of Energy, "Utility Outage Information," 2015. [Online]. Available: https://openei.org/doe-opendata/dataset/utility-outage-information

[16] ——, "Transforming the Nation's Electricity Sector: The Second Installment of the QER," 2017. [Online]. Available: https://www.energy.gov/policy/initiatives/quadrennial-energy-review-qer/quadrennial-energy-review-second-installment

[17] U.s. energy information administration - energy explained. [Online]. Available: http://www.eia.gov/energy_in_brief/article/power_grid.cfm

[18] H. Wang, C. Sanchez, R. Zimmerman, and R. Thomas, "On computational issues of market-based optimal power flow," *IEEE Trans. Power Systems*, vol. 22, no. 3, pp. 1185–1193, 8 2007.

[19] W. Hogan, "A market power model with strategic interaction in electricity networks," *The Energy Journal*, vol. 18, pp. 107–141, 1997.

[20] H. Duran and N. Arvanitidis, "Simplification for area security analysis: A new look at equivalencing," *IEEE Trans. Power App. Syst.*, vol. 91, no. 2, pp. 670–679, 3 1972.

[21] F. Harary, "Graph theory," *Addison-Wesley, New York*, 1969.

[22] R. Graham and L. Lovasz, "Distance matrix polynomials of trees," *Advances in Math.*, vol. 28, pp. 60–88, 1978.

[23] J. Plesnik, "On the sum of all distances in a graph or digraph," *Journ. of Graph Theory*, pp. 1–21, 3 1984.

[24] Z. Mihalic, D. Veljan, D. Amic, S. Nikolic, D. Plavsic, and N. Trinajstic, "The distance matrix in chemistry," *Journal of Mathematical Chemistry*, vol. 11, no. 1, pp. 223–258, 12 1992.

[25] R. Merris, "Laplacian matrices of graphs: a survey," *J. Linear Algebra and its applications*, vol. 197, no. 1, pp. 143–176, 1 1994.

[26] R. Graham, A. Hoffman, and H. Hosoya, "On the distance matrix of a directed graph," *Journ. Graph Theory*, vol. 1, pp. 85–88, 1977.

[27] M. Swamy and K. Thulasiraman, "Graphs, networks and algorithms," 1981.

[28] D. J. Klein and M. Randic, "Resistance distance," *Journal of Mathematical Chemistry*, vol. 12, pp. 81–95, 1993.

[29] B. Zhou and N. Trinajstic, "On resistance-distance and kirchhoff index," *Journal of Mathematical Chemistry*, vol. 283, no. 46, 6 2009.

[30] D. Babic, D. Klein, I. Lukovits, S. Nikolic, and N. Trinajs, "Resistance-distance matrix: A computational algorithm and its application," *Int. Journ. Quantum Chemistry*, vol. 90, no. 1, pp. 166–176, 12 2001.

[31] H. Zhang and Y. Yang, "Resistance distance and kirchhoff index in circulant graphs," *Int. Journ. Quantum Chemistry*, vol. 107, no. 2, pp. 330–339, 9 2006.

[32] J. Palacios, "Resistance distance in graphs and random walks," *Int. Journ. Quantum Chemistry*, vol. 81, no. 1, pp. 29–33, 11 2000.

[33] P. Hines and S. Blumsack, "A centrality measure for electrical networks," in *41st annual Hawaii Int. Conf. on System Sci.*, 2008.

[34] A. Barrat, M. Barthelemy, R. Satorras, and A. Vespignani, "The architecture of complex weighted networks," in *Nat. Academy of Sci. of USA*, vol. 101, no. 11, 3 2004, p. 3747âĂŞ3752.

[35] S. Boccaletti, V. Latora, Y. Moreno, M. Chavez., and D. Hwang, "Complex networks: Structure and dynamics," *Phy. Report*, vol. 424, p. 175âĂŞ308, 2 2006.

[36] M. Newman, "Analysis of weighted networks," *Phy. Rev. E*, vol. 70, no. 5, pp. 175–308, 11 2004.

[37] P. Hines, S. Blumsack, E. C. Sanchez, and C. Barrows, "The topological and electrical structure of power grids," in *43rd annual Hawaii Int. Conf. on System Sci.*, 2010.

[38] P. Lagonotte, J. Sabonnadiere, J. Leost, and J. Paul, "Structural analysis of the electrical system: Application to secondary voltage control in france," *IEEE Trans. Power Syst.*, vol. 4, 5 1989.

[39] R. Podmore, "Identification of coherent generators for dynamic equivalents," *IEEE Trans. Power App. Syst.*, vol. 97, no. 4, pp. 1344–1354, 1978.

[40] J. Undrill, J. Casazza, E. Gulachenski, and L. Kirchmayer, "Electromechanical equivalents for use in power system studies," *IEEE Trans. Power App. Syst.*, vol. 90, pp. 2060–2071, 1971.

[41] V. Sankaranarayanan, M. Venugopal, S. Elangovan, and R. Dharma, "Coherency identification and equivalents for transient stability studies," *Elect. Power Sys. Res.*, vol. 6, pp. 51–60, 1983.

[42] W. Mittlestadt, "Proposed algorithms for approximate reduced dynamic equivalents," *BPA Internal Memorandum*, 9 1973.

[43] F. Wu and N. Narsimhamurthi, "Coherency identification for power system dynamic equivalents," *IEEE Trans. on Circuits and Syst.*, vol. 30, no. 30, pp. 140–147, 3 1983.

[44] M. A. Pai and R. P. Adgaonkar, "Electromechanical distance measure for decomposition of power systems," *Int. Journ. of Electric Power and Energy Systems*, vol. 6, no. 4, pp. 249–254, 10 1984.

[45] R. Belhomme and M. Pavella, "A composite electromechanical distance approach to transient stability," *IEEE Trans. on power systems*, 1991.

[46] R. Belhomme, M. Pavella, and Y. Xue, "Electromechanical distances for identifying contingency propagation in transient stability studies," in *IFAC Int. Symp. on power systems and power plant control*, 1989, pp. 940–945.

[47] R. Belhomme, H.Zhao, and M. Pavella, "Power system reductino techniques for direct transient stability methods," *IEEE Trans. on Power Systems*, pp. 723–729, 1993.

[48] D. Wang and X. Wang, "Study on electromechanical distance of electrical power system," in *Power and Energy Engineering Conference (APPEEC)*, 3 2010.

[49] H. Liu, A. Bose, and V. Venkatasubramanian, "A fast voltage security assessment method using adaptive bounding," 5 1999.

[50] E. Nobile and A. Bose, "A new scheme for voltage control in a competitive ancillary service market," 6 2002.

[51] J. Zhong, E. Nobile, A. Bose, and K. Bhattacharya, "Localized reactive power markets using the concept of voltage control areas," *IEEE Trans. on Power Systems*, vol. 19, no. 3, pp. 1555–1561, 8 2004.

[52] M. Javadi *et al.*, "A study of reactive power margins in power system following severe generation imbalance," in *IEEE PES General Meeting*, 2015.

[53] A. Abed, "Wscc voltage stability criteria, under-voltage, load shedding strategy, and reactive power reserve monitoring methodology," vol. 1, 7 1999, pp. 191–197.

[54] Z. Feng, W. Xu, C. Oakley, and S. Mcgoldrich, "Experiences on assessing alberta power system voltage stability with respect to the wscc reactive power criteria," vol. 2, 7 1999, pp. 1297–1302.

[55] T. Cutsem, "A method to compute reactive power margins with respect to voltage collapse," *IEEE Trans. on power systems*, vol. 6, no. 1, pp. 145–156, 2 1991.

[56] C. Parker, I. Morrison, and D. Sutanto, "Application of an optimization method for determining the reactive margin from voltage collapse in reactive power planning," *IEEE Trans. on power systems*, vol. 11, no. 13, pp. 1473–1481, 8 1998.

[57] K. Visakha *et al.*, "An approach for evaluation of transmission charges based on

desired and deviations of power contracts in open access," in *6th Int. Conf. on APSCOM*, 2003.

[58] L. Willis, J. Finncy, and G. Raman, "Computing the cost of unbundled services," *IEEE Computer Applications in Power*, pp. 16–21, 10 1996.

[59] D. Shirmohmmadi, C. Rajagopalan, E. Alward, and C. Thomas, "Cost of transmission transactions: An introduction," *IEEE Trans. on power systems*, vol. 6, no. 3, pp. 1546–1560, 11 1991.

[60] J. Bialek, "Topological generation and load distribution factors for supplement charge allocation in transmission open access," *IEEE Trans. on power systems*, vol. 12, no. 3, pp. 1185–1193, 4 1997.

[61] Y. Ni, P. Wei, and F. Wu, "Power transfer allocation for open access using graph theory, fundamentals and applications in systems without loop flow," *IEEE Trans. on power systems*, vol. 15, no. 3, 2000.

[62] M. Enns and J. Quada, "Sparsity-enhanced network reduction for fault studies," *IEEE Trans. on Power Syst.*, vol. 6, no. 2, pp. 613–621, 5 1991.

[63] X. Cheng and T. Overbye, "Ptdf-based power system equivalents," *IEEE Trans. on Power Syst.*, vol. 20, no. 4, pp. 1868–1876, 7 2005.

[64] D. Shi and D. Tylavsky, "A novel bus-aggregation-based structure preserving power system equivalent," *IEEE Trans. on Power Syst.*, vol. 30, no. 4, pp. 1977–1986, 7 2015.

[65] H. Oh, "A new network reduction methodology for power system planning studies," *IEEE Trans. on Power Syst.*, vol. 25, no. 2, pp. 677–684, 5 2010.

[66] M. Rafiq *et al.*, "Average electrical distance-based bus clustering method for network equivalence," in *19th International Conference on Intelligent System Application to Power Systems (ISAP)*, Sept 2017, pp. 1–6.

[67] H. Dommel, "Digital computer solution of electromagnetic transients in single and multiphase networks," *IEEE Trans on PAS*, vol. 88, no. 4, pp. 388–399, 1969.

[68] A. Morched and V. Brandwajn, "Transmission network equivalents for electro-

magnetic transients studies," *IEEE Trans on PAS*, vol. 102, no. 9, pp. 2984–2994, 1983.

[69] H. Su, K. Chan, L. Snider, and T. Chung, "A parallel implementation of electromagnetic electromechanical hybrid simulation protocol," in *IEEE Int. Conf. DRPT*, 4 2004.

[70] Y. Zhang, W. Wu, B. Zhang, and A. Gole, "A decoupled interface method for electromagnetic and electromechanical simulation," in *IEEE Electrical Power and Energy Conf.*, 4 2011.

[71] W. W. B. Z. Y. Zhang, A.M. Gole and H. Sun, "Development and analysis of applicability of a hybrid transient simulation platform combining tsa and emt elements," *IEEE Trans on Power Syst.*, vol. 28, no. 1, pp. 357–366, 2013.

[72] P. Kundur, "Power system stability and control," McGraw-Hill, 1994.

[73] D. Povh, "Modeling of facts in power system studies," *IEEE Power Eng. Soc. Winter Meeting*, vol. 2, pp. 1435–1439, 2000.

[74] L. Gyugyi, "Power electronics in electric utilities: Static var compensators," *Proc. of IEEE*, vol. 76, no. 4, pp. 483–494, 1988.

[75] C. W. G. 31-01, "Modeling of static var systems (SVS) for system analysis," *Electra*, vol. 51, 1977.

[76] C. T. F. 38-01-02, *Static Var Compensator*, 1986.

[77] I. S. S. C. W. Group, "Static var compensator models for power flow and dynamic performance simulation," *IEEE Trans on Power Syst.*, vol. 9, no. 1, pp. 229–240, 1994.

[78] Y. Ma, A. Huang, and X. Zhou, "A review of STATCOM on the electric power system," in *IEEE International Conference on Mechatronics and Automation (ICMA)*. IEEE, 2015.

[79] L. Gyugyi, "Unified power-flow control concept for flexible ac transmission systems," in *Proc. Inst. Electr. Eng. Part C: Gener., Transmiss. Distrib.*, vol. 139, no. 4, 1992, pp. 323–331.

[80] K. Sen and E. Stacey, "UPFC-unified power flow controller: theory, modeling and applications," *IEEE Transactions on Power Delivery*, vol. 13, no. 4, pp. 1453–1460, 1998.

[81] K. Padiyar, *HVDC Power Transmission Systems: Technology and System Interactions*. New York/Chichester, U.K.: Wiley, 1990.

[82] N. Flourentzou, V. Agelidis, and G. Demetriades, "VSC-based HVDC power transmission systems: An Overview," *IEEE Trans on Power Electronics*, vol. 24, no. 3, pp. 592–602, 2009.

[83] J. Undrill and A. Turner, "Construction of power system electromechanical equivalents by modal analysis," *IEEE Trans on PAS*, vol. 90, no. 5, 1971.

[84] R. Tewerson, *Sparse Matrices*. New York: Academic Press, 1973.

[85] A. Brameller, R. Allan, and Y. Hamam, *Sparsity: Its Practical Application to Systems Analysis*. London: Pitman Publishing, 1976.

[86] W. Tinney and J. Walker, "Direct solutions of sparse network equations by optimally ordered triangular factorization," *Transactions of the IEEE*, vol. 55, no. 11, pp. 1801–1809, 1967.

[87] P. Dimo, *L'analyse Nodale des Reseaux D'energie*. Paris: Eyrolles, 1971.

[88] P. Moses, M. Masoum, and H. Toliyat, "Impacts of hysteresis and magnetic couplings on the stability domain of ferroresonance in asymmetric three-phase three-leg transformers," *IEEE Trans. on Energy Conv.*, vol. 26, no. 2, pp. 581–592, June 2011.

[89] A. Bergen and D. Hill, "A structure preserving model for power system stability analysis," *IEEE Transactions on Power Apparatus and Systems*, vol. PAS-100, no. 1, pp. 25–35, Jan 1981.

[90] A. van der Schaft and D. Jeltsema, "Port-hamiltonian systems theory: An introductory overview," *Foundations and Trends in Systems and Control*, vol. 1, no. 2-3, p. 173âĂŞ378, Jun 2014.

[91] Swedish and N. P. Companies, "Load representation in stability studies and the

effect of the load-voltage characteristics on transient stability," *Report to CIGRE Committee*, 1964.

[92] C. Concordia and S. Ihara, "Load representation in power system stability studies," *IEEE Trans on PAS*, vol. 101, no. 4, pp. 969–977, 1982.

[93] D. Sharma, K. Thulasiraman, D. Wu, and J. Jiang, "Power network equivalents: A network science based k-means clustering method integrated with silhouette analysis," in *Complex Networks and their Application VI, Lyon, France*, 2017, pp. 78–89.

[94] A. van der Schaft, *Port-Hamiltonian Differential-Algebraic Systems*. Berlin, Heidelberg: Springer, 2013, pp. 173–226.

[95] A. Malyscheff, D. Wu, F. Ma, and J. Jiang, "A probabilistic perspective for power flow and its implication to power network analysis," in *The 50th North American Power Symposium (NAPS), Fargo*, 2018.

[96] Q. Lu and S. Brammer, "A new formulation of generator penalty factors," *IEEE Trans. on Power Syst.*, vol. 10, no. 2, pp. 990–994, 1995.

[97] H.Jeong *et al.*, "The large-scale organization of metabolic networks," *Nature*, vol. 407, no. 6804, pp. 651–654, 2000.

[98] J. Doye, "Network topology of a potential energy landscape: A static scale-free network," *Physical Review Letters*, vol. 88, no. 23, pp. 1–4, 2002.

[99] M. Faloutsos, P. Faloutsos, and C. Faloutsos, "On power-law relationships of the internet topology," in *Applications, technologies, architectures, and protocols for computer communication*, 1999, p. 262.

[100] R. Albert, H. Jeong, and A. Barabasi, "Internet: Diameter of the world-wide web," *Nature*, vol. 401, no. 6749, p. 130âĂŞ131, 1999.

[101] D. Sharma *et al.*, "Advanced techniques of system restoration and practical applications," in *11th Int. Conf. on Power Generation, Transmission, Distribution and Energy Conversion, Dubrovnik, Croatia*, 2018.

[102] North American Electric Reliability Corporation (NERC), "NERC Stan-

dard EOP-005-2, System Restoration Coordination," 2009. [Online]. Available: https://www.nerc.com/docs/standards/sar/SRBSDT_EOP-005-2_Preballot_Review_Clean_2009March03.pdf

[103] ——, "NERC Standard EOP-006-2, System Restoration Coordination," 2009. [Online]. Available: https://www.nerc.com/docs/standards/sar/SRBSDT_EOP-006-2_Preballot_Review_Clean_2009March03.pdf

[104] T. Nagata, S. Hatakeyama, M. Yasouka, and H. Sasaki, "An efficient method for power distribution system restoration based on mathematical programming and operation strategy," in *Int. Conf. Power System Technology*, vol. 3, 2000, pp. 1545–1550.

[105] E. Simburger and F. Hubert, "Low voltage bulk power system restoration simulation," *IEEE Trans. Power App. Syst.*, vol. PAS-100, pp. 4479–4484, 1981.

[106] R. Kafka, D. Penders, S. Bouchey, and M. Adibi, "System restoration plan development for a metropolitan electric system," *IEEE Trans. Power App. Syst.*, vol. PAS-100, pp. 3703–3713, 1981.

[107] T. Sakaguchi and K. Matsumoto, "Development of a knowledge based system for power system restoration," *IEEE Trans. Power App. Syst.*, vol. PAS-102, pp. 320–329, 1983.

[108] T. McDermott, I. Drezga, and R. Broadwater, "A heuristic non-linear constructive method for distribution system reconfiguration," *IEEE Trans. Power Systems*, vol. 14, pp. 478–483, 1999.

[109] Y. Kojima, S. Warashina, M. Kato, and H. Watanabe, "The development of power system restoration method for a bulk power system by applying knowledge engineering techniques," *IEEE Trans. Power Systems*, vol. 4, pp. 1228–1235, 1989.

[110] K. Hotta *et al.*, "Implementation of a real time expert system for a restoration guide in a dispatch center," *IEEE Trans. Power Systems*, vol. 5, pp. 1032–1038, 1990.

[111] K. Simakura *et al.*, "A knowledge-based method for making restoration plan of bulk power system," *IEEE Trans. Power Systems*, vol. 7, pp. 914–920, 1992.

[112] M. Adibi, "New approach in power system restoration," *IEEE Trans. Power Systems*, vol. 7, pp. 1428–1434, 1992.

[113] T. Nagata, H. Sasaki, and R. Yokoyama, "Power system restoration by joint usage of expert system and mathematical programming approach," *IEEE Trans. Power Systems*, vol. 10, no. 3, pp. 1473–1479, 1995.

[114] S. Lee, S. Lim, and B. Ahn, "Service restoration of primary distribution systems based on fuzzy evaluation of multi-criteria," *IEEE Trans. Power Systems*, vol. 13, pp. 1156–1163, 1998.

[115] Power System Engineering Research Center (PSERC), "Development and evaluation of system restoration strategies from a blackout," 2009. [Online]. Available: https://pserc.wisc.edu/documents/publications/reports/2009_reports/S-30_Final-Report_Sept-2009.pdf

[116] D. R. Medina *et al.*, "Fast assessment of frequency response of cold load pickup in power system restoration," *IEEE Trans. Power Systems*, vol. 31, no. 4, pp. 3249–3256, 2016.

[117] A. Ketabi, A. M. Ranjbar, and R. Feuillet, "A new method for dynamic calculation of load steps during power system restoration," in *2000 Can. Conf. Electrical and Computer Engineering*, vol. 1, 2000, pp. 158–162.

[118] S. Lim *et al.*, "Restoration index in distribution systems and its application to system operation," *IEEE Trans. Power Systems*, vol. 21, no. 4, pp. 1966–1971, 2006.

[119] C. T. Su and C. S. Lee, "Network reconfiguration of distribution systems using improved mixed-integer hybrid differential evolution," *IEEE Trans. Power Delivery*, vol. 18, no. 3, pp. 1022–1027, 2003.

[120] Electric Power Research Institute (EPRI), "System restoration tools: System restoration navigator srn integrated into epri operator training simulator (OTS)," 2014. [Online]. Available: https://www.epri.com/#/pages/product/1020055/

[121] ——, "System restoration tools: Optimal blackstart capability (OBC)," 2012. [Online]. Available: https://www.epri.com/#/pages/product/1024262/

[122] W. Powell, *Approximate Dynamic Programming: Solving the Curses of Dimensionality.* New York: Wiley, 2007.

[123] A. Birchfield, T. Xu, K. Gegner, K. Shetye, and T. Overbye, "Grid structural characteristics as validation criteria for synthetic networks," *IEEE Trans. Power Systems*, vol. 32, no. 4, pp. 3258–3265, 2017.

[124] J. Ward, "Equivalent circuits for power flow studies," *AIEE Trans. Power App. Syst.*, vol. 68, pp. 373–382, 1949.

[125] S. Srinivasan, V. N. Sujeer, and K. Thulasiraman, "A new equivalence technique in linear graph theory," *Journal of the Institution of Engineers (India)*, vol. 44, no. 12, 1964.

[126] ——, "Application of equivalence technique in linear graph theory to reduction process in a power system," *Journal of the Institution of Engineers (India)*, vol. 46, no. 12, 1966.

[127] E. Housos, G. Irisarri, R. Porter, and A. Sasson, "Steady state network equivalents for power system planning applications," *IEEE Trans. Power App. Syst.*, vol. 99, no. 6, pp. 2113–2120, 11 1980.

[128] W. Tinney and J.M.Bright, "Adaptive reductions for power flow equivalents," *IEEE Trans. Power App. Syst.*, vol. 2, no. 2, pp. 351–360, 5 1987.

[129] M. Newman, "A measure of betweenness centrality based on random walks," *Soc. Netw.*, vol. 27, no. 1, pp. 39–54, 2005.

[130] A. Tizghadam and A. Leon-Garcia, "Autonomic traffic engineering for network robustness," *IEEE J. Selected Areas in Communication, Special Issue in Autonomic Communications*, vol. 28, no. 1, pp. 39–50, 2010.

[131] V. Chellappan, K. Sivalingam, and K. Krithivasan, "A centrality entropy maximization problem in shortest path routing networks," *Comp. Netw.*, vol. 104, pp. 1–15, 2016.

[132] P. Doyle and J. Snell, "Random walks and electrical networks," *The Mathematical Association of America*, 1984.

[133] D. Coppersmith, P. Doyle, P. Raghavan, and M. Snir, "Random walks on a 129 weighted graphs and applications to online algorithms," in *22nd Symposium on the Theory of Computing*, 1990, pp. 369–378.

[134] S. Blumsack *et al.*, "Defining power network zones from measures of electrical distance," in *2009 IEEE Power Energy Society General Meeting*, July 2009, pp. 1–8.

[135] D. Shi, D. L. Shawhan, N. Li, and D. J. Tylavsky, "Optimal generation investment planning: Pt. 1: Network equivalents," in *44th North Amer. Power Symp., Champaign, IL, USA*, 2012, pp. 1–6.

[136] J. Gutman and W. Xiao, "Generalized inverse of the laplacian matrix and some applications," *Bulletin De 1' Academie serbe des sciences et des arts.*, vol. 129, no. 29, pp. 15–23, 2004.

[137] J. Molitierno, *Applications of Combinatorial Matrix Theory to Laplacian Matrices of Graphs*. Boca Raton: Chapman and Hall - CRC, 2012.

[138] S. Brin and L. Page, "The anatomy of a large-scale hypertextual web search engine," in *Seventh International World-Wide Web Conference (WWW 1998)*, 1998.

[139] M. Newman, *Networks: An Introduction*, Oxford Univ. Press, 2010.

[140] R. Merton, *Social theory and social structure*, Simon and Schuster, 1968.

[141] F. Lorrain and H. White, "Structural equivalence of individuals in social networks," *Journal of Math. Society*, vol. 1, no. 1, pp. 49–80, 1971.

[142] R. Rossi and N. Ahmed, "Role discovery in networks," *IEEE Trans. on Knowledge and Data Engineering*, vol. 27, no. 4, pp. 1112–1131, 2015.

[143] V. Faber, "Clustering and the continuous k-means algorithm," *Los Alamos Science*, vol. 22, pp. 138–144, 1994.

[144] S. Lloyd, "Least squares quantization in PCM," *IEEE Trans. on Information Theory*, vol. 28, pp. 129–137, 1982.

[145] F. Preparata and M. Shamos, *Computational Geometry: An Introduction*, Springer Verlag, 1990.

[146] D. Arthur and S. Vassilvitskii, "k-means++: The advantages of careful seeding," in *18th Annual ACM-SIAM Symposium on Discrete Algorithms*, 2007, pp. 1027–1035.

[147] X. Sicotte, "k-means vs k-means++," Cross Validated. [Online]. Available: https://stats.stackexchange.com/q/357606

[148] R. Tibshirani, G. Walther, and T. Hastie, "Estimating the number of clusters in a data set via the gap statistic," *J. Royal Statistical Society B*, vol. 63, no. 2, pp. 411–423, 2001.

[149] G. Milligan and M. Cooper, "An examination of procedures for determining the number of clusters in a data set," *Psychometrika*, vol. 50, pp. 159–179, 1985.

[150] A. Gordon, *Classification.* London: Chapman and Hall - CRC, 1999.

[151] L. Kaufman and P. Rousseeuw, *Finding groups in data: an introduction to cluster analysis.* New York: Wiey, 1990.

[152] P. J. Rousseeuw, "Silhouettes: A graphical aid to the interpretation and validation of cluster analysis," *Journal of Computational and Applied Mathematics*, vol. 20, no. 1, pp. 53–65, 1987.

[153] T. Athay, R. Podmore, and S. Virmani, "A practical method for the direct analysis of transient stability," *IEEE Trans. Power App. Syst.*, vol. PAS-98, no. 2, pp. 573–584, 3 1979.

[154] M. A. Pai, *Energy Function Analysis for Power System Stability.* Boston: Kluwer Academic Publishers, 1989.

[155] "300 bus power flow test case dataset." [Online]. Available: http://www2.ee.washington.edu/research/pstca/pf300/pg_tca300bus.html

[156] K. Thulasiraman and M. Yadav, "Weighted kirchhoff index of a resistance network and generalization of foster's theorem," in *IEEE International Symposium on Circuits and Systems, Baltimore, USA*, 2017, pp. 1027–1035.

[157] K. Thulasiraman, M. Yadav, and K. Naik, "Network science meets circuit theory: Resistance distance, kirchhoff index, and foster's theorems with generalizations and unification," *IEEE Transactions on Circuits and Systems I: Regular Papers*, vol. 66, no. 3, pp. 1090–1103, March 2019.

[158] M. Yadav and K. Thulasiraman, "Network science meets circuit theory: Kirchhoff index of a graph and the power of node-to-datum resistance matrix," in *2015 IEEE International Symposium on Circuits and Systems (ISCAS)*, May 2015, pp. 854–857.